

DEPARTMENT OF APPLIED GENETICS AND CELL BIOLOGY



PRODUCTION OF RECOMBINANT ANTI-
MICROCYSTIN ANTIBODY VARIANTS IN
TRANSGENIC TOBACCO PLANTS FOR SIMPLIFIED
WATER PURIFICATION STRATEGIES

Master's thesis

Submitted by

MARTIN STÜBLER, BSc

Course of Studies: plant-based bioeconomy

Supervisor: Univ. Prof. Dipl. Ing. Dr. rer. nat. Eva Stöger

Co-Supervisor: Stanislav Melnik, MSc

Date of submission: 05.05.2017

Vienna, 19.10.2016

Acknowledgements

Being part of this working group has been a rewarding experience and I would like to thank all friends and colleges who supported me during my master thesis.

First of all, I am extremely grateful to, Ao. Univ. Prof. Dr. Eva Stöger, for making this opportunity available to me. I appreciate her gentle guidance, encouragement and support during this time. As well as the competent recommendations in times of doubts and uncertainty.

I want to offer a very special thanks to my personal supervisor Stanislav Melnik who guided my progress and observed it in tranquility. He was always able to answer my questions, teach me a lot of techniques and tricks and supported me with his broad knowledge and experience. But I also appreciated his classes not only in molecular biology but also in chemistry, mechanics and physics. Retrospectively I can really state, that I have learned much more than I have expected to learn during this project.

I would also like to thank Dr. Elsa Arcalis for being so helpful with the microscopy and image generation and interpretation and Dr. Verena Ibl for supporting me during the writing process.

Finally, I would like to thank Dr. Julia Hilscher, Mag. Ulrike Hörmann-Dietrich, Dr.rer.nat. Eszter Kapusi, DI Marc Tschofen and Mag. Maria Corcuera Gomez and all temporary members of this working group for their friendly support and patience during this amazing time.

Being with this research team left a lasting impression on me and will definitely shape my future decisions in one or the other way.

Abstract:

This thesis addresses the potential benefits of a plant-based production system using *Nicotiana tabacum* to produce the currently most efficient anti-[Arg4]-microcystin antibody MC10E7, which shows great potential for surveying natural water resources and for analyzing aquatic-derived food products. In collaboration with our project partners from the Technical University of Munich an inexpensive and sensitive immunoassay was developed for user-friendly on-site analysis. Future possible applications include water purification adsorbents for the efficient removal of microcystin from contaminated water.

This toxin present in all surface waters and wildlife ponds is produced by ubiquitous cyanobacteria and algae. Even small doses of the toxin induce protein phosphatase inhibition that may cause serious damage to all mammals including humans (Dawson, 1998), not only affecting individuals in direct contact with contaminated water sources but also entering the food chain (Dawson, 1998).

In 2015, monoclonal antibodies reached a market value of \$75 billion (Ecker et al., 2015), with the majority used in human therapeutic applications, e.g. Adalimumab® or Eculizumab®. Other applications are also under study e.g. the use of antibodies in bio filters for environmental sanitation measures, but this is currently only feasible if large quantities of antibodies can be produced inexpensively, e.g. by a plant expression system.

The aim of this master thesis was to produce MC10E7 starting with the experimental design and the construction of expression vectors followed by the generation of transgenic tobacco lines and their analysis.

Transient expression in *Nicotiana benthamiana* was done to achieve the required amount of antibody (AB) within a short term for analysis. However, due to the benefits of cost-efficient biomass upscale, the production of stable transgenic tobacco lines was included to reduce the overall costs for the antibody by about 40% in a theoretically assumed upscaling. To determine antibody yields a direct sandwich enzyme-linked immunosorbent assay (ELISA) was carried out to evaluate the different approaches for future investigations.

Following production, another costly step is the purification of the antibody, where mainly protein A and protein G are used. To reduce this cost factor as much as possible, we explored the use of a cellulose binding motif (CBM) fused to the antibody, to achieve attachment to a microcrystalline cellulose matrix.

Zusammenfassung:

Diese Masterarbeit befasst sich mit der praktischen Anwendung eines pflanzen-basierten Produktionssystems zur Herstellung des Antikörpers MC10E7. Der Einsatz dieses zurzeit effektivsten Antikörpers gegen Microcystin bietet großes Potenzial für die direkte Detektion in Gewässer und Lebensmittel-proben sowie zur Sanierung von Oberflächengewässern. Die Arbeit sollte dabei den gesamten Ablauf beginnend mit dem Versuchsdesign, der Klonierung sowie der Regeneration von transgenen Pflanzen bis hin zur Aufreinigung und Analyse umfassen.

Zusammen mit unseren Kooperationspartner an der TU München wurde abgesehen von der günstigen Produktion von Antikörpern in Tabakpflanzen (*Nicotiana tabacum*) auch die Möglichkeit einer schnellen und einfachen Anwendung in Teststreifen erforscht, die zur Analyse von Wasserproben auf die Anwesenheit von Microcystin genutzt werden können.

Microcystin ist ein sehr häufig vorkommendes Toxin der Klasse der zyklischen Heptapeptide und in fast allen stehenden Oberflächengewässern anzutreffen. Produziert wird es von einer Vielzahl von Algen und Cyanobakterien. Es verursacht bereits in sehr geringen Konzentration allergische Reaktionen mit teilweise schwerwiegenden Folgen für Menschen. Die Auswirkungen beschränken sich nicht ausschließlich auf den direkten Kontakt, da Microcystin sehr stabil ist, kann es auch in die Nahrungskette gelangen wie dies bei aquatischen Kulturen wie z.B. Spirulina häufig vorkommt (Morscheid, 2006).

Monoklonale Antikörper besaßen 2015 einen Marktwert von rund 75 Milliarden Euro (Ecker et al., 2015), größtenteils wurden diese in der Humanbehandlung eingesetzt wie Adalimumab® oder, Infliximab®. Ein weiteres interessantes Einsatzgebiet von monoklonalen Antikörpern liegt in der Umweltbiotechnologie, wo diese wie in dieser Arbeit gezeigt, in der Analyse und in weiterer Folge auch zur Sanierung von Gewässern genutzt werden können (Harris, 1999).

Der teuerste Faktor zur Herstellung von Messstreifen ist die Herstellung des Antikörpers. Große Erfolge konnten hierbei durch das transiente Expressionssystem mit *Nicotiana benthamiana* erzielt werden. Welches bereits einen klaren Kostenvorteil gegenüber den ursprünglich verwandten Hybridoma Linien darstellt. Durch die Verwendung von *Nicotiana tabacum* als Produktionssystem, konnten die Kosten für den Antikörper, um insgesamt 40% gesenkt werden.

Ein weiterer kostenintensiver Schritt ist die Aufreinigung des Antikörpers durch chromatographische Schritte welche im Labormaßstab zumeist auf dem Einsatz von Protein A und G basieren. Um diese signifikante Kostenstelle weiter zu senken, wurde an den Antikörper eine Zellulose bindende Domain angebracht um die direkte und kostengünstige Aufreinigung durch eine mikrokristalline Zellulose Matrix zu ermöglichen.

Aim of this work

The main focus of this work was the production of a stable transgenic tobacco line, producing an anti-microcystin monoclonal antibody in reasonable amounts and to explore its use in water survey devices, which was also preliminary tested by the partners at the Technical University of Munich. This was accomplished in close collaboration with our cooperation partners who developed a highly sensitive dip stick assay from our plant derived antibody for fast and easy on-site analysis of drinking water. The next step leads to the exploration of possible water purification devices of the AB, as it was conducted in this work.

To obtain a stable *Nicotiana tabacum* production line two approaches were taken. The first was a breeding approach. To this end, two transgenic lines were produced based on already available plasmids, expressing either heavy or light chain. The other approach involved assembly of a full length antibody expression plasmid and required more time.

This first step is followed by an analyzing procedure to determine the best parents for defined crossing.

A further goal was to produce sufficient amounts of antibody within a short time frame for the development of a dip stick assay by our project partners in Munich. This fast production was done by *Agrobacterium tumefaciens*-mediated transient expression of antibody MC10E7 in *N. benthamiana*.

A final aim of the work was to generate a c-terminal fusion of this antibody to a CBM from to facilitate low cost purification. The transient expression of the full length antibody carrying a CBM at the C-terminus of the heavy chain was carried out to study the attachment properties to cell wall derived cellulose and artificial micro fibrillated cellulose for high through-put water purification.

Table of Content

1.1	Introduction	1
1.2	The plant expression system	2
1.3	Microcystin	4
1.4	Antibodies	5
1.5	Plant transformation and regeneration	6
1.6	Enhanced Transient Expression	8
1.7	CBM and bio filters	9
2	Materials and methods	10
1.	Molecular biology procedures	10
2.1.1	Restriction digest	10
2.1.2	DNA ligation	11
2.1.3	Polymerase Chain Reaction	12
2.1.4	PCR-based cloning	14
2.1.5	DNA electrophoresis and purification	17
2.1.6	Transformation of chemically competent <i>E. coli</i>	18
2.1.7	Transformation of chemically competent <i>A. tumefaciens</i>	19
2.1.8	Preparation of chemically competent <i>A. tumefaciens</i>	19
2.1.9	Generation of master plates	19
2.1.10	Plasmid extraction	19
2.1.11	Isolation of genomic plant DNA using a Nucleo Spin®	20
2.1.12	Plant genomic DNA isolation by the CTAB method	21
2.1.13	Colony cracking screen	21
2.1.14	Sequencing and storing of DNA	22
2.1.15	Primer design	22
2.1.16	Cryopreservation	22
2.1.17	Preparing of acrylamide SDS gels	23
2.1.18	SDS PAGE	23
2.1.19	Western blotting	24
2.1.20	ELISA	25
2.1.20.1	Coating of plates:	25
2.1.20.2	Blocking and Washing:	25
2.1.20.3	Sample preparation and application to the plate:	25
2.1.20.4	Incubation with the secondary antibody	26
2.1.20.5	Color reaction and analysis	26

2.1.20.6	Material preparation for Cellulose and protein-A comparison	26
2.1.21	Fixation and embedding of samples	26
2.1.22	Sample cutting	27
2.1.23	Immunolocalization of recombinant protein	27
2.1.24	Immunofluorescent Fixation of fresh tissue	28
2.1.1	In silico calculation of the isoelectric point	29
2.2	Bacterial media	30
2.2.1	LB-medium	30
2.2.2	LB-agar	31
2.2.3	SOC-medium	31
2.2.4	YEB-medium	31
2.2.5	YEB-agar	32
2.2.6	Induction-medium for <i>A. tumefaciens</i>	32
2.2.7	Infiltration medium	32
2.2.1	MS-Vitamin stocks 1000x	32
2.2.2	MS-Shooting medium	33
2.2.3	MS-Rooting medium	33
2.2.4	AB-salts	33
2.3	Transformation of plants	34
2.3.1	Preparation of Agrobacteria for infiltration	34
2.3.2	Infiltration of <i>Nicotiana benthamiana</i> using vacuum infiltration	34
2.3.3	Infiltration of <i>Nicotiana tabacum</i> using syringe infiltration	35
2.4	Harvesting of plant Material	35
2.4.1	Ammonium sulfate precipitation	36
2.4.2	Antibody harvest and purification	37
2.4.3	Protein quantification	37
2.5	Stable transformation of tobacco plants	38
3	Results	40
3.1	Cloning of the single vector delivery system	40
3.1.1	Integration of the light chain into the cloning vector	41
3.1.2	Addition of DsRed to cloning vector	43
3.1.3	Transfer of LC and DsRed into the HC- expression vector	44
3.2	Fusion of the CBM to the C-terminal end of the HC	47
3.2.1	CBM binding capacity	49

3.2.1.1	Western blot CBM distribution pattern	49
3.2.1.2	ELISA - CBD binding specificity	57
3.3	Regeneration of transgenic plants	59
3.3.1	Tandem delivery system	59
3.3.2	single vector delivery system	61
3.4	Yields of the Plant derived antibody	63
3.4.1	Infiltration pilot experiments	63
3.4.2	Transient plant derived antibody yield determination via Bradford assay	63
3.4.3	Stable plant derived antibody yield determination	64
3.4.4	Subcellular localization	69
3.4.4.1	Antibody fluorescent-microscopy	69
3.4.4.2	Confocal microscopy	69
4	Discussion	71
4.1.1	Cloning of the single vector delivery system	72
4.2	Tandem vector delivery system	74
4.3	Regeneration of transgenic plants	74
4.4	Transient antibody production	76
4.4.1	Yield of transient antibody MC10E7	77
4.5	Antibody yield of Transgenic <i>N. tobacco</i> plants	77
4.6	Cloning of the Antibody-CBM expression vector	79
4.7	Binding capacity and specificity of the CBM	79
4.7.1	Analysis of the CBM properties	80
4.7.2	ELISA - CBD binding capacity	82
4.8	Subcellular localization	83
4.9	Introgression and Gene Flow	84
4.10	Outlook and further perspectives	85
5	Appendix A	86
6	Appendix B	87
7	Appendix C	88
8	List of Figures	91
9	List of Tables	93
1.	References	94

This work is dedicated to my parents
Andrea & Josef Stübler
All I have and will accomplish
are only possible due to their
love, endless support
and encouragement.

1.1 INTRODUCTION

Drinking and surface water is often contaminated with various types of pollutants. While some physical and chemical contaminations can be easily treated, biological contaminations are more difficult to address. Some toxins are problematic and can cause health risk when being present in surface water, e.g. water of bathing lakes (Morscheid, 2006). The toxin concentration is especially elevated in the dying-phase of the cyanobacteria, which coincides with the swimming season. The health risks involve irritations of skin and mucous membrane, allergic reactions and digestive disorders, and the reactions can be even more drastic if the person is affected by a mold allergy (Tiberg et al., 1995). The distribution of blue and green algae has greatly increased not only in marine water but also in inland water, and has therefore been subject of several concepts for monitoring and on site decontamination (Ibelings et al., 2016; Ibrahim et al., 2016; Moe et al., 2016).

In the production of food supplements from spirulina and chlorella algae a contamination with microcystin is problematic. The microcystin is derived from blue algae accompanying the crop algae in the opened production systems. Microcystin-LR (microcystin-leucine-arginine) is a potent hepatotoxic agent and may act as a tumor promotor in the rodent liver. There is also evidence that microcystin-LR can initiate DNA damage (Eisenbrand, 2007).

Therefore, already in 1999 the WHO recommended a drinking water guidance value for microcystin-LR of 1.9 µg/L, presuming a daily intake of 2 liters of water per person (60 kg bw). This value also accommodates the assumption that 80% of the microcystin-LR intake is via drinking water (Chorus and Bartram, 1999).

Antibodies are applicable for the detection and removal of cyanotoxins due to their high sensitivity and selectivity. The antibody MC10E7 is currently the most promising antibody for the selective binding to microcystin (Zeck et al., 2001) and has already been applied to analyze natural water and food samples (Gurbuz et al., 2016). Low cost antibodies directed against environmental pollutants have already been produced in plant expression systems (Barbi et al., 2011).

State of the art antibody production procedures utilize the *Pichia pastoris* system, which is mostly suitable for antibody fragments (fab fragments). Full size antibodies can be produced in hybridoma clones, which however are problematic for long-term production as they might become unstable over time, resulting in a clear loss of antibody productivity (COCO-MARTIN et al., 1992). Mammalian cell lines like CHO cells are highly suitable for long-term production and state of the art, but rather costly to maintain.

Up to now, these systems are not suitable for a cost-efficient large-scale production of antibodies, which would be needed in environmental remediation projects. Although the use of genetically modified plants for biopharmaceuticals, bioremediation, or the *in situ* cleaning of contaminated sites, has been known for quite some time, little attention has so far been paid to the production of antibodies in plants and their *ex vivo* application in full depletion.

1.2 THE PLANT EXPRESSION SYSTEM

Plants as sessile phototropic organisms have provided humans with beneficial substances for many centuries (Petrovska, 2012). The oldest written evidence of medicinal plants usage for preparation of drugs has been found on a Sumerian clay slab from Nagpur, approximately 5000 years old (Kelly, 2009). Some biological compounds (e.g. vinblastine, paclitaxel and colchicine) are too complex for direct chemical synthesis and must instead be produced by semi-synthesis or produced by plants (Stöger, 2013).

But only in the last decades methods have been developed to use plants for the production of defined molecules e.g. for the production of specific heterologous proteins. The first pharmaceutically relevant protein made in plants was human growth hormone, which was expressed in transgenic tobacco in 1986 (Barta et al., 1986). The structural authenticity of plant-derived recombinant proteins was later confirmed when the first recombinant antibody was successfully expressed in *Nicotiana tabacum* (HIATT et al., 1989). Further examples demonstrated that plants are suitable for the production of very complex mammalian proteins and are able to assemble full length monoclonal AB with different functional glycoproteins (Ma et al., 2015).

Since then, plenty of human derived proteins e.g. antibodies have been produced in a diverse range of crops. Plant molecular farming provides an alternative approach for the production of recombinant pharmaceutical proteins that is safer, provides economic benefit and a more flexible scalability than established systems based on mammalian cells (Peters & Stoger, 2011). Antibodies produced in plant expression systems showed comparable equilibrium and kinetic rate constants as those synthesized in Chinese hamster ovary cells (Ma et al., 2015)(Hensel et al., 2015).

It has also been shown that protein bodies and other plant storage organelles provide enhanced opportunities for the accumulation and bio encapsulation of pharmaceutical proteins (Hofbauer et al., 2014).

Their eukaryotic state of organization enables plants to process and assemble proteins correctly which is crucial for therapeutic applications (Mason et al., 1996), even though some glycosylation patterns are different, for example a lack β -1,4-galactose and sialic acid and the addition of plant-specific β -1,2-xylose and core α -1,3-fucose residues (Schahs et al., 2007).

Plants are also suitable for pharmaceutical production as they do not host any known viral human pathogens (Pogue et al., 2010). While some antibodies expressed in plants are intended to function within the plant itself e.g. to protect it against potential pathogen invasions which is achieved directly or by modulating the signaling pathway (Safarnejad et al., 2011), the following is intended to refer exclusively to the *ex situ* application. A comparison of different production systems is listed in table 1.

One very advantageous aspects of recombinant protein production in tobacco is the diversity of expression strategies, each with its own strengths. Stable chromosomal transformation is able to meet long-term demands for specific glycoproteins such as antibodies. Alternatively, chloroplast-based expression can yield large quantities of proteins that require minimal post-translational modification. When a product is required for rapid turnaround, transient

expression would be chosen to produce useful amounts of the desired protein in a very short period of time. Tobacco offers the flexibility to meet many different demands at (Tremblay et al., 2010). Relatively high levels of protein expression can be achieved within a short time with transiently transformed plants. The absolute amount of harvestable protein can be particularly high with technologies based on viral vectors like magnICON® which allows to speed up the production of recombinant proteins in plants. It is perfectly suited for the production of recombinant proteins for patient-specific immunotherapy that have to be available for application on short notice (Komarova et al., 2010). Stable transgenic plants provide other significant advantages. First of all they do not require repeated labor intensive infiltration procedures and just need to be harvested and processed, their yield is more predictable and they are able to produce larger quantities of biomass.

Table 1: Comparison of production systems for recombinant human pharmaceutical proteins, (Ma et al., 2015).

System	Overall costs	Production timescale	Scale-up capacity	Product quality	Glycosylation	Contamination risk	Storage costs
Bacteria	Low	Short	High	Low	None	Endotoxins	Moderate
Yeast	Medium	Medium	High	Medium	Incorrect	Low risk	Moderate
Mammalian cell culture	High	Long	Very Low	Very high	Correct	Viruses, prions, oncogenic DNA	Expensive
Transgenic animals	High	Very long	Low	Very high	Correct	Viruses, prions, oncogenic DNA	Expensive
Plant cell culture	Medium	Medium	Medium	High	Minor differences	Low risk	Moderate
Transgenic plants	Very low	Long	Very high	High	Minor differences	Low risk	Inexpensive

Producing immunogenic vaccines by plants can be less costly than through more conventional production systems. Several plant-derived vaccines have already completed early-phase clinical trials and many more are in the pipeline. Plants have been used extensively for the production of single chain antibodies as well a complex full size antibodies (Orzaez et al., 2009; Sack, Hofbauer, Fischer, Stoger, 2015a). Transient systems are rapid and high-yielding, stable transgenic plants are more scalable and may provide economical large-scale production (Peters & Stoger, 2011). In contrast to pharmaceuticals, non-pharmaceutical proteins have the big advantage, that they can reach the market faster due to less regulatory requirements. The plant expression platform led to uncertainties for the industry about the quality and consistency of mAbs produced in plants, which might not be as reliable as sterile cell cultures, resulting in an uncertain environment for industry (Ma et al., 2015). As a consequence, alternative applications have developed in other sectors ranging from cosmetic products to technical enzymes.

But up to now, only a handful of molecular farming products have reached the market, produced by companies in Iceland (e.g. ORF Genetics and Sif Cosmetics), Israel (e.g. Coll-Plant). However, the area has flourished in the research environment, allowing the diversity of different plant expression systems to be explored.

This has resulted in new products that have specific advantages over those produced in mammalian cells, as well as particular platforms that offer unique benefits. In terms of safety, efficacy and quality, purification procedures have been developed to meet the GMP requirements.

Many early bottlenecks in the development of molecular farming have already been overcome, yields are now more competitive and the issue of non-human glycan structures can be addressed in a variety of ways. Although high-level expression is a prerequisite for good yields, the efficient downstream procedure of recombinant proteins should be also addressed to maintain the cost advantages of plant-based production systems. Therefore the use of affinity tags to facilitate the purification of proteins is a widespread strategy, and if required the tag can be removed after purification to restore the native structure of the protein (Fischer et al., 2014). One low-cost opportunity would be the use of a CBM for the downstream purification coupled with an easy elution procedure. This method could be also applied for the whole plant application of environmental antibodies which would benefit from the same cost advantages that hold true for the PDs above.

1.3 MICROCYSTIN

Some of the ubiquitous cyanobacteria and brown algae produce a class of tumor promoting hepatotoxins (Fujiki and Suganuma, 2011; Xu et al., 2013), that can pose significant health risk to all mammals (including humans) due to their remarkable stability in the environment and their ability to enter the food chain (Dawson, 1998). It can also induce liver and lung damage (Robinson et al., 2015)

or disrupt the gene expression and DNA replication (Li et al., 2015). Especially

during algal bloom the microcystin levels are significantly elevated and the consumption of freshwater fish and seafood is a potential food chain hazard (Poste et al., 2011).

Structure of Microcystin-LR (Fig. 1): Microcystin-LR is composed of a “monocyclic heptapeptides composed of D-alanine at position 1, two variable L-amino acids at positions 2 and 4, g-linked D-glutamic acid at position 6, and 3 unusual amino acids: b-linked D-erythro-b-methylaspartic acid (MeAsp) at position 3; (2S,3S,8S,9S)-3-amino-9-methoxy-2,6,8-trimethyl-10-phenyldeca-4,6-dienoic acid (Adda) at position 5; and N-methyl dehydroalanine (MDha) at position 7.

There are over 50 different microcystins which differ primarily in the two L-amino acids at positions 2 and 4 and methylation/demethylation on MeAsp and MDha”. Laboratory experiments using low levels of microcystin-LR about 10 mg/L in static stored water, found that primary degradation occurred in less than 1 week. It was stable over 27 days in deionized water, indicating that the instability is due to biodegradation (Dawson, 1998).

The non-ribosomal synthesis of microcystin, a cyclic peptide, is performed through the activity of mainly two enzymatic systems: The non-ribosomal peptide synthase NRPS and the polyketide synthase PKS.

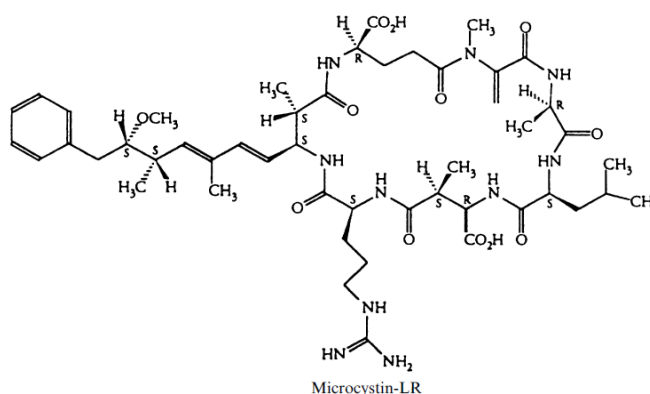


Fig. 1: Structure of Microcystin-LR (Dawson, 1998).

The detection of the microcystin-producing cyanobacteria can be performed using rapid molecular test, such as lateral flow immunoassay (dipstick). The expression of the microcystin biosynthetic genes can be quantified using real time PCR. The elimination on the other hand can happen by bacterial biodegradation, ozone treatment, photo degradation by the UV exposure or by using traditional adsorbents (El Semary, 2010).

1.4 ANTIBODIES

The production of monoclonal antibodies was first described in 1975 by Köhler and Milstein by fusing a mouse myeloma cell and a mouse spleen cell and selecting individual heterogeneous lines on hypoxanthine-aminopterin-thymidine media (HAT-media) (Plattner and Hentschel, 2006). The impact of this unique biological tool was not immediately apparent, but led to a Nobel Prize ten years later. The potential of antibodies was used in polyclonal antisera first and improved to monoclonal antibodies after decades of research and investigation. First applications were dedicated to pathological diagnosis and basic research (Weiner et al., 2009).

Monoclonal antibodies are generated by a procedure comprising multiple steps: First, an adequate protein (the antigen) is injected into an experimental animal. The immunologic reaction of this laboratory animal leads to the formation of antibodies in the B-lymphocyte cells that are derived from the spleen which is removed and utilized to initiate a cell culture. Every B- lymphocyte produces a unique antibody which is only able to detect a specific part (the epitope) of the whole antigen. This antibody possesses a unique binding capacity and needs to be selected adequately to achieve an antibody with suitable binding capacities.

Therefore the B-lymphocyte cells are transformed to immortal cells via the fusion with a myeloma cell. The successfully transformed hybrids are then selected in a HAT-media and separated into monoclonal cell lines. Although there are several classes of antibodies the most common class is the so called IgG type (γ -globulin). It consists of two identical parts, each composed of two separate molecules called heavy chain (HC) and light chain (LC) (Plattner and Hentschel, 2006).

The light chain is covalently linked to the heavy chain by the formation of disulfide bridges (Fig. 2) as well as the heavy chains among themselves to form the core structure.

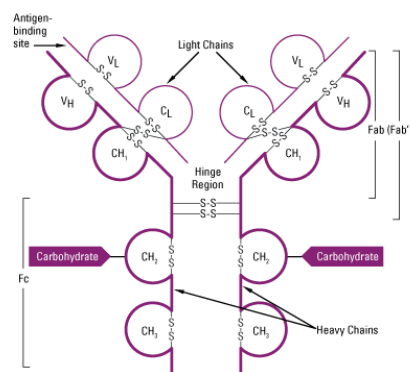


Fig. 2: Schematic drawing of an IgG antibody Thermo Fischer, 2016.

A large part of the IgG molecule is conserved and is called the constant region whereas the terminal structures of the HC and LC are variable and form the paratope. The amino acid sequence present in this region leads to the unique binding capacity to the antigen. Due to the symmetric structure of the IgG it can bind two antigen molecules in parallel. The constant region is also carrying several glycosylation sites which do not affect the antigen binding capacity but several other properties of the antibody.

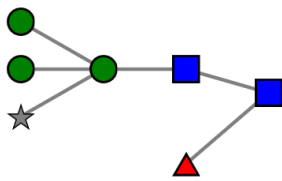


Fig. 3: N-glycosylation pattern for secreted glycoproteins, typical for plant derived glycosylation pattern are the beta(1,2)-xylose and alpha(1,3)-fucose residues.

1.5 PLANT TRANSFORMATION AND REGENERATION

Strains of the soil bacterium *A. tumefaciens* has the natural ability to genetically engineer plants with this system, the bacteria is triggered by signals of a surface wound of a plant secreting several chemical components e.g. acetosyringone. *A. tumefaciens* makes contact with the cell wall or the due to damaging directly with the plasma membrane of the plant cell. A series of steps follow, which are still not fully understood. Then a segment of the Ti-plasmid (the T-DNA) is transferred from the bacteria to the nucleus of the plant cell and becomes integrated into the chromosomal genome and subsequently the genes encoded in the T-DNA are expressed. The original Ti-plasmids have been modified for the use as gene delivery mechanism especially into dicotyledonous plants. Modifications include the removal of tumor inducing phytohormone genes as well as the genes responsible for opine metabolism from the T-DNA region and the modified T-DNA region has been cloned into a simple plasmid that can stably exist in both, *A. tumefaciens* and *Escherichia coli* strains. The gene of interest is then inserted into this T-DNA region and is transferred to the nucleus of

the recipient plant cell. To achieve this transfer *A. tumefaciens* is utilized as a delivery system. The *A. tumefaciens* strain needs to carry a compatible plasmid with genes (vir-genes) for the transfer of a T-DNA region into a plant cell. Alternatively to this binary vector system also a cointegrated vector system has been implemented, which combines the expression plasmid and the vir-gene plasmid in one single construct, which however is more difficult to handle.

Several plant expression vectors, e.g. pTRAKT-vector, equipped with genes for antibiotic resistance, selective marker, an origin of replication and a multiple cloning site, are available for performing an Agro transformation. . These cloning plasmids are much smaller than the original R-plasmids, which are less suitable for genetic engineering due to their low copy number, about 1-2 per cell, their immense size of up to 100 kbp, the handling is difficult and a natural R-plasmid would be easily transferable between bacteria and would be counterproductive for an efficient separation process of transformed and non-transformed cells (Knippers, 1997).

The techniques of plant organ, tissue and cell culture have been established in the mid of the last century in research laboratories around the globe and are still an important basis for research in plant science. Methods to propagate plants and free them from virus infections using shoot tip culture or commercial regenerations from callus cultures for a high throughput production of ornamental plants have revolutionized the availability and market value of the plant production system (Reinert and Yeoman, 1982).

All approaches are based on the totipotency of plant cells. This unique ability within the eukaryotic kingdom of pluricellular organisms describes the regenerative capacity of plant cells, including the ability of one single cell to create a whole functioning and reproductive organism being able to complete its life cycle (Feher et al., 2003).

The tobacco leaf-disc system is a well-established plant cell culture technique able to regenerate embryos, shoots, roots and complete plantlets (AN et al., 1985). It is also known, that the morphogenic capabilities of plant cells can be regulated by changes of growth regulatory substance in the nutrient media on which the tissues are cultured. The decline balance of the two main growth regulatory substances namely auxins and cytokinins determine whether roots are formed, shoots are built or mainly callus will be produced (Reinert and Yeoman, 1982).

1.6 ENHANCED TRANSIENT EXPRESSION

Plants have developed effective defense systems for artificial DNA. Which are mainly targeted against virus infections (Baulcombe, 2004). A viral counter action is the post-transcriptional gene-silencing response. However the usage of this technique has been limited to transient expression only (Siddiqui et al., 2008). Plants own two main cellular gene-silencing mechanisms, the small interfering RNA (siRNA) and the micro-RNA (miRNA)-silencing pathways which are collectively referred to as interfering RNA (RNAi) (Carthew and Sontheimer, 2009).

P19 is a multifunctional protein that is active as a dimer and found in both the cytosol and the nucleus it is capable of binding siRNA and miRNA molecules in a nonspecific fashion (Park et al., 2004; Zheng et al., 2009). reported that the expression of green fluorescent protein (GFP), is boosted approximately 50-fold when co-expressed with P19 while the expression of antibodies have only been enhanced by fivefold (Saxena et al., 2011). It was proven, that the P19 is compatible with various *Nicotiana tabacum* and *Nicotiana benthamiana* cultivars for transgenic expression as well as an intact glycan profile of a recombinant glycoprotein co-expressed with P19 but the choice of expression cassette makes a substantial difference in how well an antibody is expressed and in both transiently infected plants and stable transgenic plants (Garabagi et al., 2012).

The tomato bushy stunt virus (TBSV) p19 suppressor system of post transcriptional gene-silencing (Silhavy et al., 2002,) can be used for enhanced production of recombinant proteins. The gene-silencing machinery of plants is involved in regulating expression of endogenous gene transcripts as well as reducing or eliminating the effects of invading pathogens such as viruses (Baulcombe, 2004). As a countermeasure to the plants defense mechanism, viruses encode for proteins that serve as suppressors of gene silencing (SGS). P19 from the Tomato bushy stunt virus (TBSV) is a well-known example of proteins known to function as a potent suppressor of gene silencing in plants (Voinnet et al., 2015).

Except the already mentioned P19 silencing suppressor system, other non-viral approaches have been developed to increase and speed-up transient yields. It has recently been shown that flanking the GOI sequence with a modified 5' – leader sequence and a 3' untranslated region (UTR) from Cowpea mosaic virus (CPMV) significantly enhances the mRNA stability and thus improves expression levels. In case of an expressed full size AB it was possible to observe an improvement of +10% total soluble protein without the application of RNA virus-derived replicons (Sainsbury and Lomonossoff, 2008).

1.7 CBM AND BIO FILTERS

Cellulose binding motives (CBMs), (Fig. 5) were initially described as CBDs, based on the initial discovery of some modules that bind cellulose (O'NEILL, 1986). However more modules in carbohydrate-active enzymes that bind carbohydrates rather than cellulose are being found. These findings prompted the need to reclassify these polypeptides with more-comprehensive terminology. A CBM is defined as a contiguous amino acid sequence within a carbohydrate-active enzyme with a discrete fold having carbohydrate binding activity (Shoseyov et al., 2006). The

sequence used was a α -D-glucanase [Cellulomonas fimi] first described in, Gene 44 (2-3), 325-330 (1986).

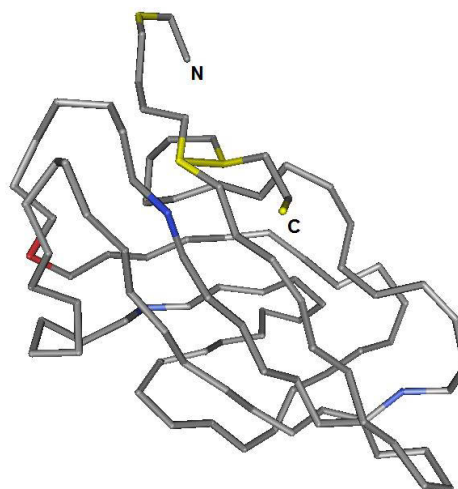


Fig. 5: α -D-glucanase derived from *Cellulomonas fimi*, showing the sulfide double bonds and the N terminal end, pointing inwards where the linker is attached.

These CBMs could be utilized to attach certain functional units e.g. AB to polymeric support films enabling the removal of toxins from water. Recently synthetic polymers were developed to remove microcystin from water. Three hydrophilic polymers were significantly effective and all the tested polymers showed more than 99.5% adsorption of microcystin-LR (MC-LR) in aqueous solution during 15 min of incubation. The physicochemical characteristics involve the maximization of the specific surface area, total pore volume and the positive zeta potential of the surface. The main structure was synthesized based on N-vinylformamide (NVF) structure cross-linked with divinylbenzene (DVB) and, after reaction with glutaraldehyde (GA) (Bialczyk et al., 2014; Tippkotter et al., 2009). Also some non-selective approaches have been developed to remove organic compounds from water which are either based on the adsorption to carbon or more selective artificial polymers derived from molecular imprinting (Le Noir et al., 2007).

The CBM was linked to the AB to facilitate the downstream which is the most expensive part of the antibody production in plants. The intention was to elute the AB-CBM conjugate at proper conditions from the bulk solution, as performed during regular extraction and to activate the CBM binding affinity by suitable environmental conditions and attach the conjugate to a cellulose matrix, which is inexpensive and available in multiple qualities. After a successful fixation to the cellulose matrix and several washing steps the binding conditions were once again changed to elute the purified AB-CBM conjugate.

2 MATERIALS AND METHODS

To deal with the diverse challenges of this project, molecular, biochemical microbiological and tissue culture techniques had to be applied.

The first stages of the project were mainly characterized by cloning, microbiological culture upscale and handling tissue culture while the later stages involved more screening related approaches like Western blot and ELISA as well as statistics for the breeding of the best lines from several candidate plants.

The C-terminal attachment of the CBM to the C-terminus of the heavy chain was carried out in parallel to the cloning of the construct containing the heavy and light chain.

1. MOLECULAR BIOLOGY PROCEDURES

2.1.1 RESTRICTION DIGEST

For the expression of fusion protein, the single polypeptides were expressed from a single cassette to ensure their simultaneous integration into the genome. The separate heterologous genes of heavy chain, light chain and DsRed (Baird et al., 2000) in a single pTRAKT vector as well as the final insertion of the CPEC assembled CBM-HC fusion into the cloning vector required different restriction digestions.

The reaction conditions such as temperature, molarity of the enzymes and buffers as well as the concentration of the substrate DNA were adapted according to manufacturer's recommendations and executed as stated below.

Table 2: Restriction digestion

Restriction digestion	
Distilled deionized H ₂ O (dd H ₂ O)	Add up to 30 µL
plasmid DNA	1-17 µL
restriction enzyme 1	1.5 µL
restriction enzyme 2	1.5 µL
10x fast digest buffer (NEB B72045)	3 µL
Total Volume 30 µL	

The reaction was kept at 37 °C for 30 min. After that the DNA was separated on a 1% agarose gel (low melting point agarose) and the appropriate band was excised on a UV screen with protection to minimize the harmful effects of the UV radiation.

The gel slice was treated further with a Gen-Jet purification Kit to obtain the linearized DNA fragment which was further analyzed with a Nano-drop 2000 to determine the concentration and purity.

2.1.2 DNA LIGATION

The T4 DNA ligase (Fig. 6) catalyzes the ATP-dependent formation of a phosphodiester bond between the 3' hydroxyl end of a double stranded DNA fragment and the 5' phosphate end of the same or another DNA fragment. Ligation of blunt ends is less efficient, the process requires higher concentrations of enzyme and DNA, a longer incubation time and a lower reaction temperature than for cohesive ends. To reduce the number of colonies containing self-ligated plasmids the fragments were treated with shrimp alkaline phosphatase (SAP) to remove the 5' phosphate groups from each strand of the vector molecule, preventing T4 DNA ligase from forming phosphodiester bonds between the two ends.

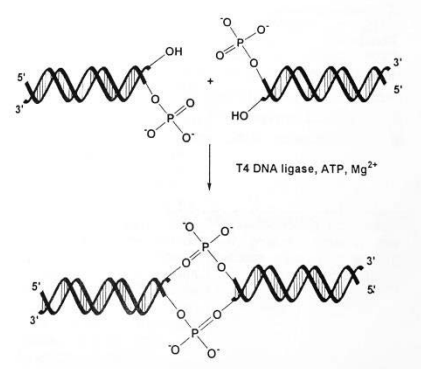


Fig. 6: T4 Ligase catalyzed ATP dependent phosphodiester bond formation (Hardin, 2001).

Ligation was performed using T4 DNA ligase (NEB, #M0202S) and quick DNA ligase buffer 5x (NEB, #B0202S). The minimum amount of Vector DNA was determined with 150 ng per 20 μ L reaction volume, according to the nucleotide concentration this would lead to a Volume of 1-2 μ L.

$$V_{vector} = \frac{150 \text{ ng}}{c_{vector}}$$

The insert was mixed with the opened vector in a molar ratio of 3:1.

$$k = \frac{L_{vector} (bp)}{L_{insert} (bp) \times 3}$$

Depending on the nucleotide concentration this would lead to a specific amount of insert.

$$m_{insert} = \frac{m_{vector}}{k}$$

According to the nucleotide concentration of the insert, this would lead to a Volume of 1-9 μ L, depending on the concentration.

$$V_{insert} = \frac{m_{insert}}{c_{insert}}$$

Table 3: Quick ligation reaction

Quick ligation reaction	
double distilled H ₂ O (or other Type I (mqH ₂ O)	1 µL
Vector linear DNA	2 µL
Insert linear DNA	6 µL
T4 DNA Ligase (TS #EL0011)	1 µL
2x Quick Ligase Buffer (NEB B2200S)	10 µL
Total Volume 20 µL	

The reaction was set to 25 °C for exactly 15 min and further used for a heat shock transformation of ultra-competent *E. coli*. See protocol *E. coli* transformation.

2.1.3 POLYMERASE CHAIN REACTION

The colony screening during cloning as well as the CPEC-assembly of the CBM domain were executed utilizing a PCR (Polymerase Chain Reaction). All primers for the assembly and screening were designed exclusively for this approach and ordered at Sigma – Aldrich.

The polymerase chain reaction is an enzymatic process which is employed to amplify specific sequences of DNA or RNA. A PCR consists of three stepwise operations which are performed sequentially. First DNA denaturation, in the second step the primer annealing takes place and finally the primer extension and amplification of the template. The whole procedure is performed by varying the temperature and repetition of this steps 20-30 times.

The first reaction step involves denaturation of the template DNA at 95°C. This is performed with a molar excess of the primers, dNTPs and Mg²⁺. The temperature is then lowered to the optimum annealing temperature which is typically no more than 5 °C below the T_m of the primers. Ranging from 55 °C to 59 °C, primers are now annealing to their complimentary target sequence. Now the temperature is raised to 72 °C which is the optimum operation temperature of the *Taq* DNA Polymerase that can survive extended incubation at 95 °C, which is now extending the primers from the 3' end complimenting the guiding strand till it reaches the location of the second primer. The initial quantity of template DNA necessary for PCR ranges typically from 0.05 – 1 µg of single copy genomic target (Hardin, 2001).

For the *E.coli* colony screen a *Taq*-Polymerase was used because no proof reading ability was required. Therefore a small amount of the colony, about 1 µL was dissolved in the PCR mix and then denatured with a 5 minute heating period at 95 °C. The composition of the PCR mix for one reaction containing 20 µL total volume was as follows.

Table 4: Colony touch down mix

Colony touch down	
distilled H ₂ O	14 µL
green Go-Taq buffer 10x	2 µL
dNTPs (2mM)	2 µL
primer forward (10 µM)	0.4 µL
primer reverse (10 µM)	0.4 µL
Go-Taq polymerase	0.2 µL
DNA template	1 µL
Total Volume 20 µL	

The following thermocycler program was used and the temperatures Ta (annealing temperature) and Tm (melting temperature) were adapted according to the used primers. Calculations for annealing temperatures were performed with the Thermo-Scientific Tm calculator. The temperature was then adopted to $T1 = Tm - 5\text{ }^{\circ}\text{C}$

Table 5: General temperature profile for thermocycler

1	Initial denaturation	95 °C	5 min
2	Annealing of primers	Tm	35 s
3	Amplification	72 °C	80 s
4	Go to line 1		4 x
5	Denaturation	95 °C	30 s
6	Annealing of primers	T1	35 s
7	Amplification	72 °C	80 s
8	Go to line 4		25 x
9	Final extension	72 °C	5 min
10	On hold	4 °C	∞

2.1.4 PCR-BASED CLONING

The PCR-based cloning (Fig. 7) facilitates the fusion of sequences without adequate restriction sites; it was therefore used to combine a pTrAkt expression vector and a pTRAKc expression vector one containing the humanized heavy chain and the other containing the CBM.

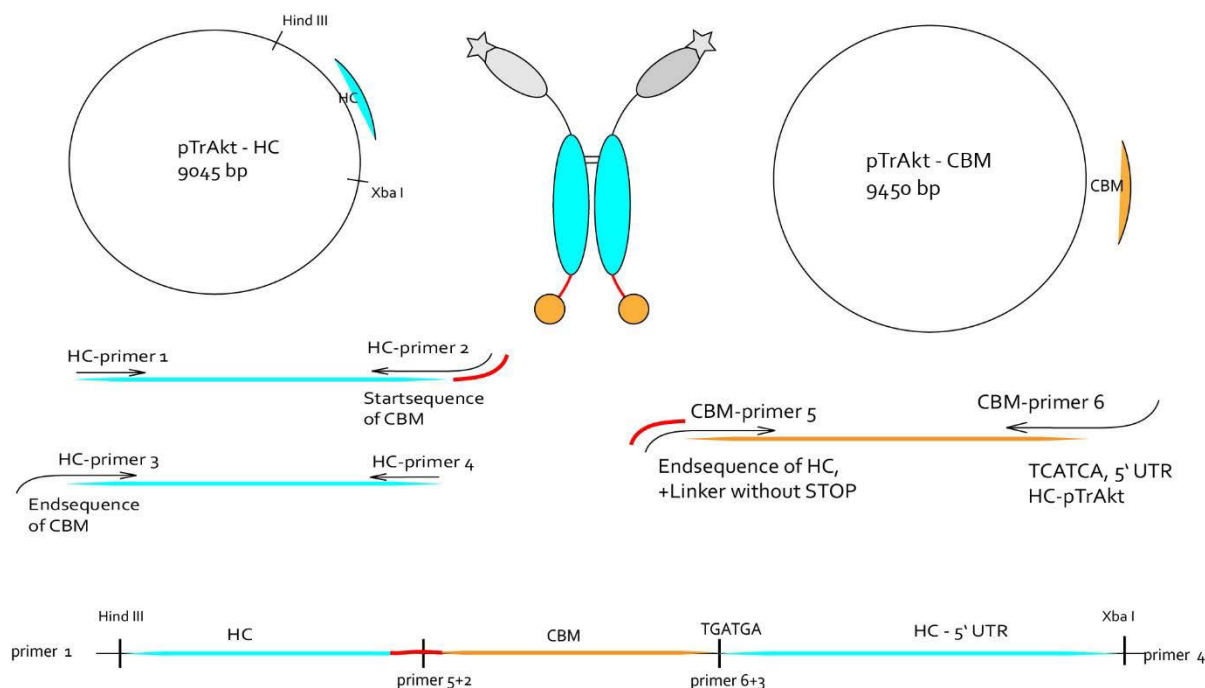


Fig. 7: Graphical illustration of the PCR-based cloning for the CBM attachment to the HC, shown in three different excise reactions and one final assembly reaction.

Initially the two specific sequences of the cloning vectors need to be reproduced in reaction one to four. Therefore the first two reactions are prepared and run by the same thermocycler program. The final assembled linear construct was carrying two distinct restriction sites at both ends, which were used to insert it in the correct orientation into the pTRAKc vector.

Reaction 1:

Reaction one amplifies from pTRAKt-HHC-MC, to achieve the C-terminal end of the HHC and complementary parts of the CBM domain on the primers achieving a linear fragment of 525bp.

Table 6: Excise reaction one

525 bp	Tm [°C]	Primer sequence
HHC882_F	full: 60.6	CAACTGGTACGTGGATGG
HHC_CB2_R	partial: 56.1 full: 68.9	GTAGGACCCTTTCCAGGAGAAAGAGAC

Construct:

CAACTGGTACGTGGATGGTGTGAGGTTTACAACGCTAAGACTAAGCCAAGGGAAGAGCA
GTACAACTCTACTTACAGGGTGGTGTCTGTGCTTACTGTTCTTCACCAGGATTGGCTTAA
CGGAAAAGAGTACAAGTGCAAGGTATCAAACAAGGCTCTTCCAGCTCCAATTGAAAAGAC
TATTTCTAAGGCTAAGGGACAACCTAGAGAGCCACAGGTTTACACTCTTCCACCATCTAG
GGATGAGCTTACTAAGAACCAGGTGTCACCTTACTTGCTTGGTGAAGGGATTCTACCCATC
TGATATTGCTGTTGAGTGGGAGTCTAATGGACAACCAGAGAACAACCTACAAGACTACTCC
ACCAAGTGCTTGATTCTGATGGATCTTTCTTCTTTACTCTAAGCTTACTGTGGATAAGTC
TAGGTGGCAGCAGGGAAATGTTTTCTCTTGCTCTGTGATGCATGAGGCTCTTCACAATCA
CTACACTCAGAAGTCTTTGTCTCTTTCTCTGGAAGGGTCTAC

Table 7: Master-mix, excitation reaction

Mastermix reaction 1	
distilled H ₂ O	30 µL
HF buffer 5x	10 µL
dNTPs (2mM)	5 µL
primer_F (10µM)	2.5 µL
primer_R(10µM)	2.5 µL
Phusion HotSt II Pol.(2U/µL)	0.5 µL
DNA template, pTRAkt-HHC-MC (10ng/µL)	1 µL
Total Volume 51.5 µL	

Reaction 2:

Reaction two amplifies from pTRAkt-HHC-MC, to achieve the C-terminal end of the HHC and complementary sequences of the CBM domain on the primers achieving a linear fragment of 289bp. The low Ta for the first few cycles results from the relatively shorter part of the initial complementary primer sequence than the total primer length

Table 8: Excise reaction two

289 bp	Tm [°C]	Primer sequence
TRA-CBM2_F	partial: 55.6 full: 64.1	CTGTTGGATGATGATCTAGAGATATCAC
TRA-HHC1629_R	full: 59.7	GAGTCGCAAATATTTCTAGGG

construct:

GCTCCTTGCACTGTTGGATGATGATCTAGAGATATCACTAGAGTCCGCAAAAATCACCAG
TCTCTCTCTACAAATCTATCTCTCTATTTTTCTCCAGAATAATGTGTGAGTAGTCCC
AGATAAGGGAATTAGGGTTCTTATAGGGTTTCGCTCATGTGTTGAGCATATAAGAAACCC
TTAGTATGTATTTGTATTTGTAAAATACTTCTATCAATAAAATTTCTAATTCCTAAACC
AAAATCCAGTGACCGGGCGGCCGCGCCGCTAGAAATATTTGCGACTC

Table 9: Thermocycler program for reaction 1 and 2

1	Initial denaturation	98 °C	1 min
2	Cycle denaturation	98 °C	20 s
3	Annealing of Primers	55 °C	30 s
4	Amplification	72 °C	30 s
5	Go to line 2	4 x	
6	denaturation	98 °C	20 s
7	Annealing of Primers	64 °C	30 s
8	Amplification	72 °C	30 s
9	Go to line 5	25 x	
10	Final extension	72 °C	5 min
11	On hold	4 °C	∞

Reaction 3:

In reaction three, the amplification from pTRAc-CBM was performed, to achieve the excised CBM domain from the initial vector, achieving a linear fragment of 408 bp.

Table 10: Excise reaction three

408 bp	Tm [°C]	Primer sequence
CBM2-HHC_F	partial: 63.7 full: 76.4	CCTGGAAAGGGTCCTACACCTACGCCAAC
CBM2-TRA_R	partial: 63.3 full: 74.0	CTCTAGATCATCATCCAACAGTGCAAGGAGC

Construct:

CCTGGAAAGGGTCCTACACCTACGCCAACACGCCCACACCAACCCCAACTACACCCACA
 CCAACCCCGACAAGCGGCCAGCAGGATGTCAGGTATTATGGGGGTCAACCAGTGGAAT
 ACAGGTTTTACAGCCCAAGTCACTGTTAAGAACACAGGTTCCGGCACCTGTTGATGGGTGG
 ACCCTTACCTTTTCATTCCCATCAGGCCAGCAAGTAACACAAGCGTGGAGTTCAACTGTG
 ACTCAATCTGGATCTGCAGTGACTGTTAGAAATGCCCGTGGAATGGAAATATTCCTGCT
 GCGGTTACTGCTCAATTCGGTTTCCAAGGTTCCCATACTGGAATAATGCTGCTCCTACT
 GCTTTTTTCCTTGAACGGTGCTCCTTGCACTGTTGGATGATGATCTGAG

Final reaction:

The four excised segments are then assembled in a final reaction to achieve the final construct. Primers for C-terminal fusion to HC of MC10E7H:

Table 11. final assembly reaction

	Tm [°C]	Primer sequence
CBM2-HHC_F	partial: 63.7 full: 76.4	CCTGGAAAGGGTCTACACCTACGCCAAC 63.7°C
CBM2-TRA_R	partial: 63.3 full: 74.0	CTCTAGATCATCATCCAACAGTGCAAGGAGC

Final construct:

CAACTGGTACGTGGATGGTGTGAGGTTCAACAACGCTAAGACTAAGCCAAGGGAAGAGCA
GTACAACTCTACTTACAGGGTGGTGTCTGTGCTTACTGTTCTTCACCAGGATTGGCTTAA
CGGAAAAGAGTACAAGTGCAAGGTATCAACAAGGCTCTTCCAGCTCCAATTGAAAAGAC
TATTTCTAAGGCTAAGGGACAACCTAGAGAGCCACAGGTTTACACTCTTCCACCATCTAG
GGATGAGCTTACTAAGAACCAGGTGTCACCTTACTTGCTTGGTGAAGGGATTCTACCCATC
TGATATTGCTGTTGAGTGGGAGTCTAATGGACAACCAGAGAACAACCTACAAGACTACTCC
ACCAGTGCTTGATTCTGATGGATCTTTCTTCTTTACTCTAAGCTTACTGTGGATAAGTC
TAGGTGGCAGCAGGGAAATGTTTTCTTCTGCTCTGTGATGCATGAGGCTCTTCACAATCA
CTACACTCAGAAGTCTTTGTCTCTTTCTCCTGGAAAGTGATGATCTAGAGATATCACTAG
AGTCCGCAAAAATCACCAGTCTCTCTCTACAAATCTATCTCTCTATTTTTCTCCAGAA
TAATGTGTGAGTAGTTCCAGATAAGGGAATTAGGGTTCTTATAGGGTTTCGCTCATGTG
TTGAGCATATAAGAAACCCTTAGTATGTATTTGTATTTGTAAAATACTTCTATCAATAAA
ATTTCTAATTCCTAAACCAAAATCCAGTGACCGGGCGGCCGGCCGCCCTAGAAATATT
TGCGACTC

Restriction site enzyme 1

Restriction site enzyme 2

2.1.5 DNA ELECTROPHORESIS AND PURIFICATION

Separation of DNA as well as confirmation of the correct fragment size were undertaken with agarose gel electrophoresis at 50 V utilizing a 1% low melting agarose gel in TAE (Tris, Acetate, EDTA) buffer.

Table 12: Low melting point agarose mix for 1% separation.

Agarose	0.5 g
1x TAE buffer	50 ml
Ethidium bromide 0.5 %	2.5 µL

After mixing agarose and TAE buffer the temperature was raised to boiling point in a microwave. Once the agarose was fully dissolved the solution was cooled down to 70 °C and the EtBr was carefully added under constant shaking.

The detection of DNA is possible due to the interaction of the ethidium bromide and the nucleic acids. The molecular structure of ethidium bromide enables the local base pairing of the dye and the nucleic acid, in our case usually double stranded DNA molecules, which was

shown by (Sharp et al., 1973). The interaction of ethidium bromide and their intercalating compounds follows the “nearest neighbour exclusion principle” because of the geometric structure of the oligo peptide. A Gel-Doc XR from Sigma was used for visualization, while for preparative gels in the cloning procedure a conversion screen (XcitaBlue™) was used in addition. It converts UV to blue light, which is not ideal to excite EtBr but prevents UV damage of the DNA sample. In aqueous solution the λ_{max} = 480 nm (water) is red shifted to longer wavelengths upon binding to nucleic acid.. The electrophoresis mobility of linear double-stranded DNA is reduced by approximately 15% in the presence of the ethidium bromide. Quantitation was performed by estimation of ethidium bromide fluorescence which absorbs ultraviolet light at 360 nm and emits it at 590 nm in PBS. The fluorescent signal of bound ethidium bromide molecule is much greater than that of unbound molecules. Therefore the bromide–DNA complex shines much brighter than the unbound ethidium bromide in the surrounding gel (Hardin, 2001).

After excising of the desired band with a scalpel from the low melting point agarose, which melts already at 65 °C usually well below the melting point of most duplex DNA(Hardin, 2001) the sample was weighed and placed in a 2 mL tube for further treatment.

Binding buffer was added to the tube in a gravimetric 1:1 ratio and placed at 65 °C for 10min. After that the DNA was extracted with a NucleoSpin® gel and PCR clean-up kit according to manufacturer’s recommendations, except the elution procedure after the washing and drying step the NucleoSpin® column was placed in a 1.5 mL micro centrifuge tube and the plasmid DNA was eluted in a two-step elution. 20 µL of elution buffer were applied to the center of the column, incubated for five minutes at 65 °C and centrifuged for one minute at 13 kg.

The quantification of the DNA concentration was performed using Nanodrop® and spectrophotometric reading (Nanodrop® 2000) at 260/280nm which gives an estimation of the quantity from the exposure at 260nm and an indication of quality when comparing the excitation at 260 and 280nm.

2.1.6 TRANSFORMATION OF CHEMICALLY COMPETENT *E. COLI*

The transformation process was carried out immediately after the ligation process and carried out with the competent *E. coli* strain DH10β.

A cryo-stock was thawed on ice for about 30min, and 3 µL of ligation reaction was gently mixed with the *E. coli* and incubated on ice for further 30 minutes. In the meanwhile the water bath was set to 42 °C.

The tube was placed into the bath for exactly 30 seconds and afterwards placed on ice for 2 - 5 minutes to reduce stress. After that 250 µL of SOC media was added under sterile conditions and incubated for about 1h at 37 °C with constant shaking at 180 rpm.

The culture mix was spread on two LB-Agar plates containing Carbenicillin. The first plate was inoculated with 80% of the volume and the second plate with 20% to obtain plates with an optimum colony density.

After 24 h a master plate was patched to keep track of the different colonies and have more biomass for screening.

2.1.7 TRANSFORMATION OF CHEMICALLY COMPETENT *A. TUMEFACIENS*

Competent *A. tumefaciens*, strain GV3101:pMP90RK was used for all infiltration procedures. To initiate transformation the cryostock was thawed on ice. Subsequently 1 µg, about 0.5-5 µL depending on the concentration of plasmid DNA, was gently mixed with the cryo-stock. In the meanwhile the water bath was set to 37 °C.

The tube was then fully submerged in liquid nitrogen for about 5min and then quickly placed in the water bath for 5 min, then chilled on ice for 3 min. Under a laminar flow 1 mL of pre-warmed YEB media was added and then incubated static for about 2h in the dark at 28 °C.

The reaction mix was spread on two YEB-Agar plates containing Rifampicin (20 mg/L), Kanamycin (50 mg/L) and Carbenicillin (100 mg/L). The first plate was inoculated with 80% of the volume and the second plate with 20% to have some plates with an optimum colony density.

After three days a master plate was started to facilitate the separation of monoclonal colonies (Matsuhara, 2000).

2.1.8 PREPARATION OF CHEMICALLY COMPETENT *A. TUMEFACIENS*

A. tumefaciens was cultured for 24 h in 3 mL of YEB medium and antibiotics. This starter culture was now used to inoculate a 50 mL flask containing the same medium and antibiotics.

The OD- value was regularly checked till it reached 0.4 and spun down at 4 °C. The pellet was then washed with 20mM CaCl₂ precooled at 4 °C and afterwards resuspended in 1ml CaCl₂.

Aliquots of 100 µL are transferred into sterile 1 mL micro centrifugation tubes and snap frozen in liquid nitrogen and stored at -80 °C till needed.

2.1.9 GENERATION OF MASTER PLATES

After the transformation process and colony separation, the monoclonal colonies were patched onto new plates to increase the inoculum and have sufficient material for the screening with a cracking buffer as well as the starting of liquid cultures.

Usually 16 to 24 colonies were transferred on a new plate each of them spread on a 1 cm² square and incubated overnight.

2.1.10 PLASMID EXTRACTION

Plasmid extraction from over-night cultures of *E. coli* ranging from 2 to 5 mL were purified utilizing a QIAprep® Miniprep Kit. This method follows a procedure, where the bacterial cultures are lysed and then cleared by centrifugation, followed by a binding, washing and elution step.

The cleared lysates are applied to the QIAprep column where plasmid DNA adsorbs to the silica membrane where it stays during several washing cycles and can be eluted with a low salt buffer in small volumes.

The bacterial overnight culture was centrifuged first at 6800 x g for 3 min at ambient temperature to obtain a pellet. The supernatant was discarded and the pellet was resuspended in 250 µL of P1 buffer and transferred to a tube.

In the next step, 350 µL of P2 buffer was added and mixed immediately by inverting until the solution becomes clear, this step should never be extended above 5 minutes.

Then 350 µL buffer N3 was added and mixed again by inverting the tube and afterwards centrifuged for 10 min at 13000 x g in a table-top centrifuge. The supernatant from the last step was applied to the QIAprep spin column by decanting and centrifuged for one minute. The flow-through was discarded. The QIAprep spin column was washed by adding 70 µL PE buffer. The column was centrifuged for one minute and the flow-through was discarded. To ensure that all washing buffer was discarded, the column was centrifuged again for one minute.

After the washing step the column was placed in a new 1.5 mL tube. To elute the plasmid DNA, a two-step elution was used applying two times 20 µL of elution buffer to the center of the column, incubating each time for five minutes at 65 °C and centrifuged for one minute at 13000 x g (Zhang and Cahalan, 2007).

2.1.11 ISOLATION OF GENOMIC PLANT DNA USING A NUCLEO SPIN[®]

Extraction of genomic DNA from plant material was performed with a Nucleo Spin[®] plant II kit (Macherey-Nagel GmbH). Plant tissue was homogenized to allow the most effective lysis procedure. The amount of fresh weight leaf material was adjusted to 100mg. The method used was manual grinding with a pestle within a micro-centrifuge-tube in the presence of liquid nitrogen. Precooled plant material was powdered under constant supply of liquid nitrogen, all equipment was precooled.

After homogenization the powder was treated with 10 µL RNase and buffer PL1, containing chaotropic salts, and vortexed thoroughly. This crude lysate was incubated for 30 min at 65 °C in the oven. The lysate was then cleared by centrifugation for 10 min at 11000 x g and the supernatant transferred to a new tube. To the clear lysate 400 µL of PC binding buffer was added and vortexed thoroughly.

The mixture was subsequently decanted to a Nucleo-Spin-column where the cap was removed, which was placed in a new 2 mL collection tube and centrifuged for 1 min at 11 kg, and the flow-through was discarded.

Followed by three washing steps, first 400 µL of PW1 buffer were applied and centrifuged for 1 min at 11000 x g, then 400 µL of PW2 buffer were applied and centrifuged for 1 min at 11 kg, this last step was repeated two times followed by 1 min dry spin

The elution procedure was optimized and was most efficient when using 2x 30 µL elution buffer at elevated temperatures (65 °C) for 5 minutes and followed by 3 min centrifugation at maximum speed.

2.1.12 PLANT GENOMIC DNA ISOLATION BY THE CTAB METHOD

To obtain PCR-grade genomic plant DNA for screening purposes, about 2 g of leaf material were harvested and placed on ice. Afterwards, 200 µl of extraction buffer were added to the sample and homogenized manually in a 1.5 ml tube using a plastic pestle.

The samples were vortexed for 10 sec and incubated at 65 °C for 5 min. Then 200 µl of Chloroform were added and incubated at ambient temperature, and subsequently vortexed for 30 sec. After that the sample was centrifuged for 5 min at 13000 x g at ambient temperature. The supernatant was transferred to a sterile 2 mL tube and filled up with 2.5 volumes of 96% ethanol and mixed by inversion.

Genomic DNA was precipitated at -20 °C for one hour and pelleted by centrifugation at 4 °C at 13000 x g for 20 min. The pellet was washed with 500 µl of 70 % ethanol (stored at -20 °C) and after air-drying at 37 °C it was dissolved in 40 µl of elution buffer for 30 min at 37 °C under gentle shaking.

Table 13: Extraction buffer for CTAB genomic DNA precipitation.

Extraction buffer	
Hexadecylammoniumbromide (CTAB)	2 % (w/v)
NaCl	1.4 M
Tris	100 mM
EDTA pH 8.0	20 mM
Polyvinylpyrrolidon sterile	1 % (w/v)
Total Volume 100 mL	

2.1.13 COLONY CRACKING SCREEN

This method allows a fast screening to check for the presence and relative size of a plasmid in *E. coli* colonies. In this procedure the bacterial cultures are lysed via cracking buffer and then cleared by centrifugation. The supernatant was loaded on an agarose gel (1% w/w) and the presence of the desired plasmid of the right size was detected.

Table 14: The cracking buffer (Sambrook & Russel, 2001).

NaOH (50 mM)	50 µg
SDS (0.5%)	5 µL
EDTA (5 mM)	5 µg
distilled H ₂ O	1 mL
Bromophenol blue	7 µL

Micro centrifugation tubes 1.5 mL were filled with 50 µL of cracking buffer as well as one tip of overnight culture from the master plate. The denaturation and lysis of the cells was carried out in a heating block (50 °C) for 5 minutes and then chilled on ice for 5 min. Finally the tubes were centrifuged at 9000 x g for 10 minutes and the supernatant was loaded on the agarose gel.

2.1.14 SEQUENCING AND STORING OF DNA

The sequencing was outsourced to MICROSYNTH for overnight sequencing.

After the QIAprep Spin Miniprep Kit plasmid extraction the premixed samples, containing 1200 µg of sample DNA and 3 µL of one of the sequencing primers (10 µM) and filled up with distilled H₂O to 15 µL of total reaction mix.

Typical Sanger-based sequencing method rarely exceeds the read length of 1000 bp, thus to guarantee accuracy a double sequencing approach was chosen, consisting of two premixed reaction mixes each having either a forward or a reverse primer flanking the sequence on both sides.

Storage of Nucleic Acid, DNA is generally very stable and can be stored either desiccated (dry) or in solution (frozen) however environmental DNases can destroy DNA, therefore DNA was dissolved in a solution containing EDTA which chelates all present Mg²⁺ and helped to preserve the sample (Hardin, 2001).

2.1.15 PRIMER DESIGN

Most screening primers were designed with NCBI primer Blast and adapted manually. The final amplicon for an analytical detection on an agarose gel should be about 300-1000 bp. All primers were checked against the whole *Nicotiana tabacum* genome to avoid possible annealing sites and guarantee a functional and specific 3' end. To perform double screens, primers with similar (only 1 °C difference) melting temperatures but different amplicon sizes (fold two difference) were chosen.

The primers for the CPEC-assembly were designed manually and blasted against the whole *Nicotiana tabacum* genome to detect similarities. The primer conditions were optimized to reach a base pair size of 18-30, mainly primers with 20 bp were chosen. At the 3' end a single G/C-clamp was desired as well as a G/C-content of 40% - 70% in the whole oligonucleotide. The melting temperature should be higher than 55 °C and lower than 72 °C. Further information on the primers used in this work is provided in Appendix B.

2.1.16 CRYOPRESERVATION

To preserve *E. coli* and *A. tumefaciens strains*, 850 µl of overnight culture in LB-medium were transferred into a pre autoclaved 1.5 ml tubes filled with 150 µl of Glycerol. Then the stock was snap-frozen with liquid nitrogen and stored at -80 °C. For the resumption of the cryo-stocks a container was taken on ice till thawed and the content scraped off with a sterile inoculation needle and streaked over a plate.

2.1.17 PREPARING OF ACRYLAMIDE SDS GELS

For a quick preparation of SDS-gels, prepared stock solutions were used and stored at 4 °C.

Table 15: Resolving gel 12%, Concentration for 50 mL

Acrylamide stock 40%	15 mL
Tris-HCl 1.5M pH 8.8	12.5 mL
SDS 10%	500 µL
Adjust to 50 mL with distilled H ₂ O	

Table 16: Stacking gel 4%, Concentration for 50 mL

Acrylamide stock 40%	5 mL
Tris-HCl 0,5M pH 6.8	12.5 mL
SDS 10%	500 µL
Adjust to 50 mL with distilled H ₂ O	

Table 17: Polymerization initiators for stacking and resolution gel

Resolving gel 12%	Stacking gel 4%
5 mL of resolution stock	2 mL of stacking stock
25 µL of APS	10 µL of APS
2.5 µL of TEMED	2 µL of TEMED

The front plate together with a spacer plate (1 mm) were put in a casting frame at a casting stand. The plates are aligned to prevent leakage when pouring the gels. The premixed stock was pipetted in a 15 mL falcon tube then the TEMED and APS were added. The gel was poured up to 1.5 cm under the edge of the shorter plate. The surface was covered with 1 mL of 70% Ethanol in order to get a plane interface between the separating and the stacking gel. Gels were left for sufficient polymerization for 30 minutes.

2.1.18 SDS PAGE

The probes were treated with 4x Laemmli buffer (62.5 mM Tris-HCl, pH 6.8, 10% glycerol, 1% LDS, 0.005% Bromophenol Blue) and boiled for 5 min at 98°C to denature and reduce the antibody and achieve separate bands for heavy and light chain. The gel was then placed in a Bio-Rad Mini-PROTEAN Tetra Cell and filled up with 180 mL of TGS (Tris, Glycine, and SDS) running buffer. The Page Ruler+, #26616 Thermo-Scientific was consistently placed to the left to avoid symmetrical gels and the positive probe right next to it. The gel was run at the following program: Initiation at 50V for 10 min, 100V for 15 min, 150V for 15 min and finally 200V for 30-40 min,

2.1.19 WESTERN BLOTTING

The SDS gel was washed and carefully cleared from stacking gel and equilibrated in the transfer buffer solution for 5 min.

Table 18: Transfer buffer

Transfer buffer	200 mL	concentration
Trizma Base (Sigma)	1.16 g	59.9 mM
Glycine (Roth)	0.58 g	48.3 mM
Methanol (Sigma)	40 mL	20 % (v/v)
distilled H ₂ O	160 mL	

Proteins were transferred onto a nitrocellulose blotting membrane (GE Healthcare #10600020) in the Bio-Rad Trans-blot SD semi-dry transfer cell for 40 min at 15 V. Afterwards the membrane was blocked for 30 min with 3% BSA solution in TBST to prevent unspecific binding of omnipresent protein to the nitrocellulose membrane. Followed by an incubation step with the secondary antibody (Sigma #A8775), in a 1:5000 dilution in TBST for 60 min. Completed by three washing steps with TBS of 10 min each.

Table 19: Tris-Buffered Saline (TBS; 10×, pH 7.5) COLD SPRING HARBOUR (2014)

Reagent	Amount for 1× solution	Final conc. (1×)	Amount for 10× stock)	Final conc. (10×)
NaCl	8.7 g	150 mM	87.7 g	1.5 M
Tris base	2.4 g	20 mM	24.2 g	200 mM
Adjust to 1 liter with distilled H ₂ O and sterilize by autoclaving				
TBST = TBS + 0.1% Tween 20				

The membrane was then blocked with a 3% BSA in TBST for 30 min at ambient temperature under constant shaking.

Table 20: Blocking buffer

TBST	10 mL	
BSA fraction V	0.3 g	3%

In the next step the membrane was incubated for 60 min at ambient temperature with primary antibody. Therefore 2 µL of antibody (Sigma #A8775) were diluted in blocking buffer

After three washing steps with 10 mL TBST for 10 min, the final washing step was performed with 10 mL TBS to get rid of Tween 20.

Table 21: Developing solution BCIP/NBT

BCIP/NBT solution	Final concentration
BCIP (5-bromo-4-chloro-3-indolyl-phosphate) Prepare 50 mg/mL stock in 70% DMF (dimethylformamide).	0.175 g/L
NBT (4-nitro blue tetrazolium chloride) Prepare 50 mg/mL stock in 70% DMF.	0.225 g/L
NBT (Nitro blue tetrazolium)	0.5 % (v/v)
Adjust to pH 9.5 by adding DEA buffer (recepty not provided) and bring to 1 liter with distilled H ₂ O	

After washing the blot was incubated with BCIP/NBT substrate in corresponding buffer (10 mL) at ambient temperature for 1 min up to 30 min. Here NBT serves as the oxidant and BCIP is the chromogenic AP-substrate. The developed blot was then flushed with distilled H₂O and scanned with a flatbed scanner.

2.1.20 ELISA

2.1.20.1 COATING OF PLATES:

Coating antibody goat anti-human IgG (no conjugate) (Sigma 13382) ($1\frac{mg}{mL}$), was diluted 1:5000 in carbonate-coating buffer. All inner wells of a 96 well-plate were filled with 250 µL, sealed with a tape and incubated at 4 °C overnight.

Table 22: Dicarboxate Coatingbuffer, pH9.6

Dicarboxate Coating-buffer, pH 9.6	Quantity (for 100 mL)	Final concentration
Na ₂ CO ₃	15.9 mg	0.159 mg/mL
NaHCO ₃	29.3 mg	0.293 mg/mL
NaN ₃ optional for conservation	0.02 g	
Adjust to 1 liter with distilled H ₂ O		

2.1.20.2 BLOCKING AND WASHING:

Subsequently the wells are blocked with 350 µL of blocking buffer (1% BSA in TBS 1x), for 1 hour to avoid all unspecific binding sites and washed manually by completely removing the blocking solution and applying 350 µL of TBST in two steps, repeating the whole procedure for three times.

2.1.20.3 SAMPLE PREPARATION AND APPLICATION TO THE PLATE:

Crude extract samples for high throughput screening were prepared by collecting 100mg of leaf material and adding 100 µL of TBS before manual homogenization. The samples were then centrifuged for 10 min at 20 kg and 150 µL of supernatant were transferred into a 1.5 mL tube and filled up to 1.5 mL to achieve an initial 1:10 dilution used for further dilution steps.

Dilutions of each crude extract sample were done using blocking buffer and 200 μL of each sample. Blanks were added to the corresponding wells and were incubated at ambient temperature for one hour.

2.1.20.4 INCUBATION WITH THE SECONDARY ANTIBODY

Two hundred microliters of the secondary antibody-anti-human conjugate, Sigma #A8775 at 1:5000 in TBST-BSA buffer were added to each well. The plate was incubated at ambient temperature for one hour followed by a washing procedure as described above.

2.1.20.5 COLOR REACTION AND ANALYSIS

For the color reaction NPP (p-NitroPhenyl Phosphate) was used in Diethanolamine (DEA)-Buffer. The development was stopped after an optimal coloration was visible by adding 50 μL of 3 M NaOH solution to raise the pH above 9 for an effective inhibition of the enzyme and better fluorescence.

The plates were then analyzed as described above at a photometer at 405 nm, the absorption maximum of p-Nitrophenolate anion.

Table 23: DEA-buffer

DEA buffer 1M	Final concentration
Diethanolamine	140 mg/mL
Magnesium Chloride	0.5 mg/mL
Adjust to pH 9.8 by HCl and fill up to 1 liter with distilled H ₂ O	

2.1.20.6 MATERIAL PREPARATION FOR CELLULOSE AND PROTEIN-A COMPARISON

The sepharose extraction and the protein-A extraction were performed in parallel to obtain comparable results. The starting material was in both cases the washed primary pellet (1g) diluted in 5 mL of PBS pH 7.4 and incubated for 1h at 5 °C at 200 rpm. After that all cell debris was removed by centrifugation at 9000 x g for 20 min at 4 °C. The pH of the supernatant was then adjusted to pH 8.0 followed by another centrifugation step and filtration through a 1 μm polypropylene filter. To every sample 150 μL of either sepharose or protein-A was added and incubated for 3 h at 5°C at 200 rpm.

2.1.21 FIXATION AND EMBEDDING OF SAMPLES

The leaf samples were pre-treated for microscopy in a way to retain an intact structure. First the leaf samples were cut on wax paper with a razor blade in squares of about 1 x 2 mm and immediately submerged in fixative for overnight fixation at 4 °C in a 2 mL tube:

Table 24: Fixation solution for sample embedding

Fixative for LRW 1 mL	Volume
Paraformaldehyde 10%	400 μL
Glutaraldehyde in PB 50%	10 μL
Phosphate buffer 0.1 M pH 7.4	590 μL

Next day the samples were placed on ice together with phosphate buffer (PB) and the diluted ethanol. To get rid of the fixative reagents the sample were washed six times for 15 min with PB on ice. Washing steps, repeated 5x with Phosphate buffer, 0.5 mL for 15 min at 4°C

After the washing steps the dehydration of the sample were performed with different dilutions of Ethanol.

Table 25: Dehydration steps

50 % Ethanol	30 min	4 °C
70 % Ethanol	30 min	4 °C
96 % Ethanol	30 min	4 °C
100 % Ethanol	Over night	4 °C

The final dehydration step is again left over night at 4 °C and the infiltration with LRWhite was continued next day.

Table 26: Infiltration steps

25% resin	75% Ethanol (100%)	120 min	4 °C
50% resin	50% Ethanol (100%)	120 min	4 °C
75% resin	25% Ethanol (100%)	120 min	4 °C
100% resin	0% Ethanol (100%)	Over night	4 °C

Following day the 100% resin was once again exchanged for pure resin and incubated for 3 hours and then placed in the including molds. The molds are than overfilled with pure resin and the sample placed there with a sterile toothpick avoiding bubbles. Place the samples at the oven at 65 °C for 48h together with the handling material to polymerize in a waste bag.

2.1.22 SAMPLE CUTTING

The glass knives were prepared at a LEICA / EM / KMR2 device. The separation of squares 25 x 25 mm was done using the glass blade in the cut mode and the application of force onto both sides. This glass peace's of 25 x 25 x 7 mm were once again separated into two triangular structures using the more precise glass cutter and a more gentle applied force on the diagonal sides. After cutting the water reservoir needs to be fixed onto the diagonal side. Therefore the glass blade and the plastic tub were slowly heated up, avoiding the knife to heat up and then brought together by wax to form a water reservoir right after the blade.

2.1.23 IMMUNOLocalIZATION OF RECOMBINANT PROTEIN

The cut samples of 1.2 µm thickness were placed into the development-cassette facing up. For the sample blocking 100 µL of 5% BSA was used and incubated for 15 minutes. For the Immunolocalization the IgG human antibody was diluted 1:300 in 0.1 M phosphate buffer (PB). For the detection separate anti-kappa and anti-gamma chain antibodies from goat were used therefore a co-localization was not possible.

After 15 minutes the BSA was removed by gently tipping the slides and adding 100 μ L of primary antibody per slide and incubating it at ambient temperatures for 2 h. The slides were washed next for three times with PB (0.1 M at pH 7.4 0.5% Tween) before about 100 μ L of the secondary antibody (diluted 1:30) was applied and incubated at room temperature for 1 h in the dark. Finally the grids were washed with PB (0.1 M at pH 7.4) for two times within 10 minutes space and flushed clean with distilled water. Slides were air dried and used for microscopy

2.1.24 IMMUNOFLUORESCENT FIXATION OF FRESH TISSUE

For microscopy the leaf samples were pre-treated to remain an intact structure and internal orientation. First the leaf samples were cut on wax paper with a razor blade in squares of about 3 x 3 mm and immediately submerged in Fixative (4% PFA) for overnight fixation at 4 °C in a 2 mL tube. Then the samples were washed in 0.1 M PB at PH 7.4 for 10 min in three repetitions.

The fixed Samples were first mounted on the platform with glue and then cut in 0.1 M PB at pH 7.4 with a LEICA Vibratome to slices of 100 μ m thickness. The samples, in total about 10, were immediately removed from the water and placed in 2 mL tubes containing 0.1 M PB at PH 7.4. After this, several dehydration and rehydration steps were performed with ethanol:

Table 27: Dehydration and rehydration steps.

concentration	duration
30 % Ethanol in PB	5 min
50 % Ethanol in PB	5 min
70 % Ethanol in PB	5 min
100 % Ethanol in PB	5 min
70 % Ethanol in PB	5 min
50 % Ethanol in PB	5 min
30 % Ethanol in PB	5 min
0 % Ethanol in PB	∞

After the last step the PB buffer was removed carefully, and 1 mL of 2% cellulase in 0.1 M PB was added and incubated at ambient temperatures for 50 min, afterwards the cellulase solution was removed and 1 mL of a 5% BSA solution was used for 5 min of blocking. The primary antibody (a human IgG – AFF, AU004) was diluted 1:50 in of 0.1 M PB at pH 7.4 and incubated overnight at 4 °C.

The slices were than washed three times in of 0.1 M PB at pH 7.4 for about 5 min and then immediately applied to the microscopy slide together with some Vaseline to keep a 0.5 mm gap between microscopy slide and the coverslip. Analyze the samples immediately at the confocal microscopy and protect the slide from light damage.

2.1.1 IN SILICO CALCULATION OF THE ISOELECTRIC POINT

The isoelectric point of the antibody molecule played a crucial role for the purification.

Several online tools were used to gather information about the specific properties of the newly designed antibody. First of all, the obtained nucleotide sequence from the cloning project was converted into the amino acid sequence via the ExPASy translation tool, data is shown in Appendix C. For the determination of the isoelectric point, required for the pH-precipitation of undesired proteins in the bulk solution, the online tool “Prot – pi” was used.

The amino acid sequences of the four subunits were inserted and an N-glycosylation site was added at position 295 (NST = Asparagine) and a fully oxidized set of Cysteines was also assumed, although a hydroxylation might occur, it was not assumed as a regular post-transcriptional modification influencing our parameters at this specific antibody.

Differences in the isoelectric point calculation with three different online tools are shown in Table 28. The average was used for the ammonium sulfate protein precipitation. The attachment of the CBM to the HC seems to acidify the antibody fusion, leading to an isoelectric point shifted by pH 0.5.

Table 28: Differences in the isoelectric point calculated by ProMoSt, ExPASy and Native.

	HHC2	HHC2-CBM
ProMoSt	pH 8.59	pH 8.76
ExPASy	pH 8.77	pH 8.95
Native	pH 9.18	pH 9.36
average	pH 8.48	pH 8.97

2.2 BACTERIAL MEDIA

For the basic cloning steps as well as the infiltration procedure different media were used to guarantee a smooth bacterial growth as well as minimal harm to explants. If not stated differently, all media components were mixed together in a flask and topped up to the 1000 mL mark with double distilled water, followed by a standard autoclaving procedure (20 minutes at 121 °C, 2×10^5 Pa).

After autoclaving the media was cooled down in a water-bath till it reaches approximately 55 °C and if needed the temperature labile vitamins were added along with the appropriate antibiotics to maintain plasmids and inhibit growth of undesired bacteria. In case of agar plates the pouring was conducted in a vertical flow laminar under aseptic conditions.

Table 29: Concentrations of antibiotics used for selection.

Stocks	E. Coli LB-medium 1 L	E. Coli Selection plates	A. tumefaciens Medium 1 L	MS plates 1 L
Kanamycin (50mg/ml)	1ml = 50 mg/L		1ml = 50 mg/L	2ml = 100 mg/L
Gentamycin (25mg/ml)	1ml = 25 mg/L			
Carbenicillin (100mg/ml)	1ml = 100 mg/L	1ml = 100 mg/L	1ml = 100 mg/L	
Rifampicin (20mg/ml)	1ml = 20 mg/L		1ml = 20 mg/L	
Cefotaxim (150mg/ml)				1ml = 150 mg/L

2.2.1 LB-MEDIUM

Table 30: Composition LB-medium

substance	concentration
sodium chloride (NaCl)	5 $\frac{g}{L}$
yeast extract	5 $\frac{g}{L}$
soya peptone	10 $\frac{g}{L}$
Adjust to 1 liter with distilled H ₂ O	
Set to	pH 7

2.2.2 LB-AGAR

Table 31: Composition LB-Agar

substance	concentration
sodium chloride (NaCl)	5 $\frac{g}{L}$
yeast extract	5 $\frac{g}{L}$
soya peptone	10 $\frac{g}{L}$
Agar-Agar Kobe I (Roth)	15 $\frac{g}{L}$
Adjust to 1 liter with distilled H ₂ O	
Set to	pH 7

2.2.3 SOC-MEDIUM

Table 32: Composition SOC-medium

substance	concentration
yeast extract	5 $\frac{g}{L}$
soya peptone	20 $\frac{g}{L}$
sodium chloride (NaCl)	0.58 $\frac{g}{L}$
potassium chloride (KCl)	0.18 $\frac{g}{L}$
magnesium sulfate (MgSO ₄)	1.2 $\frac{g}{L}$
magnesium dichloride (MgCl ₂)	0.95 $\frac{g}{L}$
Adjust to 1 liter with distilled H ₂ O	
Set to	pH 7

2.2.4 YEB-MEDIUM

Table 33: Composition YEB-medium

substance	concentration
sodium chloride (NaCl)	5 $\frac{g}{L}$
yeast extract	5 $\frac{g}{L}$
soya peptone	10 $\frac{g}{L}$
Adjust to 1 liter with distilled H ₂ O	
Set to	pH 7

2.2.5 YEB-AGAR

Table 34: Composition YEB-Agar

substance	concentration
Beef extract	5 $\frac{g}{L}$
Yeast extract	1 $\frac{g}{L}$
Soya peptone	5 $\frac{g}{L}$
Sucrose	5 $\frac{g}{L}$
Magnesium sulfate (MgSO ₄)	0.5 $\frac{g}{L}$
Agar-Agar Kobe I (Roth)	15 $\frac{g}{L}$
Adjust to 1 liter with distilled H ₂ O	
Set to	pH 7

2.2.6 INDUCTION-MEDIUM FOR *A. TUMEFACIENS*

Table 35: Composition induction medium

substance	concentration
MES	10.6 $\frac{g}{L}$
Glucose	5 $\frac{g}{L}$
AB-salts	32 $\frac{ml}{L}$
Sodium phosphate (Na ₃ PO ₄)	0.236 $\frac{g}{L}$
Acetosyringone	100 mM
Adjust to 1 liter with distilled H ₂ O and set to	
	pH 5.7

2.2.7 INFILTRATION MEDIUM

Table 36: Composition infiltration medium

substance	concentration
MS media (Sigma)	2.4 $\frac{g}{L}$
MS Vitamins	1 $\frac{g}{L}$
Adjust to 1 liter with distilled H ₂ O, set to pH 5.7	

2.2.1 MS-VITAMIN STOCKS 1000x

Table 37: Composition MS-Vitamin stocks

substance	concentration
MS Vitamin Stock, Sigma and Aldrich	0.1032 $\frac{g}{1 mL}$
Add 1 mL with distilled H ₂ O and incubate for 10 min at 37 °C under constant shaking	
Sterilize via filtration with 0.22 µm filter	

2.2.2 MS-SHOOTING MEDIUM

Table 38: Composition Murashige & Skoog shooting medium

substance	concentration
MS media (Duchefa)	4.4 $\frac{g}{L}$
MS Vitamins	1 $\frac{g}{L}$
Sucrose	30 $\frac{g}{L}$
GELRITE ® Duchefa	3 $\frac{g}{L}$
Adjust to 1 liter with distilled H ₂ O	
Set to	
0.1 $\frac{mg}{L}$ NAA (Auxin)	pH 5.7
1 $\frac{mg}{L}$ BAP (Cytokinin)	

2.2.3 MS-ROOTING MEDIUM

Table 39: Composition murashige & skoog rooting medium

substance	concentration
MS media (Sigma)	4.8 $\frac{g}{L}$
MS Vitamins	1 $\frac{g}{L}$
Sucrose	30 $\frac{g}{L}$
GELRITE ® Duchefa	3 $\frac{g}{L}$
Adjust to 1 liter with distilled H ₂ O	
Set to	
1 $\frac{mg}{L}$ NAA (Auxin)	pH 5.7
0.1 $\frac{mg}{L}$ BAP (Cytokinin)	

2.2.4 AB-SALTS

Table 40: Composition AB-salts

substance	concentration
Ammoniochloride (NH ₄ Cl)	20 $\frac{g}{L}$
magnesium sulfate (MgSO ₄) * 7 H ₂ O	6 $\frac{g}{L}$
potassium chloride (KCl)	3 $\frac{g}{L}$
Calcium chloride (CaCl ₂)	0.2 $\frac{g}{L}$
Iron(II) sulfate (FeSO ₄) * 7 H ₂ O	0.05 $\frac{g}{L}$
Adjust to 1 liter with distilled H ₂ O	0.18 $\frac{g}{L}$
Set before autoclaving to	pH 7

2.3 TRANSFORMATION OF PLANTS

2.3.1 PREPARATION OF AGROBACTERIA FOR INFILTRATION

A. tumefaciens were cultured for two days in 2 mL starter culture and then transferred to 250 mL flasks containing up to 20 mL medium and incubated at 28 °C and 180 rpm.

When an OD₆₀₀ of 0.5 was reached the culture was centrifuged at 3500 g for 10 min and the bacterial pellet was resuspended in about the same amount of induction media. To stimulate the infection process the *A. tumefaciens* culture was shaken for 2 hours at 100 rpm in the dark at ambient temperature. After the induction period the culture was once again centrifuged at 3000 g for 15 min and the bacterial pellet was resuspended in an appropriate volume of infiltration medium, calculated to reach a defined OD value.

At this stage the OD₆₀₀ was checked and adjusted to 0.5. Individual cultures bearing the single plasmid for HC, LC and p19, respectively, were mixed at a ratio of 2:2:1. In case of the final construct (pM4-27-2) the total OD ratio of M4:p19 was 4:1. The cultures were used for syringe infiltration as well as the vacuum approach.

2.3.2 INFILTRATION OF *NICOTIANA BENTHAMIANA* USING VACUUM INFILTRATION

The infiltration of *Nicotiana benthamiana* was facilitated by their low height and their low resistance against vacuum infiltration (Fig. 8), as shown in pre-tests.



Fig. 8: Equipment for the vacuum infiltration procedure.

The equipment itself was composed of a vacuum pump, the vacuum chamber containing the infiltration container, the cold trap cooled with dry ice (in this particular setting a rotary vane pump was used) and the tube system. The *Nicotiana benthamiana* plants were supported via a polymethylmethacrylic shield and immersed upside down into the infiltration container filled with at least 1 L of infiltration medium at OD=0,5 and 100 µL TritonX and the vacuum chamber was closed. The closed chamber contains now the beaker with cell suspension filled nearly to the edge, as well as the submerged plants, hanging upside down into the beaker. The chamber was then evacuated by applying a mild vacuum of about 100 mbar, measured with a capacitive vacuum sensor, for 30 seconds. When bubbles appeared from

the stomata the whole chamber was moved to detach the bubbles from the stomata. The chamber was slowly vented until atmospheric pressure was reached, and afterwards evacuated again for another 30 s (Chen et al., 2013).

This procedure was repeated two times and the plant was subsequently immersed in clear water to flush off excess of *A. tumefaciens* from the surface (Lakatos et al., 2004). These plants (Fig. 9) were watered extensively and cultured at ambient temperature (~21 °C) for seven days.



Fig. 9: A successful infiltration of the leaves is easily observable, as fully infiltrated leaves do show a transparent appearance (left) compared to non infiltrated leaves (right)

2.3.3 INFILTRATION OF *NICOTIANA TABACUM* USING SYRINGE INFILTRATION

The syringe infiltration (Fig. 10) was performed into the abaxial side of *N. tabacum* L. cv. Petit Havana SR1 due to the better accessibility of the apoplastic space in the leaf. This usually offered an easier infiltration compared with *Nicotiana benthamiana*.

The agrobacterium suspension carrying the final mixture of cultures harboring different constructs was adjusted to a final OD of 0.4 the syringe itself was pushed against the lower side of the leaf to inject the bacteria suspension. The so infiltrated areas were easily visible and not marked after infiltration.



Fig. 10: Manual syringe infiltration into the abaxial side of *N. tabacum* L. cv. Petit Havana SR1 leaves.

The plants were cultured at ambient temperatures for 7 days and then harvested.

2.4 HARVESTING OF PLANT MATERIAL

Leaf material was harvested from both species excluding the midvein (Fig. 11), weighed, and then the material was either immediately processed or stored in a container at -20 °C.

The harvesting had to be performed as quickly as possible to avoid enzymatic degradation. In the standard procedure the harvested leaves are immediately frozen in liquid nitrogen and homogenized with mortar and pestle (Fig. 12). The powder was stored on ice and then transferred to a centrifugation flask where extraction buffer (200ml 1x PBS, 2ml 100x EDTA, 500 µL PMSF pH 7.4) was added in a 1:2 ratio (w/w)



Fig. 11: Removing of the not transformed midvein before homogenization.

Table 41: Extraction buffer

PBS pH 7.4	200 mL	
EDTA 100 x	2 mL	To block metallo-proteases
PMSF 1000 x	400 μ L	Against serine proteases

Table 42: PMSF stocks 1000x

substance	concentration
PMSF crystalline	0.0174 $\frac{g}{1 mL}$
Add 1 mL with 2-Propanol and incubate for 10 min at 37 °C under constant shaking	
Sterilize via filtration with 0.35 μ m filter	

Subsequently the mixture was sonicated extensively three times on ice and placed at a 4 °C room for constant shaking at 180 rpm for 2 hours. The mixture was split in two centrifugation flasks and centrifuged at 9000 rpm for 15 min at 4 °C to get rid of cell wall compartments (pellet 1). Next the extract (supernatant 1) was filtered via a vacuum Erlenmeyer flask and a filter paper followed by a microfiltration utilizing a syringe and a 1 μ m polypropylene filter.



Fig. 12: Homogenization of leaf material with mortar and pestle under constant cooling with liquid nitrogen.

After filtration the pH of the supernatant was slowly increased to 8.0 with 1 M NaOH and incubated for 30 minutes at 4 °C under constant rotation and centrifuged at 9000 g for 15 min at 4 °C to precipitate most other proteins with different isoelectric properties than the antibody in the pellet (pellet 2). The supernatant was collected (supernatant 2) and used further.

2.4.1 AMMONIUM SULFATE PRECIPITATION

The ammonium sulfate precipitation was used to achieve pellets of adequate antibody enrichment for further testing. The method itself is used since the nineteen sixties (Herbert, 1972) and shows significant cost advantages over other purification techniques like protein G-purification. The saturation point was calculated online (www.encorbio.com) for 45 % saturation at 4 °C (Encorbio, 2016).

The supernatant 2 shifted to a 45% saturation using crystalline $(NH_4)_2SO_4$ with a purity of 99.8% from Sigma which was slowly applied to the constantly stirred liquid over about 15min at 4°C. The precipitation was usually performed overnight with slow stirring for about 12 hours and centrifuged afterwards in a precooled centrifuge in a 50 mL falcon at 9000 g for 30 min to achieve pellet 3. This pellet was suspended again in 1 mL of 45 % saturated ammonium sulfate solution and transferred to a 1.5 mL tube. After another centrifugation step at 13000 g for 10 min the supernatant was discarded and final product dried at ambient temperature, weighted and afterwards stored at 4 °C.

2.4.2 ANTIBODY HARVEST AND PURIFICATION

Purification of Antibody for analytical purpose and determination of yields was performed using a protein-G binding assay and subsequent quantification by a Bradford assay. The necessary amount of protein-G was calculated beforehand by assuming an optimal estimated yield of $300 \frac{\text{mg}}{\text{kg}}$ leaf material as well as the binding capacity of G-protein ($15 \frac{\text{mg}}{\text{mL}}$). This led to an average amount of 200 μL of drained beads per 100 mL of volume.

The supernatant 2 and G-protein was incubated at 4 °C with constant shaking at about 150 rpm for 1.5h and afterwards transferred to a column for elution. The drained beads were washed 5x column volume (CV) with precooled 4 °C 1x PBS at pH 7.8 and eluted afterwards with 1x CV of 0.1 M Glycine at pH 3 and neutralized immediately with 1 M Tris-base (about 12.5 μL of Tris for 500 μL of Glycine) to neutral pH. This procedure was repeated 3 times, till four fractions were eluted and neutralized. The highest concentration of antibody was usually obtained in fraction two and three.

The samples were weighted to determine the amount of each fraction and afterwards stored at 4 °C. The column was recovered by applying 2 mL of Glycerol, 5 mL of PBS and 2 mL of degassed 20% Ethanol which stays within the column that is immediately closed with a cap and the beads are pipetted into a collection tube to be stored at 4 °C.

2.4.3 PROTEIN QUANTIFICATION

The Bradford protein quantification assay is a color reaction of the Bradford reagent based on Coomassie G-250 dye (4 mL reagent concentrate and 11 mL distilled H₂O) and the proteins in solution, usually performed in a 96 Well plate at 596nm. The reaction, containing 50 μL of the sample and 200 μL of 1x Bradford solvent, was incubated at constant shaking for 3 min and afterwards measured with a photometer (MG-TECAN) where the absorbance rate (A) was exported to an Excel file.

The calibration curve is set up by the application of 50 μL standards containing bovine serum albumin (BSA) at various concentrations including distilled H₂O the factors (B) and (C) for the slope of the calibration curve was calculated by Excel:

$$y = B * x + C$$

The calculation of the concentration of each eluate was back calculated and complemented by the gravimetric measurement of the tube volume to calculate the total yield, by multiplication with the dilution factor (D).

$$c = \frac{A - C}{B} * D$$

2.5 STABLE TRANSFORMATION OF TOBACCO PLANTS

Infiltration of *Nicotiana tabacum* was performed according to the standard infiltration procedure by syringe and cultured for seven days post infiltration. Subsequently the infiltrated leaf was taken off as a whole and sprayed with 70% ethanol till all the epidermal layer was completely covered, and incubated for max. 30 s. The leaf was immediately rinsed with sterile water to remove the ethanol from the surface. After this first step the whole leaf was cut in a laminar flow cabinet in pieces of about 7 x 7 cm and placed carefully into a sterile glass beaker. The stomata should face down to avoid upwards bending of the leaf. Now 500 mL of a 2 % Sodium hypochlorite solution was poured over the leaf and kept under constant shaking for 5 to 10 minutes according to the state of the leaf. As soon as stomata started to appear dark the sterilizing solution was removed and the beaker immediately flushed with autoclaved water at room temperature and rotated constantly for about 2 minutes. Then the water was poured into another beaker also present in the laminar. This washing step was repeated five times and the beaker covered with sterile aluminum foil afterwards.

The scalpels and forceps were flamed and placed next to a sterile petri dish served as chopping board for the further procedure. Leaves were carefully taken out of the beaker and placed onto the petri dish where all infiltrated spots appeared a bit lighter. These spots were excised producing rhombus shaped leaf squares of about 7 x 7 mm in size which were placed on already prepared shooting medium containing Kanamycin for the selection of successfully transformed cells and Cefotaxime against the *A. tumefaciens*. The so prepared plates were sealed with parafilm and provided with two slots for air circulation and placed at 24 °C into an incubator.

Depending on the growth rate of the squares they were sub cultured every five to seven days (Fig. 13). While cutting them into smaller pieces as soon as callus was formed to separate them and facilitate the regeneration of individual shoots and to avoid shoot clusters. After the plants have developed two to three small leaves the callus was truncated and the plants were transferred to the rooting medium and into taller petri dishes. The rooting medium also contained Kanamycin to avoid the growth of *A. tumefaciens*. Then the shoots were subcultured every 7 to 14 days (Fig. 14) till reaching the lid. At that point they were transferred to magenta boxes filled up to 1.5 cm with rooting medium featuring the inverse auxin-to-cytokinin ratio to enhance the root formation.

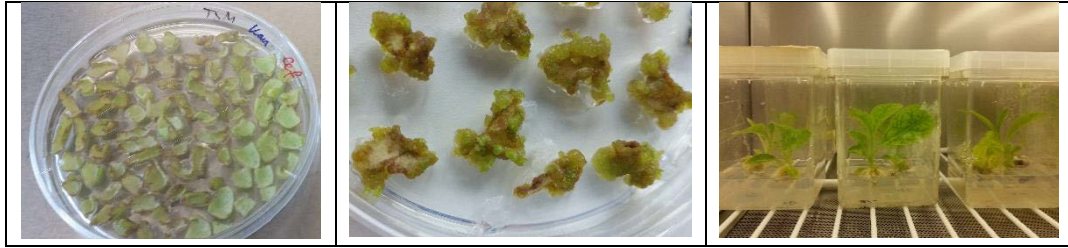


Fig. 13: developmental stages of plant regeneration, captured at one week, 5 weeks and 11 weeks

After the roots were fully established, the regenerated plants were gently removed from the magenta boxes. Then the roots were rinsed from remnants from solid medium under running tap water and all easy removable parts of the callus were discarded. After that, the cleared root system was placed in a pot half filled with soil and fertilizer and covered with topsoil. The so prepared plants were watered extensively and placed in a tray completely covered by a plastic bag for proper acclimatization. After a week, the bag was gradually removed and the plants were adapted to normal humidity and light conditions.

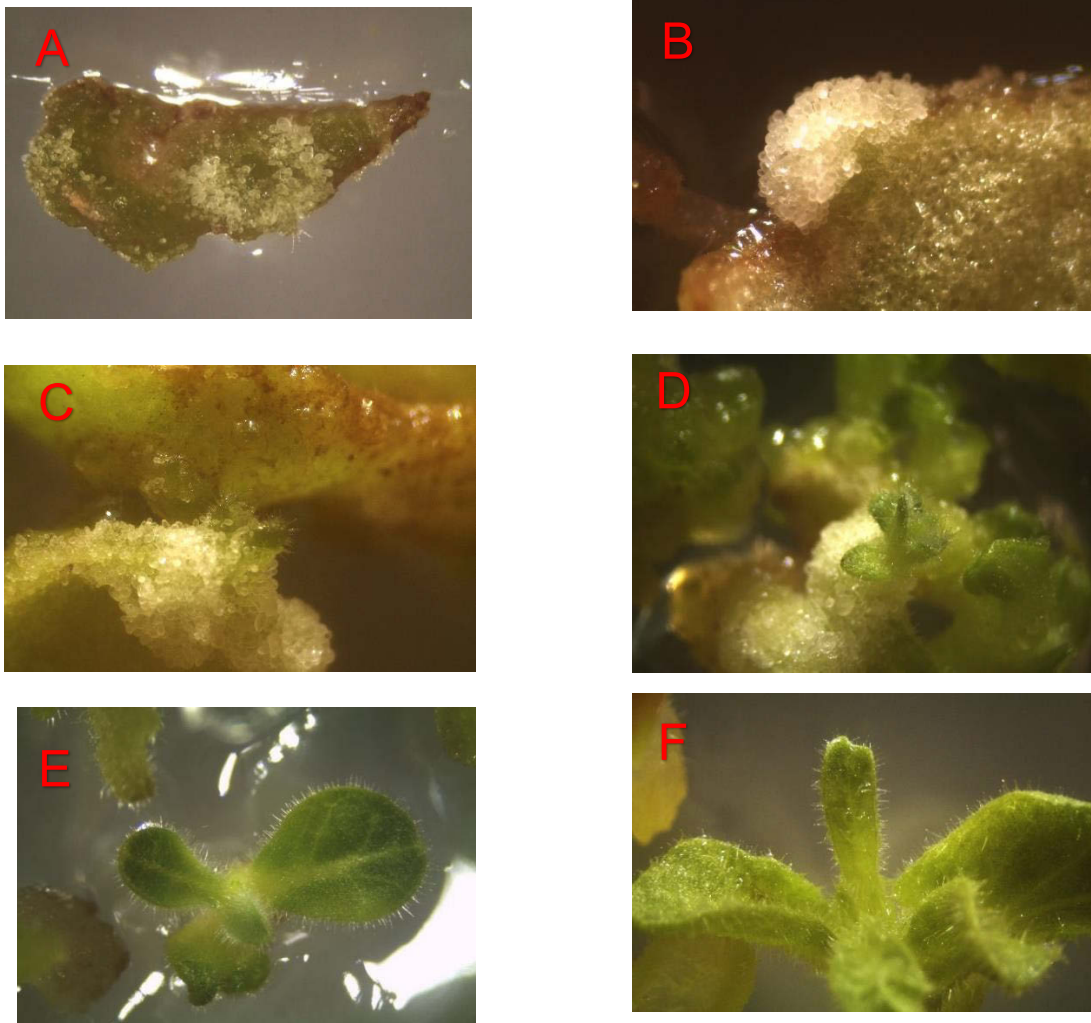


Fig. 14: Chronological observation of a single embryonal callus to plant stage. Starting at A: 1 week B: 3 weeks C: 5 weeks D: 7 weeks, E: 9 weeks transfer to rooting media, F: 11 weeks, transplantation to magenta boxes.

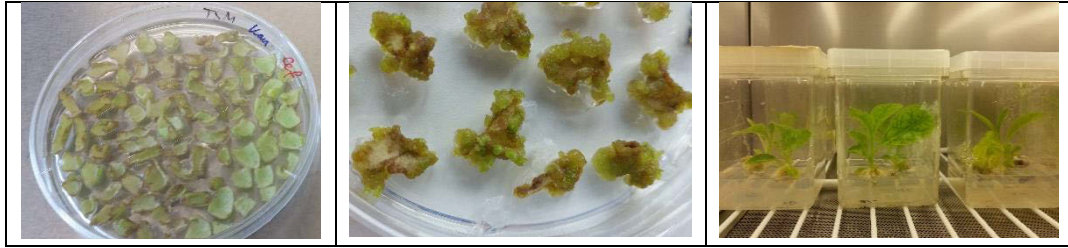


Fig. 13: developmental stages of plant regeneration, captured at one week, 5 weeks and 11 weeks

After the roots were fully established, the regenerated plants were gently removed from the magenta boxes. Then the roots were rinsed from remnants from solid medium under running tap water and all easy removable parts of the callus were discarded. After that, the cleared root system was placed in a pot half filled with soil and fertilizer and covered with topsoil. The so prepared plants were watered extensively and placed in a tray completely covered by a plastic bag for proper acclimatization. After a week, the bag was gradually removed and the plants were adapted to normal humidity and light conditions.

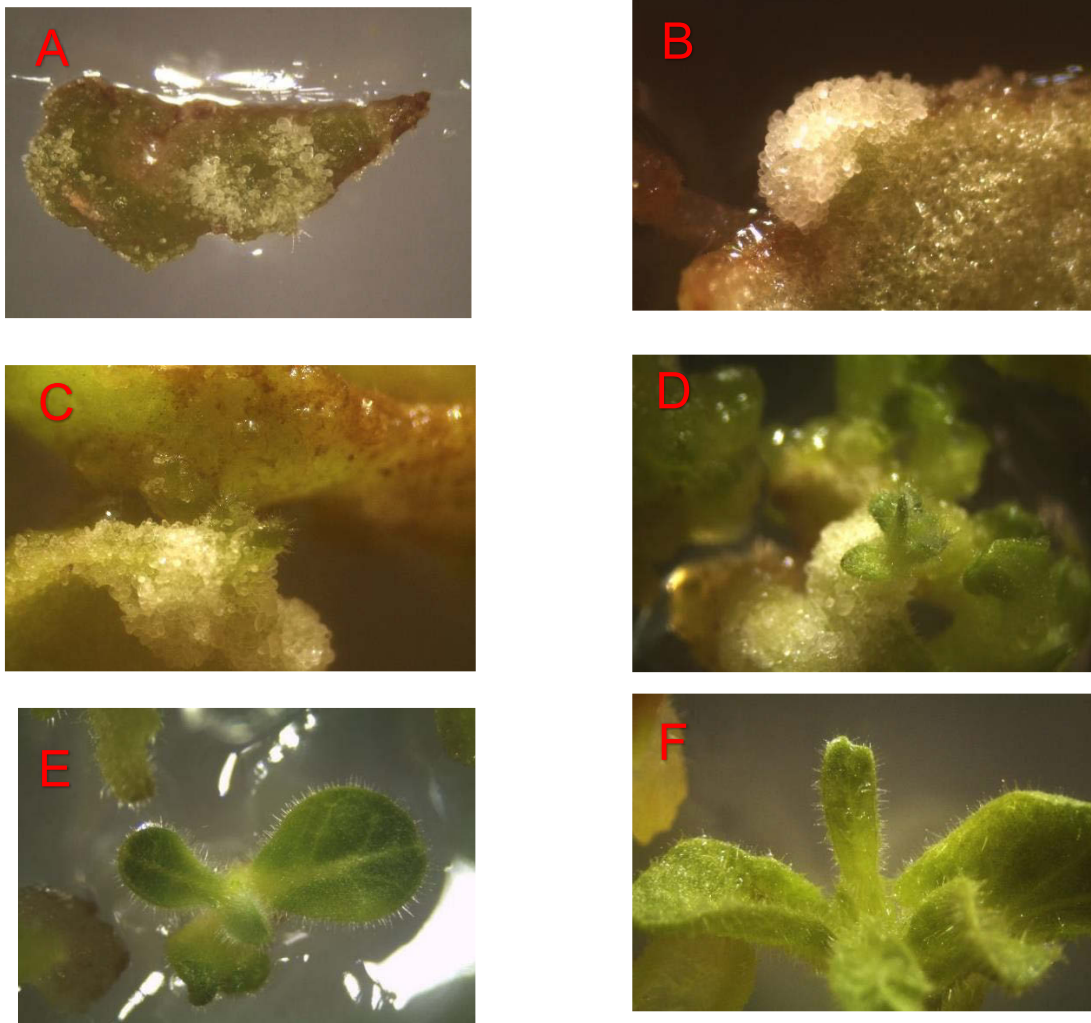


Fig. 14: Chronological observation of a single embryonal callus to plant stage. Starting at A: 1 week B: 3 weeks C: 5 weeks D: 7 weeks, E: 9 weeks transfer to rooting media, F: 11 weeks, transplantation to magenta boxes.

3 RESULTS

3.1 CLONING OF THE SINGLE VECTOR DELIVERY SYSTEM

The intention was to combine heavy and light chain into one expression vector. The final product facilitates the infiltration procedure due to the use of only one construct in one *Agrobacterium* culture, and allows to obtain stable lines expressing fully assembled antibody without any crossing of two different parental plants. Already in T0 plants the antibody is assembled in the ER and secreted into the apoplastic space. DsRed as a visual screening marker was also present on the final construct and is retained by a KDEL-sequence within the endoplasmic reticulum lumen. The three initial plasmids used are shown in figure 15.

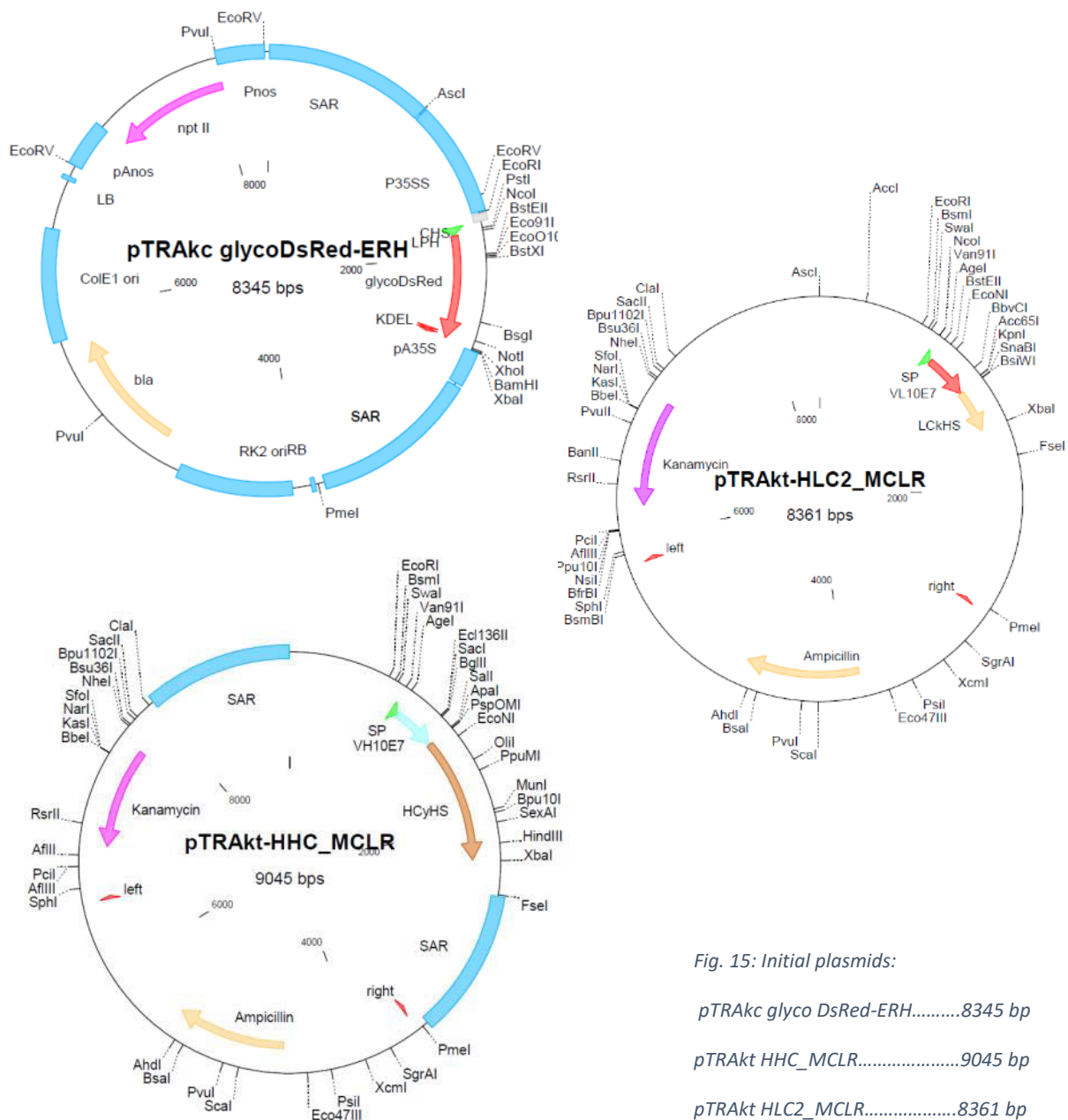


Fig. 15: Initial plasmids:

pTRAKc glyco DsRed-ERH.....8345 bp

pTRAKt HHC_MCLR.....9045 bp

pTRAKt HLC2_MCLR.....8361 bp

A “shuttle vector”, pJET 1.2-plasmid (Fig. 16) was used for the consecutive cloning steps as described below. The pJet vector (2974 bps) is composed of a rep (pMB1) section at 1162 bps originating from the pMB1 plasmid and is responsible for the replication of pJET1.2.

The β -lactamase gene confers resistance to ampicillin, which is used for selection and maintenance of recombinant *E. coli* cells. As well as the lethal gene *eco47IR* which enables positive selection for a successful recombinant insertion of the fragment. The XHO1 restriction site for the insertion is located right within the ORF of the *Eco47IR* gene thus disrupting its function and upon the application of lactose or IPTG only bacterial cells with nonfunctional ORF survive. Additionally a modified lac promoter for expression of the lethal *eco47IR* gene at a level sufficient to provide positive selection and a T7 RNA polymerase promoter for in vitro transcription of the cloned insert are located on the pJet vector.

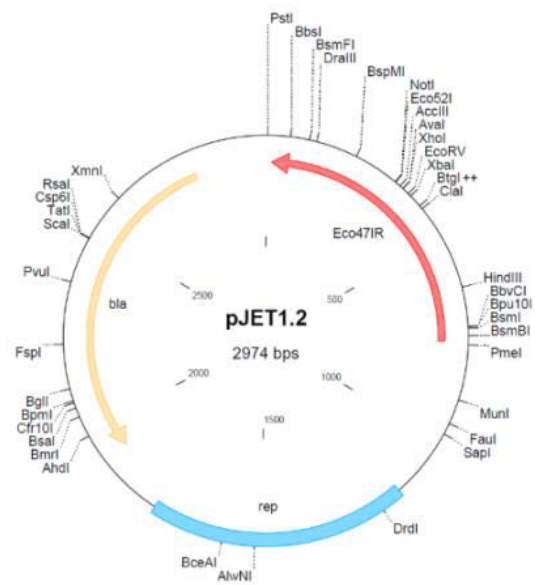


Fig. 16: pJet1.2 shuttle vector with lethal restriction site *Eco47IR*

All initial plasmids (Fig. 15) were equipped with an origin of replication for *E. coli* as well as *A. tumefaciens*. The plasmids for HC and LC contain the same selection marker, a gene conferring Kanamycin resistance. The DsRed (Baird et al., 2000) containing plasmid is also equipped with a gene expressing the β -lactamase conferring resistance to Carbenicillin. All three plasmids carry a signal peptide followed by either the DsRed gene or the HC constant region and variable region respectively the LC constant region and variable region. Also two SAR regions are included in every plasmid to expose the big cassettes efficiently to the RNA polymerase (AGARWAL et al., 1989).

3.1.1 INTEGRATION OF THE LIGHT CHAIN INTO THE CLONING VECTOR

For the integration of the HLC2 into the pJET1.2 vector (2974 bp) the vector was opened with the restriction enzyme *Xho*1, which is located within the ORF of the *Eco47IR* gene, the *Eco47IR* gene is under a lactose promoter which is activated by the presences of IPTG which is removing the lac-repressor from the double strand, mimicking the presence of lactose.

After the insertion of the LC the intermediate vector pM2 (4066bp) was generated.

The Light chain insert was excised as explained in chapter 3.1.1 from its original pTRAc vector via restriction sites *Asc*I and *Pme*1, the overhangs which were filled in by Klenow-Fragment (#EP0051), The vector was further dephosphorylated by the Shrimp-Alkaline-Phosphatase (#EF0511) (SAP) to avoid self-religation.

The simultaneously performed forward and reverse screening offered complementary information about the orientation of the insert. As checked in advance with the clone manager the correct insertion would lead to a fragment of 1200 bp amplified from the insert (35S_F primer) to the backbone (Jet_F, Jet_R) and a 2000 bp fragment if the insert is flipped. The size of the amplicon can be explained by different distance of the insert primer sequence to the backbone sequence. If the 3' ends of the primers are facing in different directions or distance is exceeding a certain length the amplicon cannot be synthesized due to a mismatch or a lack of time in the elongation step of the PCR.

3.1.2 ADDITION OF DsRED TO CLONING VECTOR

To obtain the pJET-HLC2-DsRed plasmid the pM2 clone one was scaled up together with an *E. coli* clone carrying the pTRAKT vector containing a DsRed gene. Finally plasmids from both cultures were purified, as explained in chapter 2.1.10. The concentrations for the initial pM2 clone one was $555.6 \frac{ng}{\mu L}$ and the DsRed clone achieved $80.9 \frac{ng}{\mu L}$ which were found to be sufficient for further cloning steps.

The pJet vector was now treated as explained in 2.1.1 with the restriction enzyme XhoI leading to 5' overhangs treated with the Klenow-Fragment (#EP0051) for 20min at 37°C. The vector was further dephosphorylated via the Shrimp-Alkaline-Phosphatase (#EF0511) (SAP) to avoid self-relegation.

The DsRed insert (2401 bp) was excised as explained in chapter 2.1.1 from its vector via restriction site AscI and PmeI in fast digest buffer for 60 min at 37 °C, the overhangs which were later filled in by Klenow-Fragment (#EP0051), for 10min at 37 °C. The ligation was performed as explained in chapter 2.1.2 and immediately followed by the heat shock transformation of the competent *E. coli* cells.

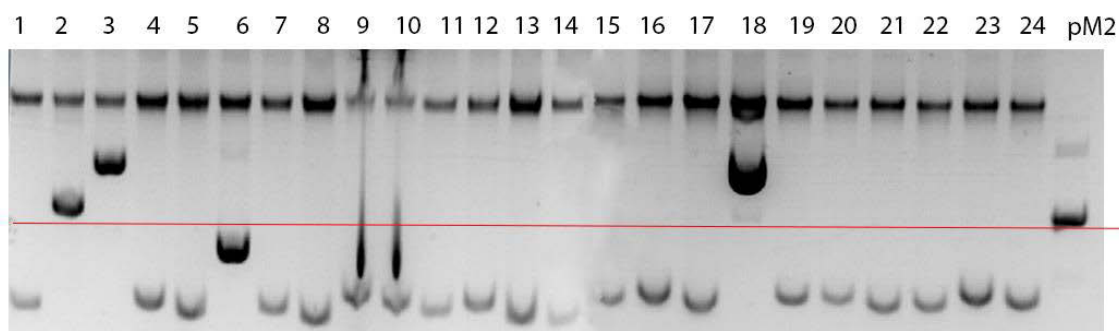


Fig. 20: Colony cracking screen for the *E. coli* transformation.

The pre-screening (Fig. 20) was implemented via a colony cracking approach, being able to roughly estimate which colonies are carrying the desired insert of the DsRed gene plus the SAR- region, for the enhancement of expression (AGARWAL et al., 1989) which would lead to a shift of about 2800 bp in size. The most promising clones M3-18 and M3-3 (Fig. 20) were used for a PCR screening with pJet_F and Ds_Red_R primers. This indicated a successful insertion in both, and pM3-18 was chosen (Fig. 21).

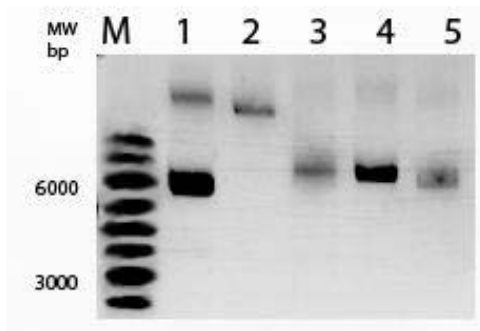


Fig. 21: PCR screening with pJet_F and Ds_Red_R primers for the correct insertion

The purified pM3-18 plasmid shown in figure 22, displays the correct total size of about 6904 bp indicated by the upper big fragment of the pM3, the lower band is supercoiled plasmid, the upper band was excised and further processed as described in chapter 2.1.10.

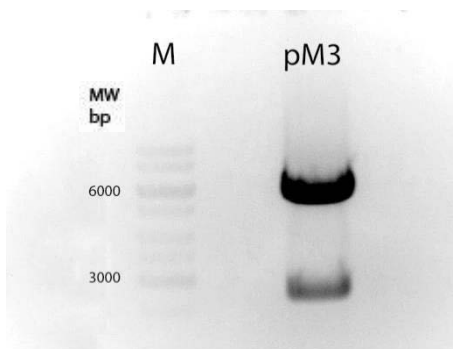


Fig. 22: gel purified product pM3 for further processing

3.1.3 TRANSFER OF LC AND DsRED INTO THE HC- EXPRESSION VECTOR

To find the correct pM4 construct, which is composed of the pM3-18 + DsRed, a prescreening of 33 colonies (Fig.23) was necessary. After incorporation into the pJet vector, eight positive candidates were selected after the prescreening and those were analyzed via PCR (Fig.24). With the promising M4-27 (15033 bps) a restriction digest was executed indicating a positive insertion (Fig. 25).

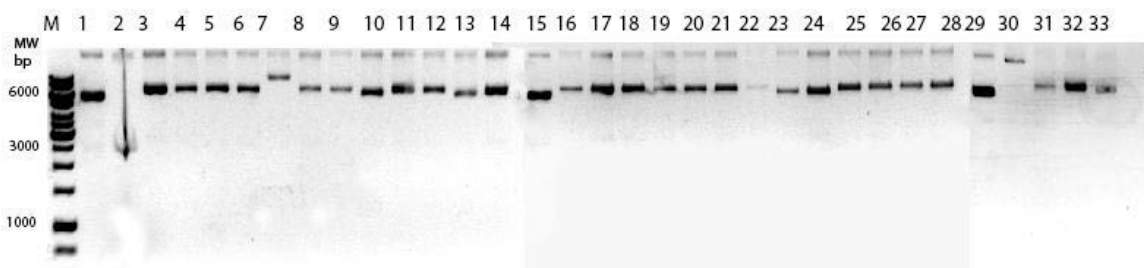


Fig. 23: Pre-screen for the E. coli transformation of LC and DsRed into the HC expression vector.

The screening with the cracking buffer was only to narrow down the number of candidates for the PCR-based screening. Several colonies were included 2, 6, 7, 9, 13, 27, 10, and 15 for the PCR screen as the results were not quite clear.

A strong band (Fig. 24) at 600 bp shows a successful integration of the LC and DsRed in colonies number 9 and 27. The other bands are probably due to a too high number of PCR cycles, which might amplify a contamination or result from

unspecific binding in the bacterial chromosomal genome. Colony 27 was chosen because of a better growth rate.

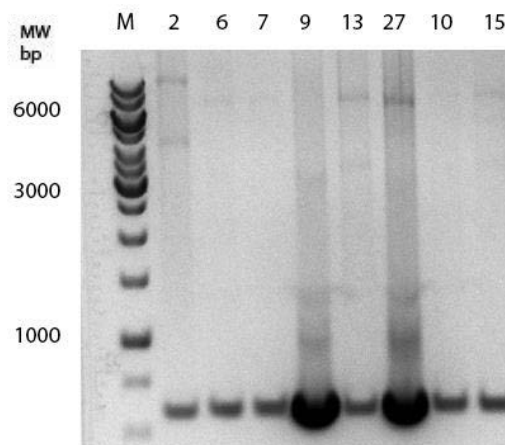


Fig. 24: PCR screening for the correct insertion of LC and DsRed into the expression vector, successful integration in colony 9 and 27.

The verification by a restriction digest offered clear and indicative data about the structure of the plasmid though the limited resolution of the gel should be taken into consideration when observing the result. While the expected forward oriented pattern for ECO_RI (8618, 3555 and 2860) was clearly apparent the pattern for ECO RV (4599, 2860, 1908, 1652, 1647, 1404 and 963 bp.) must be read with special considerations as band 1652 and 1647 cannot be distinguished and show up as one slightly darker band and band 963 is poorly visible due to the low molecular weight. (Fig. 25)

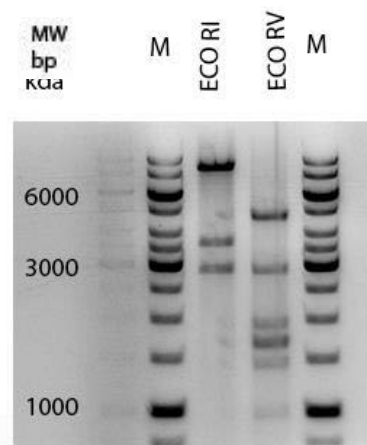


Fig. 25: restriction digest with Eco RI and Eco RV show the expected pattern for an insertion.

The E. coli clones were used to produce sufficient amounts of plasmid for the transformation of *A. tumefaciens*, which were transformed as described in 2.1.7.

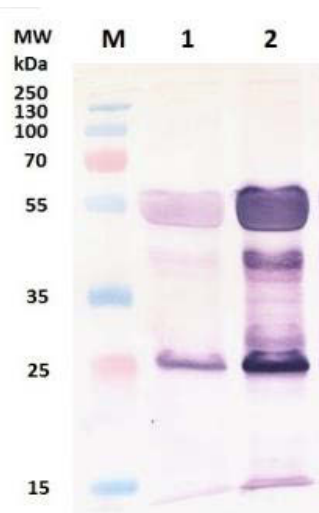


Fig. 27: Transient expression of antibody in *N. benthamiana* using the final *A. tumefaciens* clone pM4-27-2. Distinct degradation bands occurred at about 40 kDa

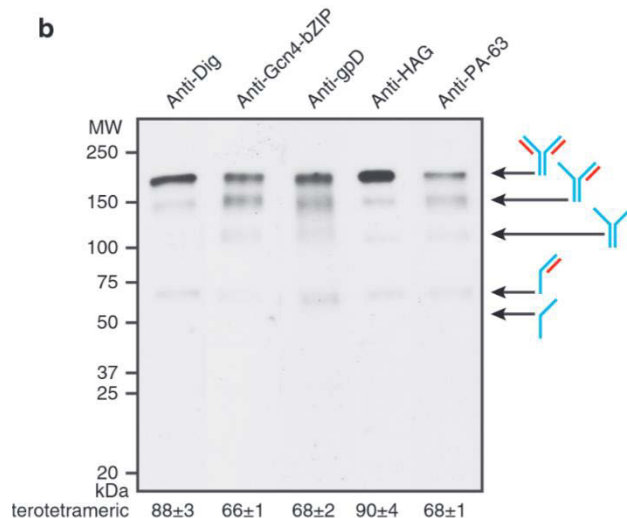


Fig. 26: (Robinson et al., 2015) showing a schematic explanation of the distinct degradation or incomplete assembly of IgG .

Then two *A. tumefaciens* colonies, M4-27-7 and M4-27-2 (Fig. 28) which were screened positive for the plasmid via PCR were used in the first experiments and led to quite different results. M4-27-7 (Fig. 29) showed a higher growth rate as well as simple separation from the culture broth by centrifugation which did not apply to M4-27-2. Although both colonies contained the correct insertion clone 2 performed better than 7 in terms of antibody yield, as shown in a western blot after infiltrating about 1g leaf material with cultures of equal density. M4-27-2 was therefore chosen to generate transgenic tobacco lines.

The yield was confirmed in four biological repetitions and found comparable to prior yield data (data not shown) achieved by the triple infiltration of separate *A. tumefaciens* colonies containing constructs encoding heavy chain, light chain or p19. The successful expression of DsRed was already observed after 4 days and showed macroscopically detectable fluorescence in *N. tabacum* (Fig. 28) and *N. benthamiana* (Fig. 29).

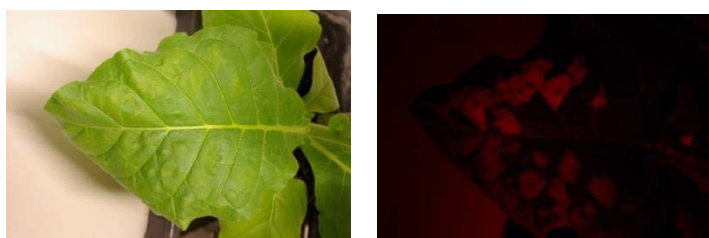


Fig. 28: Transient expression of the single construct in NT, observed after local DsRed expression.

But even here the *N. benthamiana* plants showed slightly higher expression levels compared to *N. tabacum* which was confirmed in later experiments as well.



Fig. 29: Transient expression of the single construct in NB, observed via the local DsRed expression

3.2 FUSION OF THE CBM TO THE C-TERMINAL END OF THE HC

Due to the fact, that there were no restriction sites available right at the end of the heavy chain sequence the cloning of the CBM and linker to the C-terminal region of the heavy chain construct was executed with a PCR-based cloning approach.

After the final assembly reaction utilizing only the flanking primers the whole construct has been checked on the gel for successful assembly and purified subsequently, the concentration was digested with Hind-III and Xba-I, checked at a Nano drop ($154 \frac{\text{ng}}{\mu\text{L}}$) and decided to be sufficient for the quick ligation procedure.

Then the insert containing the CBM + Linker (about 397 bp) and the C-terminal end of the HC and the backbone on the other side were joined with a blunt end cloning approach.

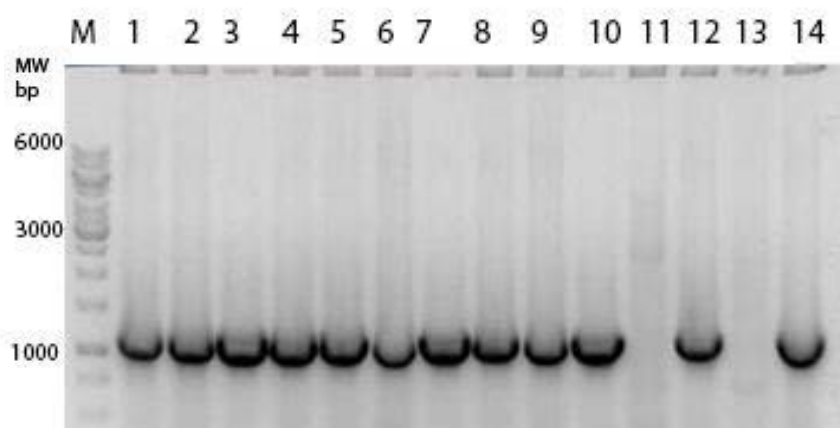


Fig. 30: PCR pre- screening (HHC-882_F and TRA-HHC1629_R) of colonies after the quick ligation procedure.

Fourteen colonies were received from the quick ligation procedure and pre-screened (Fig. 30) via a colony touchdown PCR. From 14 colonies screened via touch down colony PCR and the primers HHC-882_F and TRA-HHC1629_R, twelve colonies carried the plasmid including the desired insertion of the CBM with an expected size of 1175 bps including the CBM (397 bps) and 778 bps in case of no insertion, possible due to a re-ligated vector.

Although SAP shrimp alkaline phosphatase was utilized to dephosphorylate the 5' end of the cloning vector.

Colony one and three (Fig. 31) were up-scaled, the plasmid was extracted and sent for sequencing. The parallel transformation of *A. tumefaciens* saved about three days and enabled to start with the first infiltration right after the sequencing data arrived.

The sequencing data suggested to use colony 3 for the further cloning, although all plasmids were without any SNPs in case of colony 3 the sequencing read also covered the complete polyadenylating site. The Phusion Hot Start II polymerase was used for cloning due to the higher replication fidelity compared to regular Taq polymerase, Vent or Deep Vent DNA polymerases. Pfu DNA polymerase exhibits the greatest PCR fidelity, with an average error rate of 1.3×10^{-6} mutation frequency/bp/ duplication (Cline, 1996). In both constructs no mutations were detected, the sequencing (1224 bps) was also able to cover the upstream and downstream region and proved to be efficient.

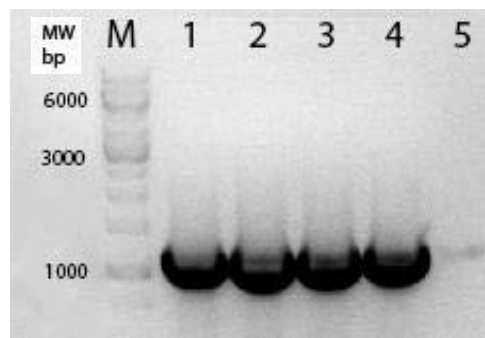


Fig. 31: PCR based screening for the correct insertion of the assembled expression vector

The agro-transformation with plasmid 3 led to 24 colonies (Fig. 32) which were again screened via PCR, this time the colony cracking screening was skipped due to the low copy number of the plasmid, which would not be detectable. All 24 colonies were screened via touch down colony PCR using the primers HHC-882_F and TRA-HHC1629_R leading to an expected product of 1175 bp which turned out to be present in 22 colonies. Therefore colony 16 and 17 were chosen for further evaluation due to their higher growth rate on media. This turned out to be a crucial selection criterion for the future performance in upscale. Especially the growth rate and the formation of polysaccharides in the media should be evaluated in this step.

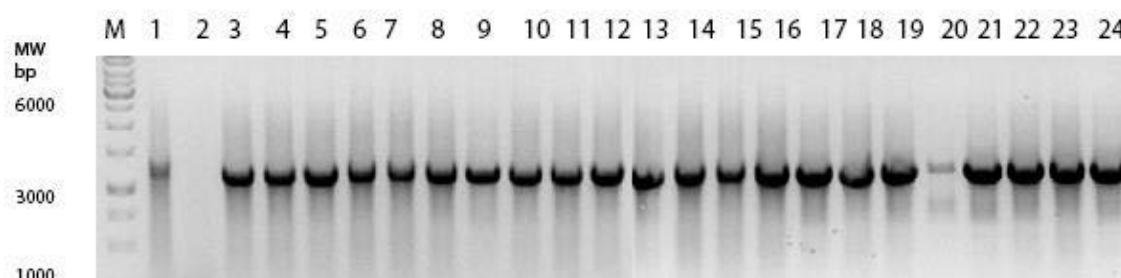


Fig. 32: Colony cracking screen after *A. tumefaciens* transformation.

Protein sequence of the heavy chain carrying the linker and CBM:

```

MVVESGGGLVKPGGSLRLSCAASGFTFSRYAMSWFRQTPERRLEWVATINSVGSYSYYPDSVKGRF
TISRDNVRNTLFLQMSSLRSEDTAIYYCTKGADYAMDYWGQGTSTVTSSASTKGPSVFPLAPSSKST
SGGTAALGCLVKDYFPEPVTVSWNSGALTSGVHTFPAVLQSSGLYSLSSVVTVPSSSLGTQTYICNVN
HKPSNTKVDKKVEPKSCDKHTHTCPPCPAPELLGGPSVFLFPPKPKDTLMISRTPEVTCVVDVSHEDP
EVKFNWYVDGVEVHNAKTKPREEQYNSTYRVVSVLTVLHQDWLNGKEYKCKVSNKALPAPIEKTISK
AKGQPREPQVYTLPPSRDELTKNQVSLTCLVKGFYPSDIAVEWESNGQPENNYKTTTPVLDSDGSFF

```

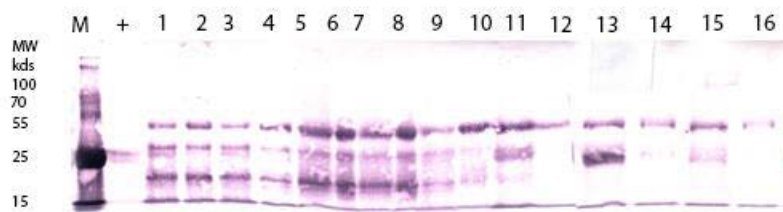



Fig. 33: The samples from *Nicotiana tabacum* (1-2 supernatant, 5-6 pellet, 9-10 pH shifted pellet and 13-14 eluate) followed by the *Nicotiana benthamiana* samples (3-4 supernatant, 7-8 pellet, 11-12 pH shifted pellet and 15-16 eluate).

Samples were taken from the first supernatant of extraction buffer, the crude pellet of the same treatment. As well as the second pellet after the pH-shift to pH 8 to precipitate bulk protein and the final eluate derived from the G-protein enrichment.

The liquid phase applied was 100 μ L and the pellet was 50 mg. Samples were loaded accordingly in two repetitions, started by *Nicotiana tabacum* followed by the two *Nicotiana benthamiana* samples showing feasible Ab concentrations. The other fractions namely pH-shift pellet (9-12), liquid before G-protein binding and the final eluate (13-16) showed only low antibody concentrations. Later tests indicated that the elution was not sufficient, due to the too high pH of the glycine and the experiment was repeated, whether the samples should be analyzed gravimetrically as it would be obvious in case of the pellet or volumetric for the liquid fraction. In later testing the gravimetric approach was favored.

Second biological repetition:

The second biological repetition (Fig. 34) yielding 20 g of leaf material was extracted regularly as described in 2.4.2 and analyzed in more detail with different elution procedures,

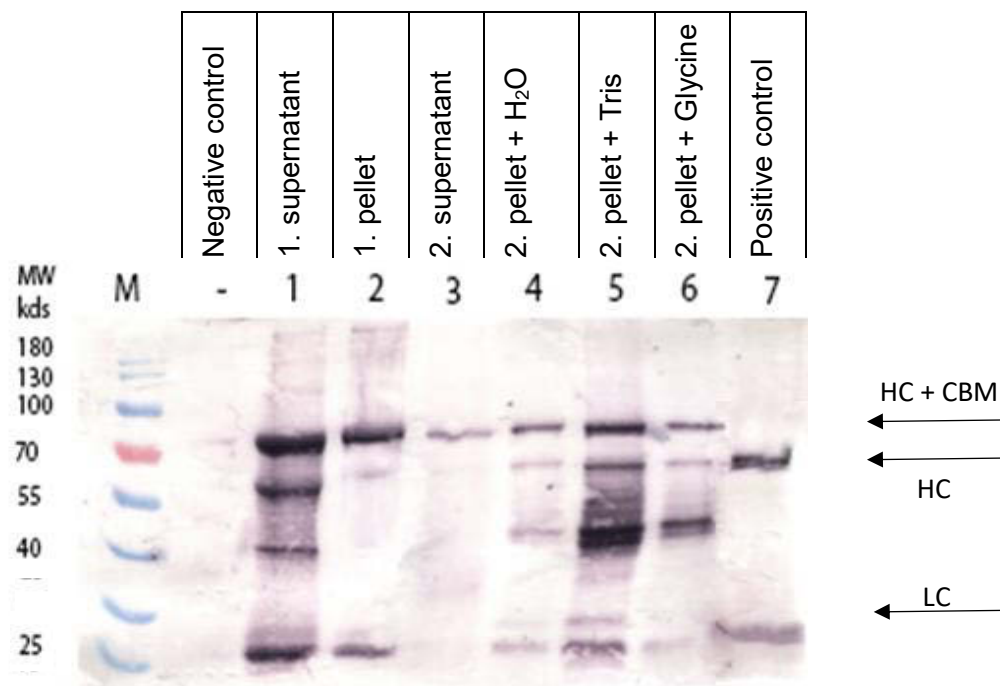


Fig. 34: Second biological repetition NT, comparison of different elution methods from the pellet-immobilized antibody. Wildtype NT served as negative control and purified AB as positive control

The intention of this experiment, shown in figure 35, was the identification of potential elution procedures for the antibody remaining in the pellet of the *Nicotiana tabacum* expression host. The two liquid phases applied indicate that the degradation products obviously visible in supernatant 1 were no longer present after the washing procedure with distilled H₂O. The positive control on the right shows a common pattern with a HC running at about 50 kilo Dalton (kD) and a LC at 25 kD; the upshift compared to the positive control is visible in lane 1-6 at about 7 kD due to the integration of the CBM to the HC. The liquid phase applied was 100 μ L and the pellet was 50 mg.

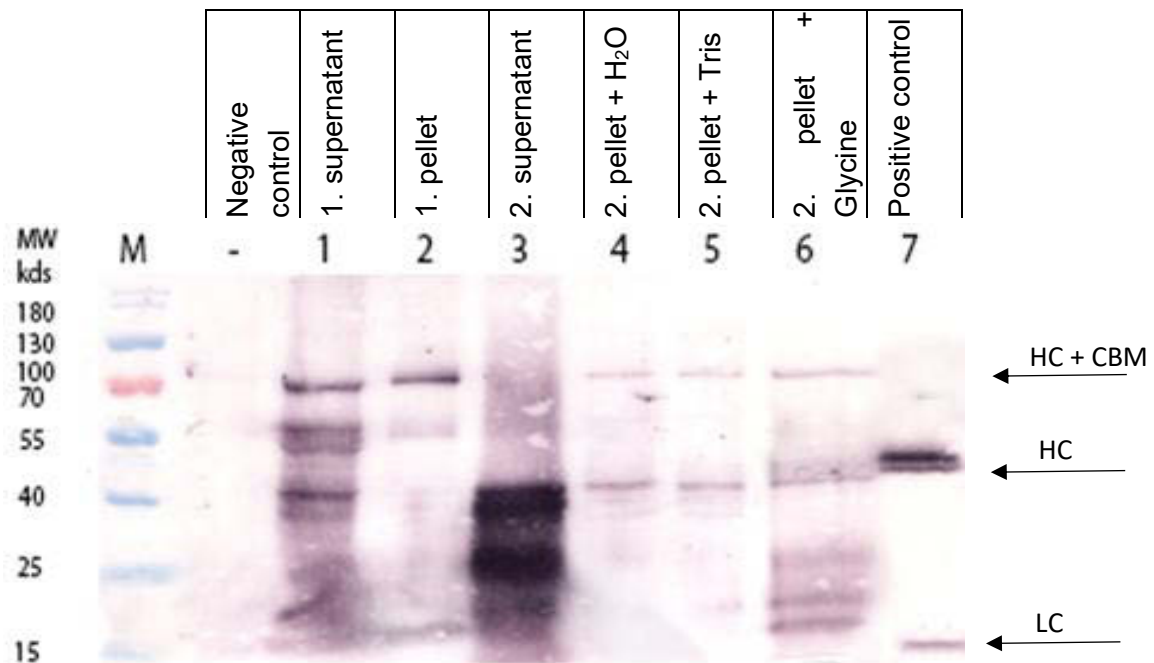


Fig. 35: Second biological repetition NB, comparison of different elution methods.

This blot (Fig. 36) shows the equivalent loading pattern as describes before but now for the NB expression system, the trials were split to identify potential differences due to cell wall specific or glycosylation which might alter the binding behavior of the CBM.

The positive control on the right shows a common distribution pattern with a HC running at about 55 kilo Dalton. In lane 1-6 the HC + CBM is clearly visible in lane 1-6 a band at 50 kDa appeared as well. In lane 1 a band for the HC as well as the HC+CBM appeared probably accompanied by a band of degradation product. In the first pellet a clear band from the HC+CBM is present at +75 kDa without a band for initial HC (50 kDa). The second supernatant shows a significant number of degradation product at 40 kDa and 35 kDa. The elution methods in lane 4 to 6 display again a band at 50 kDa and 75 kDa.

It seems that the major amount of antibody remains located in the first pellet, the liquid phase applied was 100 μ L and the pellet was 50 mg.

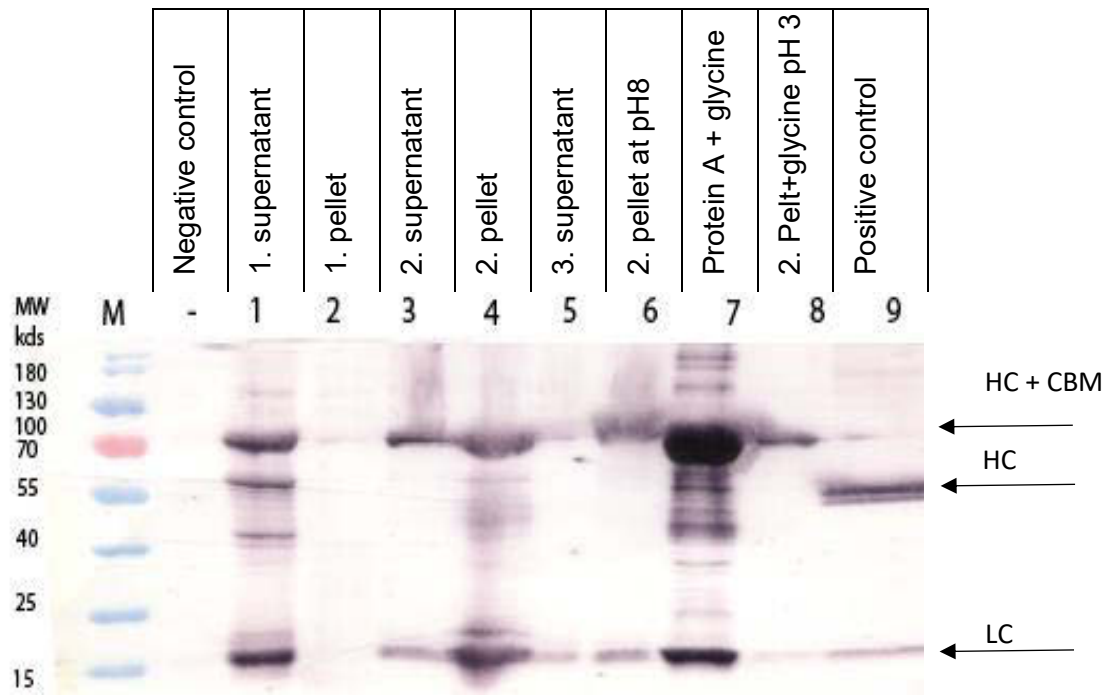


Fig. 36: Comparison of different extraction stages, and elution procedures at pH3 and 8.

The supernatant applied was 60 μ L and the pellet was 50mg. Again quite significant amounts of antibody were in the first liquid fraction (Fig. 37) and less in the first pellet, in the second supernatant we see a more purified antibody without degradation products and again some amount in the second pellet.

In lane 1-8 (except 2, due to a loading error) a clear band for the HC+CBM conjugate is present as well as a band for the LC at 25 kDa.

In lane 3, 5 and 6 little degradation product derived from HC and LC was observed , which might be due to the higher purity of the supernatant compared to the solid pellet.

We can now see the antibody eluted from the pellet is present in all fractions but is higher concentrated at the beads. The positive control (50 kD) at the right travels slightly lower than the HC+CBM (75 kD).

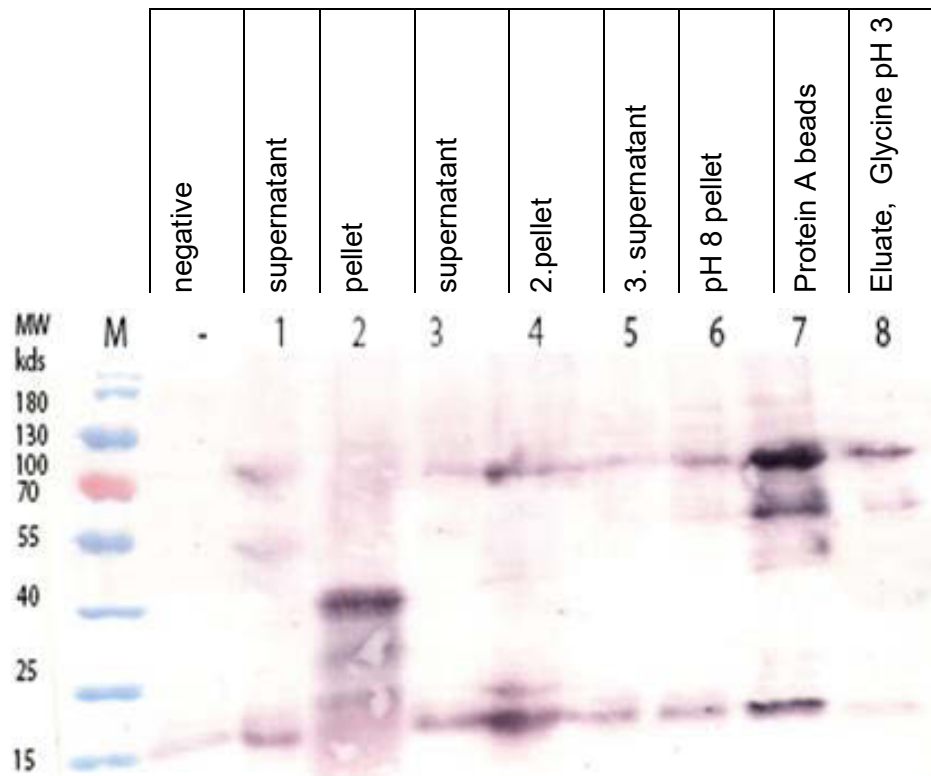


Fig. 37: The regular extraction procedure (prot A) of NT sampled at every step.

When the fractions were applied to a western blot (figure 37), the main amount of antibody seemed to remain in the first pellet and on the protein A beads. But after separation on a gel, the difference in antibody integrity became more visible. While the G protein beads carry a LC and HC including some degradation products running slightly lower, the pellet showed no clear evidence of intact antibody only a diffuse band running at around 40 kDa. The beads contained antibody, it was not fully eluted from the beads.

Due to suboptimal blotting conditions the information gained from this blot is limited, although it supports the results of the *N. benthamiana* blot. The highest recovery rate was definitely achieved with protein-A beads. But -as described above the plant derived antibody was not released upon treatment with glycine at pH 3. The beads were washed after elution with glycine and boiled directly in LB. The liquid phase applied was 60 μ L and the pellet was 50mg which hampers a direct quantitative comparison.

Third biological repetition:

The intended goal of the third experiment (Fig. 38) was to confirm potential elution methods from the second experiment and to test specific binding behaviors to Cellulose, see figure 39.

The first blot [A] again was done to compare the *N. benthamiana* and the *N. tabacum* expression system. The better binding of antibody to the *N. benthamiana* pellet than to the *N. tabacum* pellet was again confirmed, while the total antibody expression of seems to be comparable as both supernatants contained about the same amount of plant derived antibody. This was not intended as a 1M ammonium sulfate solution described by (Sugimoto et al., 2012) was used for extraction, and additional cellulose was mixed to the

crude lysate, trying to retain most of the antibody in the pellet. However, this approach did not lead to the intended retention of the plant derived antibody in the pellet. Further two steps of washing with distilled H₂O and washings with Glycine pH3 showed virtually no successful recovery of plant derived antibody from the pellet, although the elution with Glycine worked slightly better. This could either mean, that the plant derived antibody is so strongly bound to the added micro crystalline cellulose matrix that it is not possible to recover it, or the binding to the matrix was not successful and the plant derived antibody was already washed out with the first ammonium sulfate solution, where most of the plant derived antibody was detected.

For Experiment A (Fig. 38) and B (Fig. 39) the sample was split in equal portions and for experiment A with 1M ammonium sulfate was added to retain the AB in the pellet, while for experiment B a regular extraction procedure with subsequent G-protein purification was carried out.

Experiment A aimed to retain the AB in the pellet. The positive control is clearly visible in lane 1 indicating a successful detection, lanes 2-6 show bands for the LC. As the HC is virtually not detectable in this blot the Experiment was repeated (Experiment C).



Fig. 38: Experiment [A]: to analyze the fixation on the AB to the pellet, acquiring 1M ammonium sulfate and cellulose mixed to the crude lysate, trying to retain most of the AB in the pellet.

The second blot [B] (Fig. 39) was carried out to obtain information on the potential losses of the antibody during the regular extraction procedure from *N. benthamiana*. Relatively high concentrations were observed in the supernatant. The pellet, although washed once, still contained plenty of low molecular degradation products. The plant derived antibody distribution between eluate and beads might indicate, that about half of the bound antibody is not eluted from the beads when treated with Glycine pH3. This was the case when working with the standard MC10E7 antibody in previous experiments, where usually the total

recovery was around 70%, and the most significant losses occurred during pH adjustment (approx.. 14%), incomplete antibody adsorption to protein-A (approx.. 8%) as well as the losses due to incomplete elution (approx.. 5%).

In lanes 1, 3, 5, 7 a clear upwards shift of the AB-CBM fusion protein to 75 kDa indicates a successful expression of the intact AB-CBM fusion. In lane one also degradation products are present running at around 40 kDa and 30 kDa. In lane three also the additional band at 55 kDa is present. Lane 5 and 7 show the highest AB concentrations due to the enrichment with G-protein.

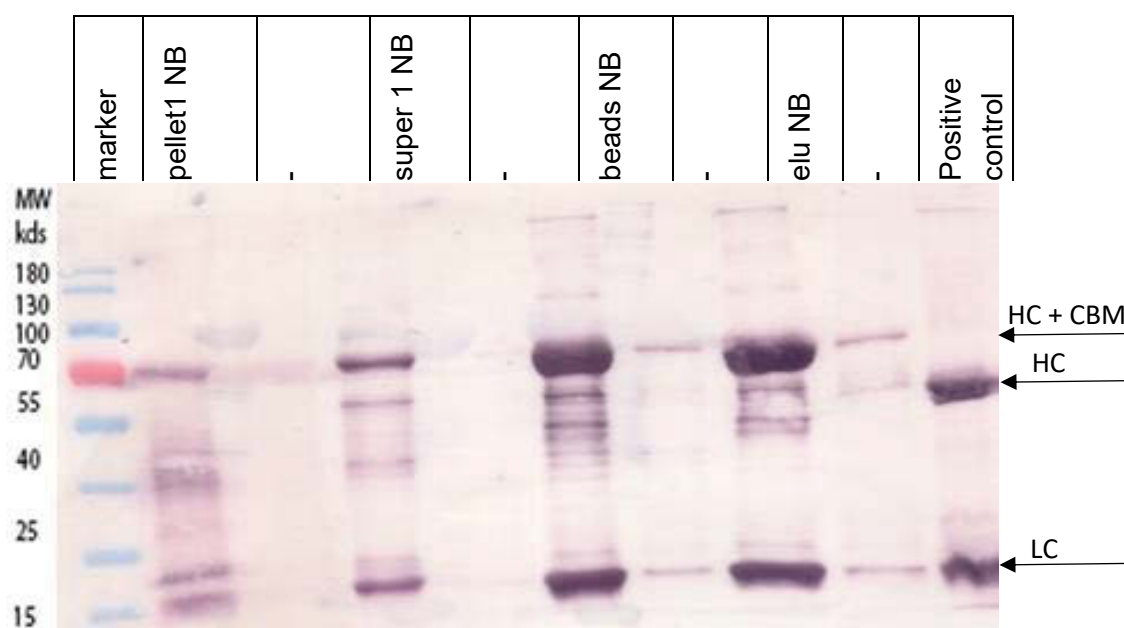


Fig. 39: Experiment [B]: Showing the extraction with A-protein. to identify the possible losses.

The third blot [C] (Fig. 40) was a repetition of experiment [A], to further investigate the retention of the antibody by the cellulose within the pellet. The elution from the pellet was attempted with distilled water as described by (Sugimoto et al., 2012). Homogenization and blending with microcrystalline cellulose in a 1:1 [w/w] ratio was repeated, followed by an extraction in ammonium sulfate (45%) solution (supernatant 1). Subsequently, two elutions with distilled water and an elution with Glycine pH 3 were carried out for comparison. The rinsed pellet after two extractions with water was loaded as pellet 2 and showed very low antibody concentrations. As there is virtually no sign of an antibody within the second pellet either the first extraction buffer or the elution with distilled water was efficient in removing some of the AB. But there is nearly no signal for the HC in both extraction procedures and only a faint signal for the ammonium sulfate extraction. It was not possible to clarify the position of the remaining antibody. The direct elution with glycine pH 3 from the pellet worked quite well and showed good recovery performance.

Lane three shows a higher AB concentration than the supernatant indicating a successful binding to the cellulose. Lanes 4-7 demonstrate different elution methods from the initial pellet. Only the band for the LC is present indicating an inefficient elution from the pellet.

Lanes 8-9 show the G-protein enriched fraction after the purification procedure for the AB conjugate. This demonstrates the proper function of the G-protein purification, also in combination with the HC+CBM fusion.

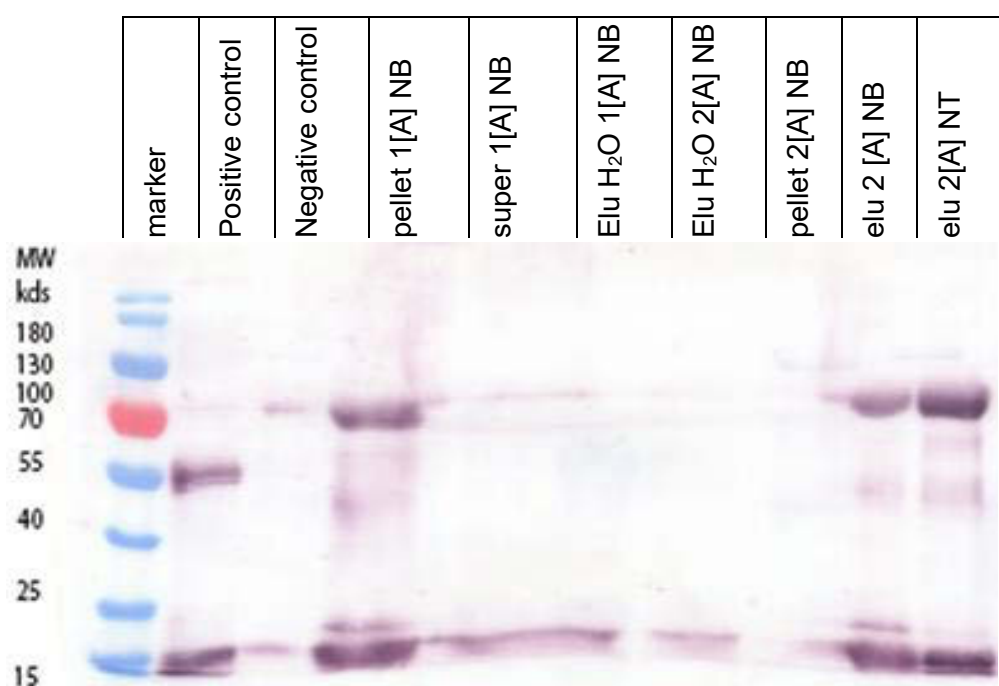


Fig. 40: Experiment [C]: repetition of experiment A, Cellulose fixation and elution with water.

Blot D (Fig. 41) finally aimed to identify the contents of the white layer, observed several times in the *N. benthamiana* pellet. The two fractions were manually collected from the pellet and examined separately. All pellets showed faint bands for the HC and LC as well as the degradation product of about 40 kDa. The white layer showed relative low concentrations of antibody, when compared to the upper pellet surface of the same biological repetition. Therefore the hypothesis of a defined chimeric particle composed of precisely degraded oligo-saccharide-units as expected after endo cellulase treatment, together with the antibody attached via the CBM leading to a defined homogenous molecular weight and thus a defined layer within the pellet had to be rejected,.

In lane 3 the pellet from the last biological repetition was applied to identify potential differences, except the increased amount of degradation product. Lanes 4 and 5 contain the regular intermediate steps for the extraction procedure showing a small loss of AB in the flow through and reasonable concentrations for the eluate..Lanes 6 and 7 contained the two fractions of denatured AB, after being denatured intentionally for longer time on G-protein. Neither the non-transparent precipitate nor the lighter phase of elution buffer contained detectable amounts of AB.

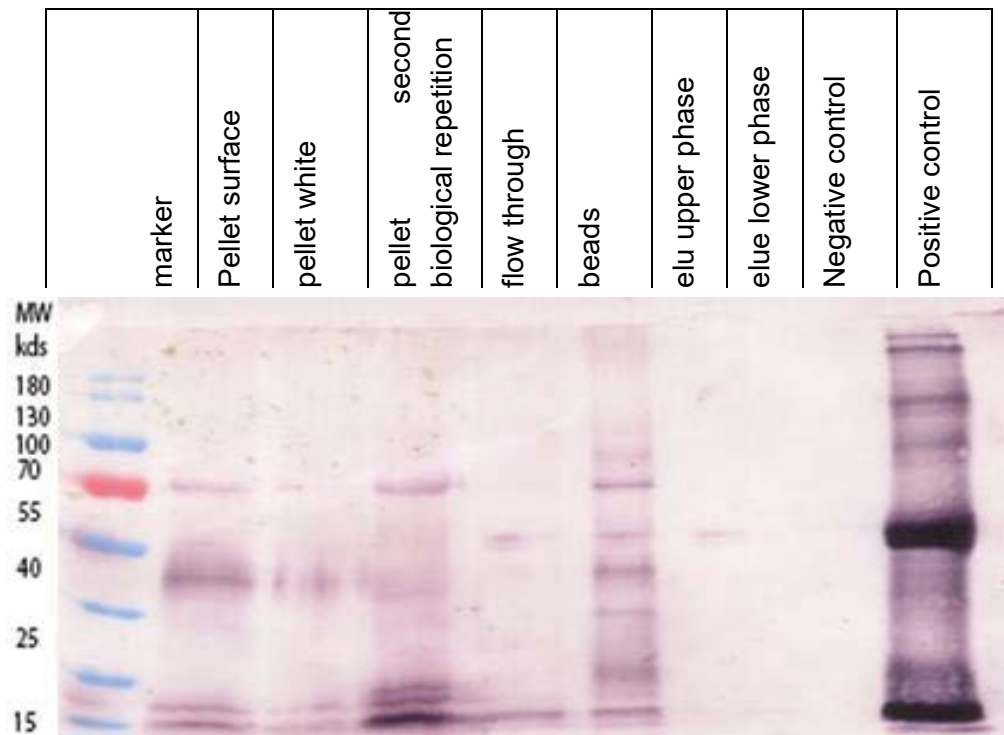


Fig. 41: Experiment [D]: regular extraction with protein A and glycine pH3: The differences of the white layer and the rest of the pellet is examined together with the pellet of the last biological repetition and the long-term stability experiment.

3.2.1.2 ELISA - CBD BINDING SPECIFICITY

With this experiment the binding capacity of the CBD to sepharose and Cellulose was analyzed. And compared to the binding capacity to protein-A beads.

For all three experiments the pellet was washed three times, (Fig. 42) with PBS pH 7,4 to get rid of weakly attached AB and dissolved in 5 ml PBS pH 7.4 for the protein A and the sepharose extraction and an adequate cellulase buffer for the enzymatic degradation.

To verify the most promising purification and elution methods the extracted CBM-antibody-conjugate was quantified in an ELISA assay. Plates were coated over night

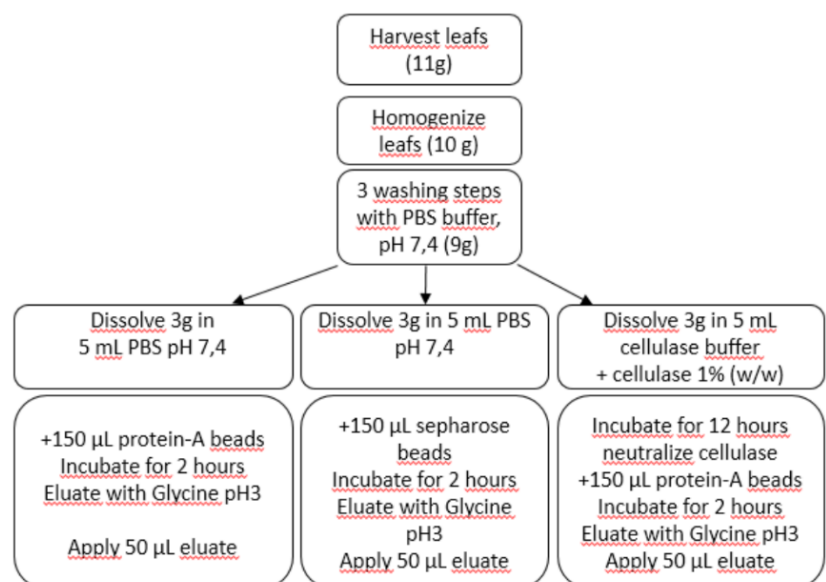


Fig. 42 Flowchart of the three compared extraction procedures

with a goat anti human gamma-chain IgG (dilution 1:5000). The calibration curve was obtained by serial dilutions of an antibody with known concentration, measured by UV-absorbance, and data points limited to obtain a linear range ($1\text{-}50\frac{\text{ng}}{\text{mL}}$).

Leaf extracts were applied in several dilution steps to meet the linear range. The secondary antibody was an anti-human AB-conjugate as the constant region of the MC10E7 was human and developed by a p-Nitrophenyl phosphate substrate according to manufacturer's recommendations.

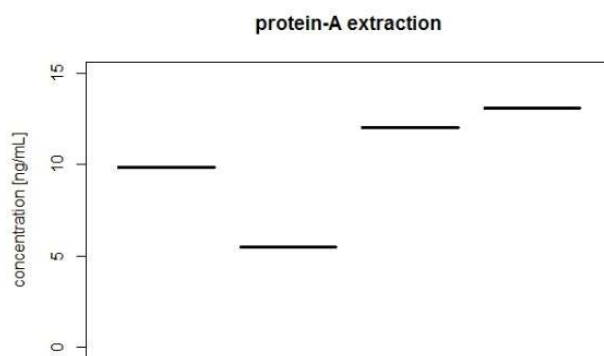


Fig. 43 ELISA analysis for the protein-A extraction.

The ELISA assay was used to clarify the affinity of the CBM-antibody-conjugate to the highly cross linked sepharose. The results (Fig 44) can be compared with the same pellet treated with a protein-A extraction procedure (Fig. 44).

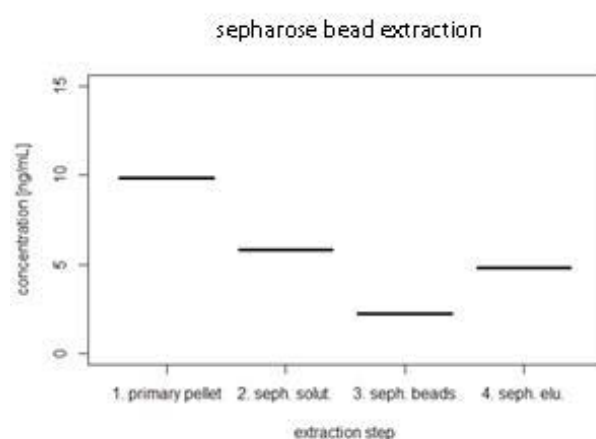


Fig. 44: ELISA analysis for the sepharose beads extraction procedure sampled at the four main stages.

The primary pellet obtained by a extraction in regular 0.1 M PBS- buffer, which was not included in the ELISA was again dissolved and blended with 150 μL sepharose beads, incubated for 2 h at 5 $^{\circ}\text{C}$ and followed by a regular extraction with glycine at pH 3.

Another extraction procedure tested was the degradation of cellulose via a cellulase treatment to recover the AB attached to defined polysaccharide fragments, such as β -glucose or shorter polysaccharides, derived from the degraded cellulose is shown in figure 45. The washed pellet was dissolved in a cellulase buffer (20 mM MES, 20 mM potassium chloride, 10 mM Calcium chloride, 1% [w/w] cellulase) and incubated at ambient temperatures overnight. Afterwards the cellulase was deactivated by a shift to pH 8 followed by a regular extraction with protein A (150 μL) to determine the recovery rate and compare it to the regular extraction method.

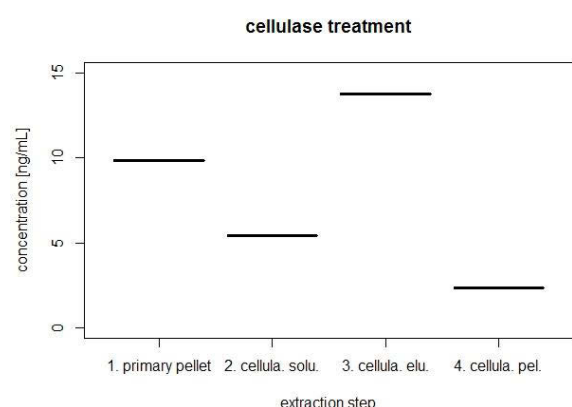


Fig. 45: ELISA analysis of the cellulase treatment of the first pellet.

The results indicate a high affinity of the AB-CBM-conjugate to the protein-A beads (Fig. 43) and nearly no affinity to the pure sepharose beads. The incubation with cellulase on the other hand did not improve the extractability of AB from the pellet as a recovery of 14 ng/mL was also achieved just by protein-A extraction.

3.3 REGENERATION OF TRANSGENIC PLANTS

3.3.1 TANDEM DELIVERY SYSTEM

The regenerated transgenic tobacco plants containing either the HC or the LC cassette were screened at the protein level using a Western blot for the semi quantitative detection of the antibody (Fig. 46). A pre-screen was performed to optimize the blot conditions and estimate the necessary amount of plant material for a clear signal.

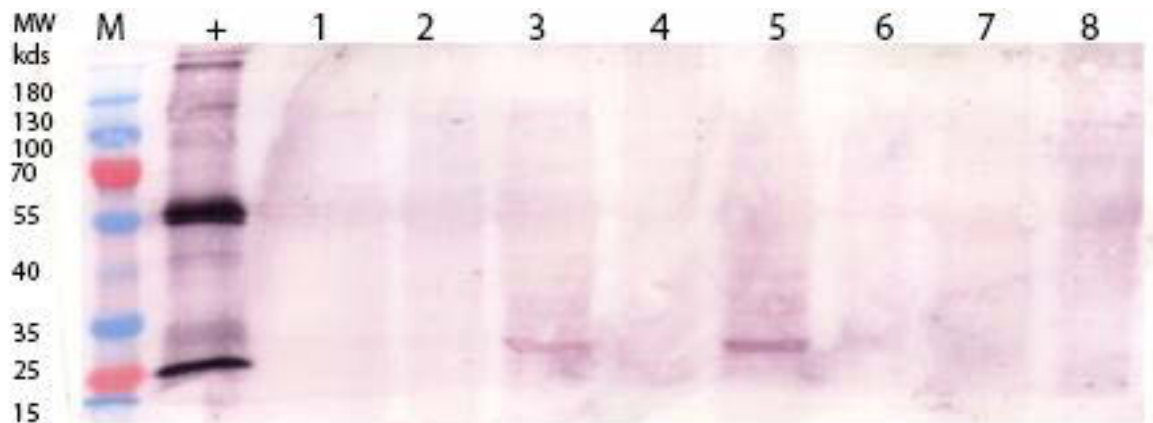


Fig. 46: First screening to optimize the blotting conditions, successful detection of the LC in plant 3 and 5.

For the first screening 1g leaf material was sampled from eight plants and extracted and the crude supernatant was separated on an SDS PAGE and transferred to the blot. Although the applied antibody recognizes both kappa and gamma chain only the LC showed up, although at a slightly higher MW than expected. Plant 5 and 3 were used for further crossing as LC parent.

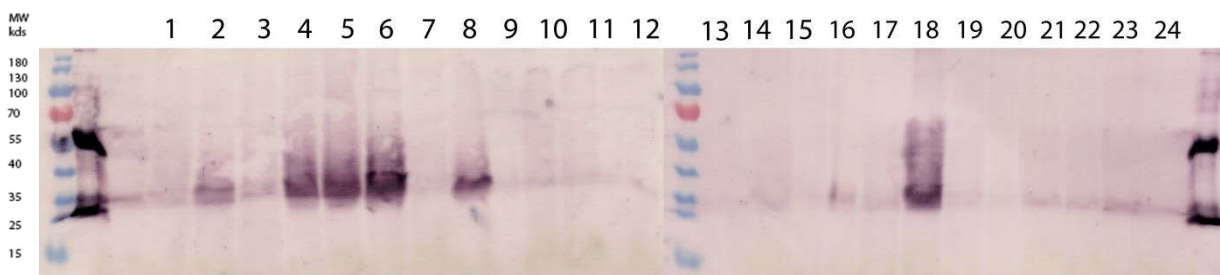


Fig. 47: Full screen for LC detection.

To detect other LC positive clones the procedure was repeated again utilizing now 5 g leaf material enriched and concentrated via a binding step with protein G (Fig. 47). For further crossing, the plants 2, 4, 5, 6, 8, 18 were used as crossing partners for the LC plants.

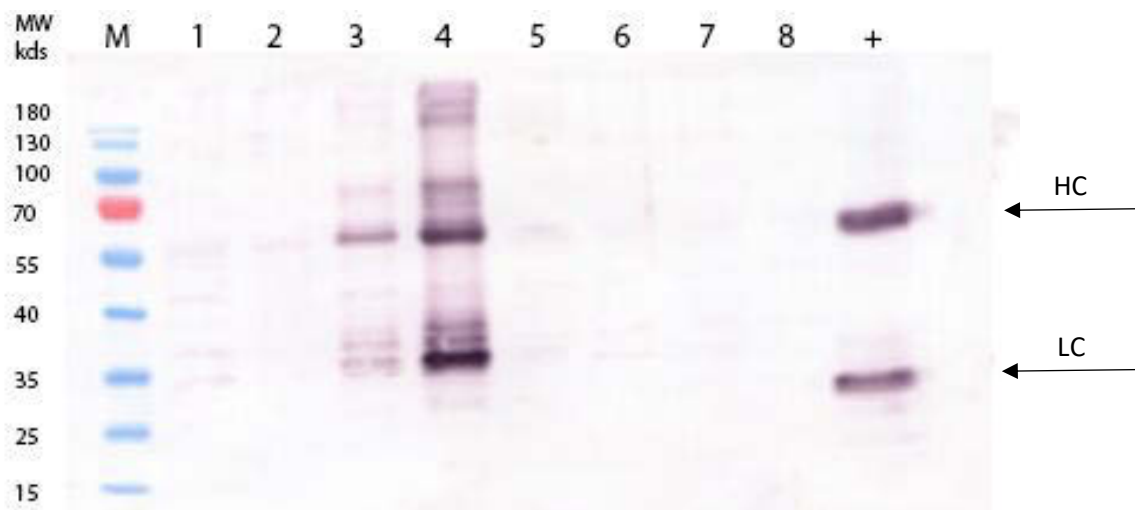


Fig. 48: For the HC detection the procedure was repeated enriched and concentrated via a binding and several washing steps with protein A.

For the HC detection (Fig. 48) the procedure was repeated again utilizing about 10 g leaf material enriched and concentrated via protein A. The plants involved were 11, 13, 14, 15, 19, 22, 24, WT and positive control assembled antibody consisting of heavy and light chain. The light chain is traveling slightly below the heavy chain degradation product. The abundance of degradation product could be explained by the harsh conditions in the apoplastic space where it is secreted to.

For the further crossings the plants number 3 and 4 were preferentially used.

In total 6 individual pairings within 5 lines were obtained, leading to 23 successful individual crosses of 5 plants (Fig. 50). As one tobacco flower (Fig. 49) is capable of producing around 1000 seeds leading to 23 000 potential plants for screening the amount had to be reduced. Three pots were selected (17 x 5, 5 x 5 and 15 x 7) and eight plants per pot were regenerated.



Fig. 49: Targeted pollination of HC plant 15 with pollen from LC plant 6.

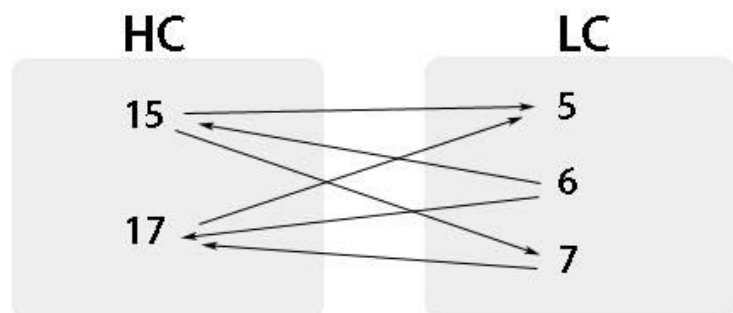


Fig. 50: Schematic drawing of the crossed HC and LC containing plants.

The final screening for the best producer was performed by an ELISA approach and all 24 plants were screened.

3.3.2 SINGLE VECTOR DELIVERY SYSTEM

The final construct pM4-27-2 was also transfected to *Nicotiana tabacum* via an agro infiltration procedure according to a regular Infiltration procedure 2.3.3.

The leaf material remained on plant for seven days and plants were regenerated from leaf discs as described in section 2.5.

This time the regeneration time from infiltration to the first flower could be significantly reduced and dropped from 3 month to 2 month, a possible reason for that was the fine tuning of antibiotics to keep the selection pressure up but not too high. After one month a second transformation step was performed (Fig. 51) to obtain more transgenic plants. This turned out to be necessary due to overgrowing *A. tumefaciens* which were not fully eliminated and remained viable after the first transfer to Cefotaxime-containing medium..

Due to this *A. tumefaciens* contamination nearly half of the plants from the first batch had to be discarded, and as a fact the Cefotaxime concentration was raised to $300 \frac{mg}{L}$ and kept constant on rooting as well as on shooting plates. There were some efforts made to inhibit further *A. tumefaciens* growth with two local treatments of 40 μ L Timotaxim which turned out to be not very efficient at this stage of bacterial growth. In total 40 individual plants were regenerated. Only one regenerating shoot was kept per successfully dividing callus to avoid screening more than one plant with the same genotype.



Fig. 51: Overview of the regenerative stages of NT from leaf-disc to rooting media.

The plants were transferred to soil earlier this time and screened for the presence of DsRed and by an additional dot blot for the presence of the antibody. Before selecting for potential clones the presence of DsRed was screened (Fig. 52) with green light (source: 552 nm) combined with a red filter (filter: 610 nm). The emitted light is interacting with the fluorophore in the leaf epidermis cells and reflects the visible green light but also portions of red light. The red light spectra is able to pass through the filter, where all the green light is absorbed, resulting in a red appearance of transformed leaves on the picture

With this method about half of the plants (15 of all 30) were identified to express at least the DsRed from the construct of interest.

day light

filtered light

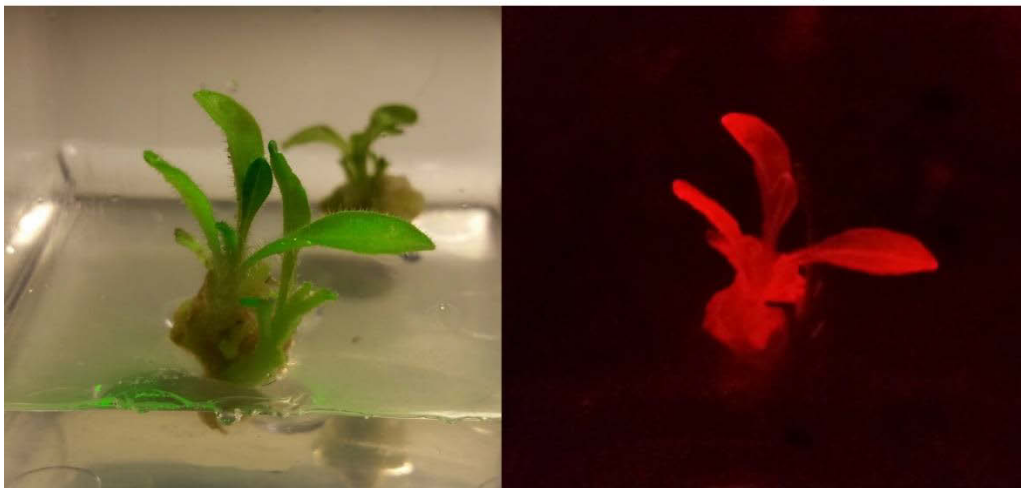


Fig. 52: Selection based on the expression of DsRed for the detection of successfully transformed clones, the shoot arising from the lower part of the callus was detected as negative due to the absence of DsRed. Both plants were irradiated but only the anterior shoot was emitting red light indicating the presence of DsRed and therefore likely the presence of the antibody transgene.

The younger shoot arising from the callus did not seem to be transformed and somehow escaped the Kanamycin selection pressure. Then a reducing SDS page was used to gain more information about the presence of the antibody heavy or light chain.

One month after transferring the shoots from the magenta boxes to the soil they were again observed under green fluorescent light (Fig. 53-55) and red filter to check their expression of DsRed of the epidermal cells of the leaves. Surprisingly, all four observed plants showed completely distinct distribution patterns of DsRed.



Fig. 53: Clone B and C showed homogenous distribution all over the surface, but especially strong in the flower buds and the tips of the youngest leaves. Both plants showed a weak growth and slightly untypical leaves.

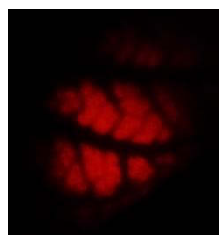


Fig. 54: Clone D showed an inverted phenotype to Clone A with no DS-Red in the younger leafs and strong expression in the first three lower leaves.

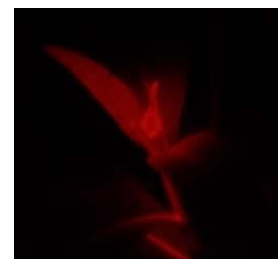


Fig. 55: Clone A showed enriched fields of DS-red in the younger leaves but exclusively adjacent to the veins. While the first four leaves and their internodes showed no signal at all the younger leaves especially their veins were shining bright.

3.4 YIELDS OF THE PLANT DERIVED ANTIBODY

3.4.1 INFILTRATION PILOT EXPERIMENTS

For up-scale two expression systems were compared (*N. benthamiana* and *N. tabacum*) as well as two infiltration techniques. To maximize yield while reducing manual work experiments were set up to compare the usability of the different methods. This led to the decision to go for a transient expression of the antibody in *N. benthamiana*, using the vacuum infiltration technique for a short-term production. In addition, a stable production system using transgenic *N. tabacum* plants was chosen for long-term production. Although small batches of *N. benthamiana* were also performed using syringe infiltration, this turned out to be very tedious and was preferentially replaced by vacuum infiltration.

Before starting production with the first procedure, the parameters were fine tuned. The short-term expression system of choice was *Nicotiana benthamiana* and the vacuum infiltration technique as described in section 3.4.1, the optimal ratio of concentration for *A. tumefaciens* was also determined by pre-tests and set to 1:2:2 for p19:HC:LC.

Another consideration was the optimized harvest point, and here different results have been reported in the literature. Finally two favorable intervals were chosen, 5 days post infiltration and 7 days post infiltration and evaluated for the MC10E7 construct. After running two trials where plants were infiltrated in two day intervals and sampled separately but at the same time, about 10g were obtained from six *N. benthamiana* plants per trial and processed as stated in 2.4.2 and 2.4.3. In both trials a ~25% higher yield was achieved with the seven day setting, as listed in table 43, and used as a basis for further investigations.

Table 43: Comparison of yield for the five and seven day expression system.

5 days post infiltration				7 days post infiltration				
Elu 1	Elu 2	Elu 3	Elu 4	Elu 1	Elu 2	Elu 3	Elu 4	Eluate number
0.795	1.4195	1.6252	0.7405	0.7865	1.4823	1.2514	0.7542	UV-absorption
308.8889	4711.515	1986.061	198.7878	291.7171	5092.121	1230.909	226.464	concentration [mg/ml]
0.45	0.65	0.65	0.6	0.5	0.75	0.7	0.65	Elution volume [ml]
139	3062.485	1290.939	119.2727	145.8586	3819.091	861.6364	147.20	Individual mass [mg]
			4611.69				4973.78	Total Mass [mg]
			238.9				316.8	Yield(mg/kg)

3.4.2 TRANSIENT PLANT DERIVED ANTIBODY YIELD DETERMINATION VIA BRADFORD ASSAY

To produce sufficient amounts to perform the lateral flow immunoassay (dipstick) as well as for the surface plasmon resonance spectroscopy of the chimeric version of the antibody MC10E7 was transiently expressed in *N. benthamiana*. In total 7 batches of plants were infiltrated, harvested after seven days, extracted and purified. The individual yields and concentrations for each are summarized in the table below (Fig. 56). Individual yields reached a maximum of $288 \frac{mg}{kg}$ after 7 dpi.

Table 44: Total harvest of Antibody.

Date	harvest (g)	AB (μg)	yield $\frac{\text{mg}}{\text{kg}}$	construct
10. February	10	850	85	MC10E7
16. February	35	1800	51	MC10E7
24. February	45	9000	200	MC10E7
21. March	80	23000	288	MC10E7
13. April	100	6000	60	MC10E7
18. April	60	7000	117	MC10E7
02. Mai	42	9000	214	MC10E7 + CBD
13. June	10	1200	120	MC10E7 + CBD
06. July	6	400	67	MC10E7 + CBD
28. July	180	19600	109	MC10E7 + CBD
Σ		77850	total harvest in μg	
Σ		78	total harvest in mg	

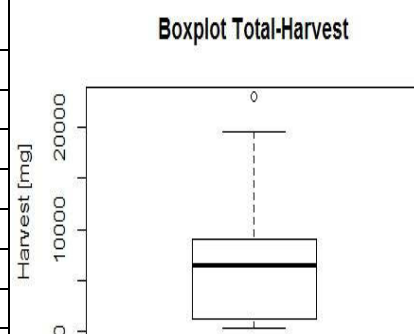


Fig. 56: Yield distribution for the total harvests.

3.4.3 STABLE PLANT DERIVED ANTIBODY YIELD DETERMINATION

Regenerated stable transgenic F1 plants from the breeding trial were screened for antibody concentrations by an ELISA assay. Therefore the 96-well plate was prepared as described in section 2.1.20 and crude extracts of the plants were applied in a 1:10 dilution to determine the presence of the AB in the first run (Fig. 57).

To distinguish between successfully expressing clones and background noise, the six σ -rule was applied. Which implies an addition 6 times the standard deviation of the blanks, which was added afterwards to the mean blank to obtain a positive threshold limit of $4\frac{\text{mg}}{\text{kg}}$.

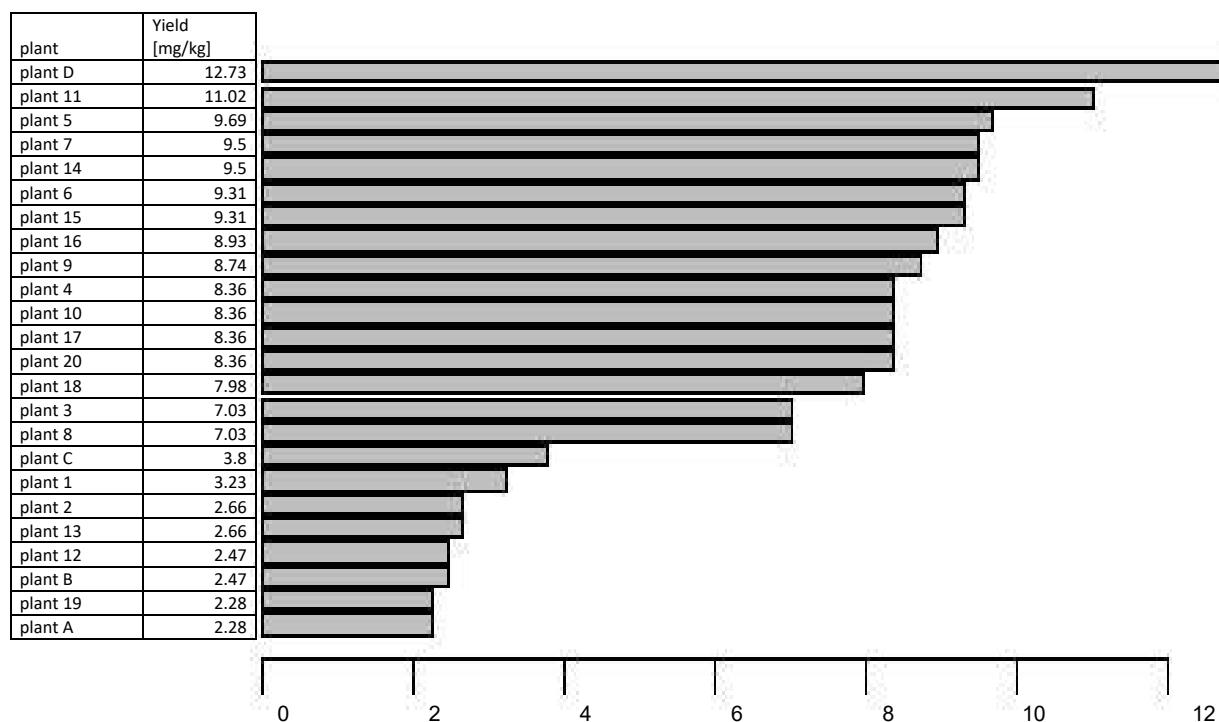


Fig. 57: Distribution of the antibody yield for the prescreen procedure.

In total 22 blanks were measured with an average of 0.13 and a standard deviation of 0.01034. This data was used to determine of positive limit for plants which was calculated as shown and lead to a positive limit of 0.192.

$$\text{Positive limit} = \bar{\phi}_{blank} + 6 * \sigma_{blank}$$

$$\text{Standard deviation} = \sigma_{blank} = \sqrt{Var_{blank}}$$

For a more accurate yield determination the highest producers (all plants above 0.5) were selected and analyzed in a quantitative ELISA. This was repeated three times to obtain statistically valuable data.

The best producing plants 5, 6, 7, 11, 15, 16, D were analyzed by ELISA a second time, to verify the concentrations measured and obtain information of the changes in concentration within the first weeks after regeneration. Plants were sampled from the tip of the third youngest leaf in a nine day interval. Data was analyzed with R-studio to determine the levels of significance.

Three different measurements were taken, 10.10.2016, 19.10.2016 and 28.10.2016 to monitor the changes in yield. To obtain a higher accuracy double measurements were taken for each plant on each sampling date.

Before computing an analysis of variance tables for one or more fitted model objects the normal distribution has to be verified. Data was therefore analyzed with a QQ-blot and decided to be normally distributed. Another prerequisite for the ANOVA is the variance-equality for the given set of samples, this is verified with a Levene-Test, which is a test for significance testing the H_0 = that all individual and group variance is not significantly differing from each other and is identical with the variance of all samples.

According to literature (Köhler et al., 2012), most living systems are normally distributed when it comes to physical properties such as height and weight, therefore it was assumed to continue with an ANOVA.

An ANOVA is a computed analysis of variance for various characters, comparing a numeric value with a factor. When given a sequence of objects, the ANOVA tests each models against one another in the order specified. The linear model chosen estimates no interaction between the investigated characters of data, plant and yield.

Table 45: Analysis of Variance Table, response: yield

	Df	Sum Sq	Mean Sq	F value	Pr(>F)
plant	7	158.208	22.601	77.052	< 2.2e-16 ***
trial	2	286.955	143.478	489.147	< 2.2e-16 ***
Residuals	38	11.146	0.293		

Signif. codes: 0 '***' 0.001 '**' 0.01 '*' 0.05 '.' 0.1 ' ' 1

This ANOVA estimates the influences on the yield according to the parameters of the individual plant and the trial (in total three trials at three dates). Significant influences are marked with three asterisks, according to the significance code. The F value is 77.05, and p-value is very low too. In other words, the variation of plant yield means among different plants is much larger than the variation of AB yield within each trial. Hence it can be concluded that for the confidence interval (p-value is less than 0.05) the alternative hypothesis H1 can be accepted and stated, that there is a significant relationship between the time of sampling as well as a significant difference between the individual plants.

The single factorial ANOVA only states, that within a group of means there is a significant difference. The post-hoc-test (Fig. 58-59) offers a comparison in pairs and provides information which means significantly differ from each other.

Posthoc test for comparison of trials
Study: model.trial ~ "trial"

HSD Test for yield
Mean Square Error: 3.763431

	yield	std	r	Min	Max
trial 1	3.88125	1.845795	16	2.2	8.6
trial 2	9.20000	2.002998	16	7.3	14.5
trial 3	8.92500	1.967570	16	7.1	13.9

alpha: 0.05 ; Df Error: 45
Critical Value of Studentized Range: 3.427507
Honestly Significant Difference: 1.662304

Trial means labeled with the same letter are not significantly different from each other.

Table 46: Posthoc test for comparison of individual AB yields per plant.

	Trial	Means $\frac{mg}{kg}$	Groups
1	Trial 2	9.2	a
2	Trial 3	8.925	a
3	Trial 1	3.881	b

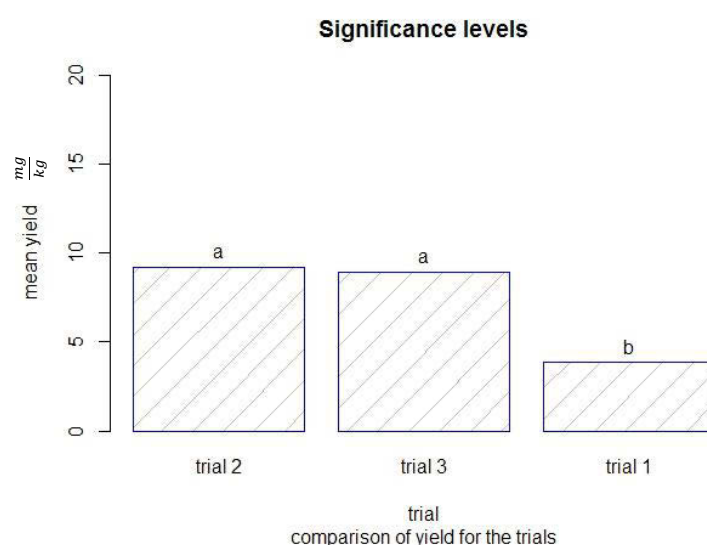


Fig. 58: Illustration of significance levels for the individual trials.

Posthoc test for comparison of yields

Study: model2 ~ "plant"

HSD Test for yield

Mean Square Error: 7.452542

	yield	std	r	Min	Max
11	7.283333	3.257248	6	3.0	10.0
15	6.433333	2.601282	6	2.9	8.6
16	6.650000	2.893268	6	2.2	9.1
17	6.550000	2.413918	6	3.4	8.4
5	6.116667	2.706597	6	2.2	8.4
6	6.233333	2.631856	6	2.8	9.0
7	7.416667	2.325869	6	4.0	9.1
D	12.000000	2.895514	6	8.0	14.5

alpha: 0.05 ; Df Error: 40

Critical Value of Studentized Range: 4.520535

Honestly Significant Difference: 5.038096

Means with the same letter are not significantly different.

Table 47: Posthoc test for comparison of individual AB yields per plant.

	plant	Means $\frac{mg}{kg}$	Groups
1	D	12	a
2	7	7.41	ab
3	11	7.28	ab
4	16	6.65	b
5	17	6.55	b
6	15	6.43	b
7	6	6.23	b
8	5	6.11	b

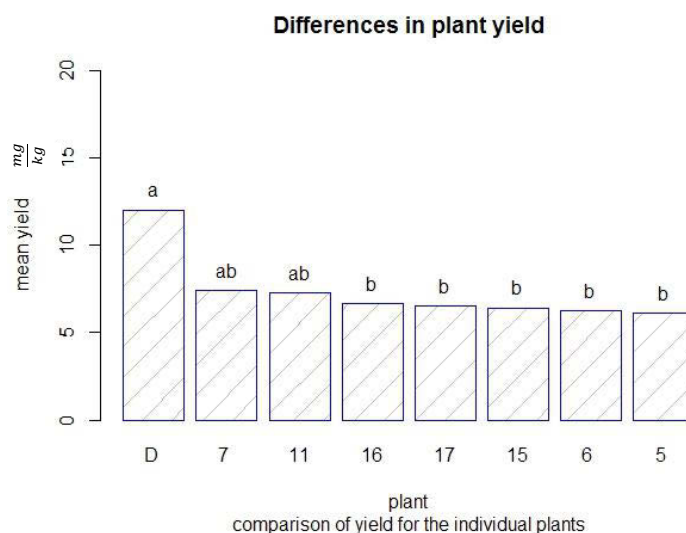


Fig. 59: Illustration of significance levels for the highest producing plants..

Another side experiment in terms of plant derived antibody expression was the investigation of postinfiltration leaf chlorosis (Fig. 60-63) and partial necrosis due to environmental or infiltration stress. This approach was not intended to evaluate the effects on a semi-quantitative or even statistical basis but just to get an impression of the visible symptoms and the potential effects on the plant derived antibody yield. Four different leaf samples were collected. First of all *NB* leaf infiltrated by vacuum infiltration (7dpi), then a highly chlorotic *NT* leaf of an intentionally for this experiment overwatered plant (7dpi), followed by a conventional infiltration pattern of *NT* (7 dpi) and a highly necrotic tissue of *NT* (7 dpi) probably induced by an insufficient removal of medium and thus elevated sucrose concentrations.





NB (7dpi) Sample 1	NT (7 dpi) Sample 2	NT (7 dpi) Sample 3	NT (7 dpi) Sample 4
			
Fig. 60: regular infiltration pattern.	Fig. 61: massive yellow chlorosis.	Fig. 62: Regular sized spots.	Fig. 63: sclerotic spots.



Fig. 64: Crude lysate for the individual patterns.

The MC10E7 was infiltrated in a tandem delivery approach

The crude lysate, containing the AB, displayed already several different levels of coloured compounds (Fig. 64). Where the yellow necrotic leaf sample showed the highest concentrations of stress induced discolouration. The main intention was the comparison of all our observed patterns and their corresponding AB expression levels



Fig. 65: Antibody production, comparison of expression.

By western blot (Fig. 65) it was possible to monitor the related expression levels. The expression level of MC10E7 in NB was quite clear as it would have been expected from the bright green leaf. The yellowish NT leaf instead showed virtually no antibody, as it might be the case due to elevated oxygen stress and reduced metabolic capacity. Both sclerotic spotted leaves of NT showed unexpected similar results although due to the sclerosis in sample four I expected a reduced overall plant derived antibody yield. This data might be an indicator, that also half-strength MS medium used for the infiltration procedure is not reducing the expression due to plant induced stress..

Finally it can be stated, that overwatered plants seem to produce significantly less AB than normally cultured plants. Secondly, the stress induced in the leaves due to infiltration with low amounts of glucose containing buffer is not significantly reducing the AB expression, as the comparison of sample 3 and 4 show that also obviously, glucose damaged leaves can still produce reasonable amounts of AB.

3.4.4 SUBCELLULAR LOCALIZATION

3.4.4.1 ANTIBODY FLUORESCENT-MICROSCOPY

For the fluorescence microscopy the best producer, clone D was selected. The kappa chain was successfully detected via an immunostaining assay, as explained in chapter 2.1.22 to 2.1.24 and was visible in the apoplastic space shown by the red arrows. Although the signal obtained is rather low, consistent with the WB results, it can be observed as faint deposits in the apoplastic space (Fig. 66).

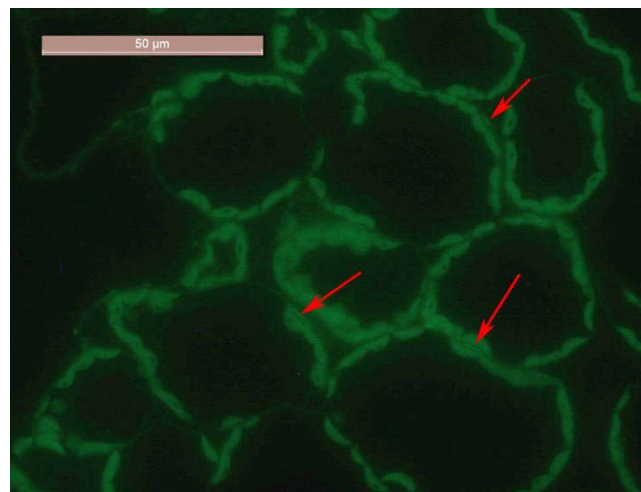


Fig. 66: Fluorescent microscopy image for the subcellular localization of the AB in clone D. The spots of successfully secreted AB is marked with red arrows

3.4.4.2 CONFOCAL MICROSCOPY

Given the low expression level of the protein, a different localization approach was tried in order to improve the signal to noise ratio.

Images were captured using the Leica SP5 CLSM with filter settings for autofluorescence, secondary antibody (excitation 488 nm, emission 500–530 nm), ER-Tracker (excitation 488 nm, emission 500–531 nm). Images were processed using Leica confocal software, ImageJ and Adobe Photoshop CS5.

The confocal images of Clone D derived from the single construct cloning project were prepared as described in Chapter 2.1.25 and localized with a mouse anti human antibody. The images indicated a strong accumulation of AB either in the cytoplasm or ER area. The AB was only hardly visible in the apoplastic region. In contrast to the Cytoplasm / ER where real clusters of antibodies were located.

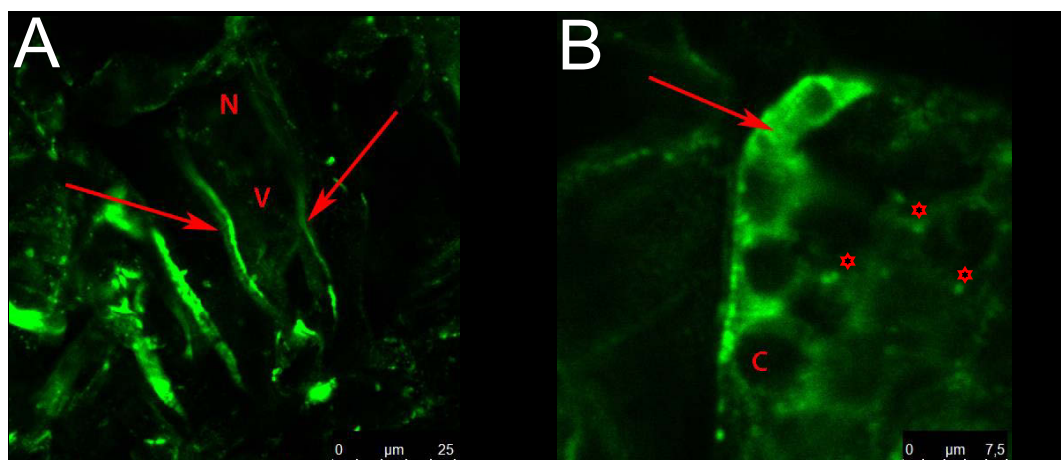


Fig. 67: [A] Localization of the AB in the apoplastic space, indicating a successful secretion. [B] Subcellular localisation of the AB still on the way to secretion, dark circular areas are excluded chloroplasts

Significant signals (Fig. 67 A) derived from the apoplastic space (arrows), could be an indication for successful secretion of the AB. Russel body like inclusion bodies (next to the asterisk).

The arrows indicate an antibody which is already on the way to secretion. See also the signal in between the chloroplasts (c) corresponding to the HC (γ -chain) in the endomembrane system.

Second observation:

In the second observation, an ER marker was used (Fig. 68) to better determine the nature of the punctuate structure where the antibody seems to accumulate to confirm the ER origin of the RB like structures (Clone D). The ER Tracker has a high affinity for the potassium channels, very abundant in the ER and therefore it stains preferably this organelle.

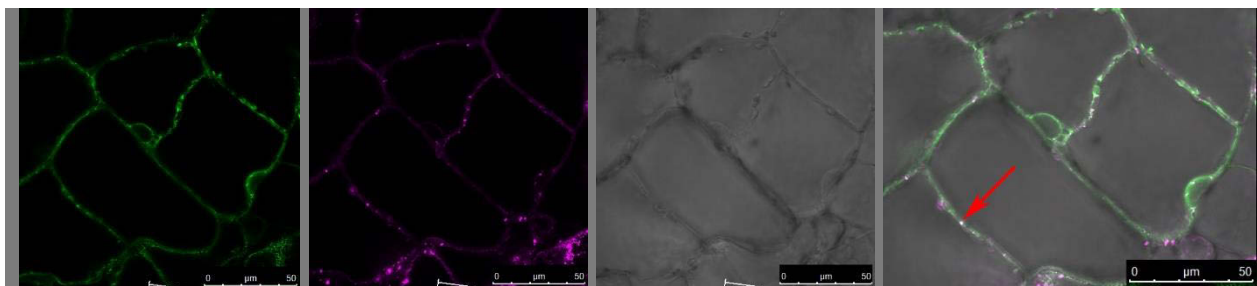


Fig. 68: The following pictures show the (1) an emission of the antibody, (2) emission ER-tracker and (4) a confocal image. A partial colocalization was observed as bright structure in the middle (red arrow) which is a result of the overlay of the magenta and green wave spectra, leading to a white signal, which indicates that a fraction of the antibody is still within the endomembrane system.

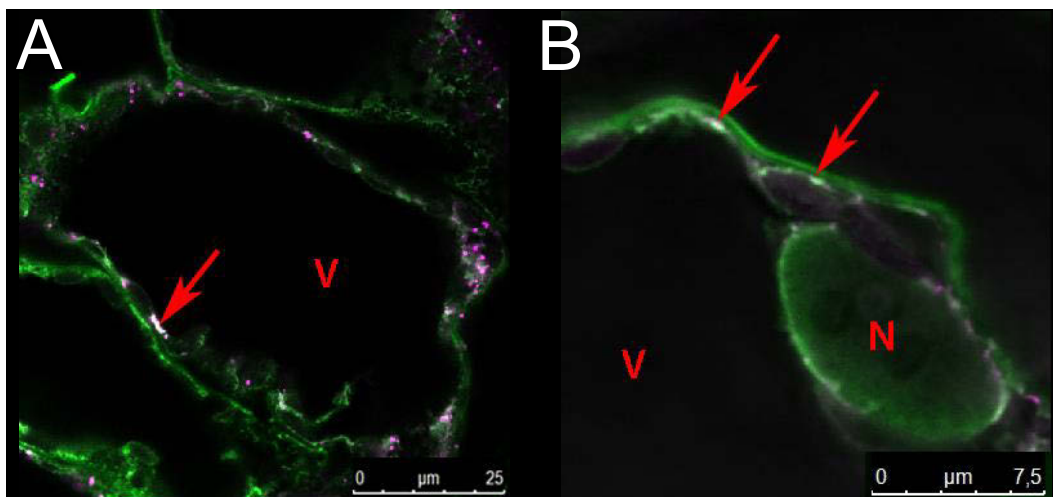


Fig. 69: [A] Detection of the Antibody within the endomembrane system. The colocalization of the AB (red arrows) signal and ER tracker results in white area that indicate that part of the antibody is retained within the ER forming RB-like structures.

In image (Fig.69 [B]) the nucleus is shown in detail surrounded by chloroplasts. In both sub compartments of the cell no antibody was detected, whereas in the region of the plasma membrane, in the upper part of the picture. For the above mentioned reasons, the antibody can therefore be confirmed as successfully secreted into the apoplastic space (Fig.68 A). Although the ER-tracker-red, seems to reveal the presence of diluted structures of accumulated HC as shown in Fig. 69.

4 DISCUSSION

Plants are a favorable expression system for biopharmaceuticals proteins, with certain advantages as well as drawbacks compared to other expression systems. These points should be discussed in more detail as far as related to the two main goals of this thesis, the production of a stable antibody-producing tobacco line and the facilitated downstream processing of the plant derived antibody.

For decades the unknown effects of heavy metals caused severe health problems and were only successfully tackled after developing sufficient methods to detect these toxins. As ADI levels for heavy metals and other organic and inorganic components are established the tracing of specific biological components such as those of the Microcystin group is still difficult.

The market for ABs tracing bio indicators for environmental toxins is relatively small as the high production costs of Abs limit the application to products with at higher financial return rate, like for example human medicinal products.

But the demand for antibody-based and user-friendly assay formats is shown by the desire to trace e.g. estrogens in marine environments associated with food production. For decades, it was not possible to directly detect estrogens but only indirectly by the detection of vitellogenin (Vtg) and zona radiata proteins (Zr-proteins) in male and juvenile salmon. This method required only a general antibody targeting those two proteins (Meucci and Arukwe, 2005). This method required about 1-3 weeks and the handling of laboratory animals. Today it's possible to detect estrogens directly by a simple immune assay (ELISA) and commercially available monoclonal AB's as the SP1-strain targeting direct the palindromic oestrogen response element (ERE) sequence (AGRISERA, 2016).

A similar problem is faced today by blue-biotechnology producing food additives and biopharmaceuticals with algae and their by-product microcystin. Although there are already several polyclonal AB on the market today the main hosts are still rabbit, mouse and hen. Which display in direct comparison to our MC10E7 a lower affinity (Zeck et al., 2001).

Other targets for environmental antibodies are e.g. Exoenzyme S (ExoS) a toxin directly translocated into eukaryotic cells by the type III secretory process of *Pseudomonas aeruginosa*. Or catalase peroxidase (EC 1.11.1.7) is a bifunctional antioxidant enzyme encoded by the *katG*-gene. The enzyme is present in a number of bacterial taxa, including cyanobacteria. Other AB target pathogens of the Enterobacter, *Candida* and *Helicobacter* subfamily which are also part of the microbial flora of aquatic production systems (AGRISERA, 2016).

4.1.1 CLONING OF THE SINGLE VECTOR DELIVERY SYSTEM

The intention to combine HC and LC in one expression vector turned out to be the most successful strategy. Co-expression of ER-retained DsRed facilitated the detection of successful clones under green light.

Although some minor difficulties at the start could have been avoided e.g. the utilization of an expression vector turned out to be the method of choice. It was possible to obtain a successful clone combining HC + LC cassettes (clone M1.2-9) within the expression vector. Retrospectively this first clone should have been used for a first infiltration instead of the individual HC-LC vectors because the possibility to regenerate positive plants from this single construct without the ease of a visible selection marker would be lower but possible. . In the absence of DsRed, which was targeted and tracked to the ER, the full ER processing capacity would be available for the processing of the target protein.

The blunt-end ligation of the light chain led to several hundred successfully transformed colonies. The LC insertion into the pJet vector was a good choice, as the pJet shuttle vector facilitates positive selection significantly. The lethal gene *eco47IR* was sufficiently precise to obtain exclusively positive colonies.

The incorporation of the DsRed gene into the pJET-HLC2 vector was performed with blunt-end cloning and didn't cause any problems, several hundred colonies were successfully recovered and a pre-screen by the "colony-cracking" method had to be conducted to limit the colonies for the PCR-based screen. Three promising colonies were observed together with two other colonies and showed that 4 out of 5 clones carried a positive insertion. Although both potential colonies showed quite promising results in the colony cracking screen one was carrying the plasmid while the two negative controls showed signals very similar to the expected plasmid size.

The final step was achieved by the transfer of the LC:DsRed cassette from the shuttle vector to the pTRAKt vector already containing the HC. In total 33 colonies were obtained and screened. But this time the PCR screen has not verified any of the most likely candidates but colony 9 and 27, showing no significant upshift in prior assay. The result of this screening method might therefore be misleading and should be evaluated critically. The main benefit of this fast procedure which only requires two hours of work is therefore in balance with the time required to set up a PCR screen.

After the transformation with *A. tumefaciens* two positive colonies were checked for growth rate and sedimentation behavior as some strains caused difficulties in centrifugation, probably due to the formation of polysaccharides. This problem is quite common in cultures containing carbohydrates, and *Agrobacterium tumefaciens* produces vast amounts of extracellular polysaccharides. This results in colonies having a voluminous, slimy appearance (Pawar Sandip, 2017).

Despite both *A. tumefaciens* colonies showing the correct insertion of the plasmid the final transient yield differed significantly as shown by the first western blot. This could be explained by a different transfection potential of the individual strain. Colony 2 showed reasonable AB yields in a transient trial, whereas colony 7 resulted in virtually no AB expression; this was also confirmed by a second biological repetition but not further explored because the stable plants were produced with colony 2.

The individual *N. tabacum* clone D of the full length antibody showed the highest expression. Thus leading in this trial to a higher success of the single vector delivery approach than the tandem delivery approach, which could also be coincidence as the number of regenerated plants was very low. Although the individual clones regenerated from the single construct delivery project were only a fraction in quantity compared to the individual plants regenerated from the tandem delivery approach.

The expression of DsRed facilitated the screening process enormously and reduced the amount of plants brought to soil from 23 individuals to 8 individuals expressing DsRed. The fluorescent protein (FP) proved to be expressed efficiently in the chosen system to provide sufficient signal above autofluorescence to be reliably detected and imaged. The sufficient photo-stability was also fit for the intended use, although other FP like mCherry would offer a six fold higher stability. The brightness is another factor to consider, where mCherry has a fourfold higher brightness to be imaged thus leading to a clear observation with much lower expression levels (Shaner et al., 2005).

Except the stability issues the retention of the DsRed within the ER might also lead to a bottle neck in ER-processing where it accumulates and limits the capacity for HC and LC processing. It can be concluded that there is a need to incorporate the DsRed gene, despite the amount of DsRed produced could have been also kept at a moderate level by changing the 35S promoter with the double enhancer to a regular 35S promoter or another less strong constitutive promoter. A weaker promoter could lead to less expressed DsRed, which is primarily needed during selection in the tissue culture and for the selection of heterozygote seedlings but afterwards obstructive for production. A more attractive possibility would be to target DsRed to plastids (Sack, Rademacher et al., 2015), where a tandem-construct containing HC and LC and a second construct containing also DsRed were tried in parallel. Resulting in several lines containing just AB and AB + DsRed, with no significant difference in AB yield although DsRed was expressed at quite high levels. This would suggest, that the expression and targeting of DsRed to plastids does not significantly decrease the yield of the target protein.

This project utilized a constitutive promoter to facilitate the selection in tissue culture. It turned out to be quite useful, but maybe a limiting factor for high yield expression. As those clones are probably experiencing severe growth difficulties. The application of an inducible plant promoter, stimulated by e.g. day-light-length (Weisshaar et al., 1991) or the application of chemicals (Zuo et al., 2000) might be a challenge for the selection procedure but could lead to a higher biomass production as plants are able to grow unhindered to full size without the burden of additionally expressed protein.

4.2 TANDEM VECTOR DELIVERY SYSTEM

This trial was intended to gain statistically comparable information about the two approaches and evaluate them. The constructs were delivered separately having one pool of plants carrying HC and one pool carrying LC. After a four month regeneration process these plants were screened for the highest producer of either heavy or light chain and then crossed. While crossing of *N. tobacco* was relatively easy compared to other crop plants especially of the poaceae family the screening proved to be quite difficult. The expression of only one chain of the antibody leads to a higher susceptibility to degradation explained by a limited folding ability and consequently a reduced stability.

The amount of time required for the identification and crossing of the parent plants as well as the time required for growing two plant generations were not proportional to the final result of about $7,4 \frac{\text{mg}}{\text{kg}}$. The pre-screening procedure at the T1 level (transformation generation 1) required about 10g leaf material when screening for the HC.

It can be concluded that the delivery of HC and LC cassettes on separate plasmids was faster as no plasmid construction was necessary to start with this project.

However, the single construct delivery system (four plants regenerated) was leading to significantly better yield (clone D 12 mg/kg) than the best expressing tandem delivery system derived plant (plant 7 with 7.5 mg/kg). Nevertheless, the average yield was similar when comparing the tandem delivery system to the single construct delivery system. The potential of this tandem delivery system was also shown by (Tremblay et al., 2010) who crossed individual tobacco plants expressing single HC or LC, sexual crossing resulted in progeny lines that expressed and accumulated a fully length mouse AB at levels up to 1.3% of total soluble protein (TSP).

4.3 REGENERATION OF TRANSGENIC PLANTS

Two repetitions of infiltration (vacuum), sterilization (2% NaOCl for 8 min) and regeneration (150 mg/l Cefotaxime and Kanamycin to 100 mg/L) were performed. As shown from the first trials many plants were lost due to overgrowing *A. tumefaciens* from the first batch and less in the second batch by a better balancing of antibiotics. Also the regeneration time was significantly lowered from the first experiment to the second experiment from about 100 days to about 70 days.

A lower antibiotic stress positively affected the regeneration speed at the beginning, leading to a less strict selection for the plant cells for the formation of the primary callus. Then the plants were subjected to a higher concentration of Cefotaxime $150 \frac{\text{mg}}{\text{L}}$ to inhibit the growth of *A. tumefaciens*. This approach although leading to a fast regeneration had certain problems with overgrowing *A. tumefaciens* appeared again and infected about 30% of the first experiment. The adjustment of the antibiotic level as a crucial factor for the regeneration speed and quality, and the time taken for regeneration could be cut back by 30% from 100 days in the first round to about 70 days for the M27-3-2 construct.

The plants derived from the single construct delivery system had the additional metabolic burden of producing DsRed. The time necessary to generate a homozygous and highly producing stable transgenic plant line is very long, and frequently exceeds two years or more (Christou and Klee, 2004).

In transient expression systems, the total expression level is determined by many factors including promoter strength and translation efficiency of the recombinant mRNA. In transgenic plants the site of T-DNA insertion is an additional factor and the number of inserted copies also affects the expression levels. Therefore, multiple stable transgenic plants should be established for each expression construct to manage insertion-site position effects (Christou and Klee, 2004). In this survey about 25 to 50 transgenic events were created for each delivery system. The construct expression range was in both delivery systems about the same and ranged for the tandem delivery system from 0.15-7.45 mg/kg and for the single construct delivery system from 0.14-12 mg/kg. About 25 plants were regenerated from the tandem delivery system. From the single construct delivery system 4 plants were finally regenerated after DsRed pre-screening. It is also important to take multiple samples, e.g. extracts from 6-8 harvested leaves per single clone to avoid too big variation (Ma et al., 2015)

We used PT-Havanna variety, which is mainly a fast cycling clone and not a commercial variety for high biomass accumulation. A comparison of different tobacco varieties might lead to better expression clones producing up to 100 000 kg/ha (Gutierrez et al., 2013). This problem could be targeted by crossing with high biomass producing *Nicotiana* varieties and backcrossing to industrial *Nicotiana tabacum* varieties.

During this project the selection was conducted until T2 which is quite short compared to other projects, which progressed until T5 generation, and might explain the relatively low yields. Further work to obtain a master seed bank (MSB) will continue at least until T5 using homozygous seed stocks for a single transgene locus of the GOI, with confirmed single-gene Mendelian segregation. For all subsequent selection steps both HC and LC should be addressed and checked. (Ma et al., 2015) confirmed that T5 to T10 of a 2G12 expressing tobacco line, showed a constant number of transgene copies per genome and constant transcript size, as determined by Northern and Southern blotting. Further on it was shown, that antibody yields are positively influenced by a selection procedure and can increase from ~10 µg/g in T1 plants up to ~25 µg/g in plants of the T3 generation. Thereafter, the yield was effectively stable. Subsequent testing from T3 extending up to T10 plants showed no difference in leaf biomass or plant height across all the generations of plants. (Ma et al., 2015)

In conclusion, it may be stated that the life cycle of one tobacco generation may have been finalized earlier when applying the water-soluble compound Ethylene or commercially available products like Ethyrel, which is absorbed by the plant and cracked into Ethylene, chloride and phosphate to speed up the seed formation. But due to the very narrow range of Ethylene, starting already at 0,1 ppm (Hart et al., 2002) and difficulty in dosage this idea was rejected. Also the cultivation of plants for the infiltration should be conducted under

fluorescent light and not under high pressure sodium or equivalent lamps. Low radiation intensity should be preferred, as the development of densely packed palisade parenchyma, which is difficult to infiltrate is directly enhanced by the application of stronger radiation, where the loosely packed mesophyll tissue contains a higher volume of gas space for a successful infiltration. And compared to the plants growing under high light conditions, they also have less thick cell walls (Tosens et al., 2012).

4.4 TRANSIENT ANTIBODY PRODUCTION

The transient production of mAb in plant-expression systems provides a fast and scalable method to meet the marked demand especially in case of pandemic events which require immediate response as it has been demonstrated during the EBOLA crisis in 2014 (BOSELEY, 2015). Currently, there are no licensed vaccines for the EBOLA virus available on the market, although it has been declared as an important goal by the U.S. Department of Health and Human Services. A cooperation of BOKU researchers around Herta Steinkellner and Mapp Biopharmaceuticals developed, produced and tested three different glycosylation patterns for the mAb. The variable region of the 13F6 was therefore grafted to a human IgG₁ and expressed in a transgenic *N. benthamiana* line, lacking plant specific N-linked glycoforms. It was possible to produce highly human like mAb glycoforms with enhanced affinity and stability tested in a mouse model (Zeitlin et al., 2011).

The utilization of plant viral vectors, commercially known as magnICON vectors, enabled a simultaneous expression of HC and LC from two replicating viral segments (Giritch et al., 2006). These vectors were introduced separately by an *A. tumefaciens* mediated infection and led to a rapid transient expression of protein, usually within 3-4 days. This system can also provide a fast scale up of functional full size IgG1 mAbs in plants, if all HC and LC are introduced independently (Marillonnet et al., 2004). The difficulty of a co-expression of multiple proteins, as it is required for a full length antibody, is overcome by using vectors based on two different viruses that can access the same cell and trigger the GOI expression (Sainsbury and Lomonosoff, 2008). Together with Mapp Biopharmaceuticals and Kentucky BioProcessing it was possible to produce sufficient amounts of mAb to start clinical tests earlier than with any other expression system (Hiatt and Pauly, 2006). Demonstrating, that this technology is fit for the intended use and highly flexible for potential future endemic crisis to be applied.

Non-viral approaches for increased transient yields are mainly depending on vacuum infiltration procedures and highly efficient expression plasmids. In addition to the already mentioned P19 expression also other non-viral approaches have been developed to speed-up transient yields. It has recently been shown that flanking the GOI sequence with a modified 5' – leader sequence and a 3' untranslated region (UTR) originally derived from Cowpea mosaic virus (CPMV) significantly improves expression levels. The pEAQ vectors derived from this first vector series led to an increase of +10% total soluble protein. The expression of the 2G12 monoclonal AB from a single pEAQ plasmid represents the highest reported yield of transient antibody from plant tissue, infiltrated with only a single *Agrobacterium* culture (Sainsbury et al., 2009).

Protein yields can also be improved by the implementation of stabilizing domains as well as fusion sequences. Such modifications may not be suitable with clinical applications but might work out very well with nonclinical applications, as industrial or cosmetic applications or environmental sanitation. The genesis of protein bodies (PB) derived for example from the endoplasmic reticulum (ER) can be induced in plant tissues not adapted for storage functions e.g. leaves by fusing polypeptide sequence tags derived from, elastin-like polypeptides (ELPs) (Gutierrez et al., 2013), cereal prolamins or fungal hydrophobins with the protein, which increases the stability of stored proteins due to PB formation (Sack, Hofbauer, Fischer, Stoger, 2015b).

4.4.1 YIELD OF TRANSIENT ANTIBODY MC10E7

The preparation for the vacuum infiltration was time consuming method. Despite this effort was it was a fast and satisfying method to infiltrate big batches of plants. Although the accumulation of polysaccharides during growth hindering the centrifugation lead to a big loss of cells, which was also observed by (Pawar Sandip, 2017). The first spin down was usually the most difficult and exceeded the maximum recommended spin down acceleration of 8000g for 7 min, as explained in (Bechtold et al., 1998) when using 9000 g for 15 min where the cultures were always clearly separated from the media. But after the induction procedure the acceleration was reduced to 3500 g for 20 min to avoid any harm to the induced plants.

The plants used for the infiltration were selected to be healthy and not exceeding the bolting stage. The plants should also be completely immersed and the maximum number of transformed plants should not exceed 50 individuals using the same infiltration suspension due to the dilution of the media and the repeated stress at low vacuum for the plant cells (Bechtold et al., 1998).

As shown in table 43 the total extractable AB reached a value of more than 300 mg/kg and could therefore be considered about 25x times higher than the yield of the stable plants.

4.5 ANTIBODY YIELD OF TRANSGENIC *N. TOBACCO* PLANTS

To accomplish one major task of this work, the comparison of the stable plant derived from the tandem vector delivery system and the plants regenerated from the single vector delivery system. Therefore a big screen for the plant derived antibody concentrations was conducted by an ELISA assay.

The sample number was limited by the number of positive regenerated plants and reached about 50 plants in total, 26 of them derived from the tandem vector delivery system and another 24 from the single vector delivery system where only 4 were transplanted to soil due to the pre selection via DsRed. Thus the total amount of plants was too small to obtain a normal distribution. The standard deviation of the yield for all screened plants was unexpectedly high for the tandem vector delivery system (0.14) and even higher for the single vector delivery system (0.22) which could be explained by the small number of clones

regenerated. As well as potential silencing effects or site effects depending on the chromosomal region inserted.

The determination of yield was performed in three biological repetitions for the highest producers, while a double measurement was undertaken with every plant. The two hypotheses were

H₀₁: The AB yield is stable within the time of observation.

H₀₂: Every plant has the same level in AB yield.

To answer these questions an analysis of variance was conducted. All following calculations were undertaken with an alpha of 0.05. Before answering the H₀₁ a linear model of additive quality was chosen thus assuming that there is no plant AB expression level affecting another plants AB expression level. This ANOVA estimates the influences on the yield according to the parameters of the individual plant and the trial (in total three trials at three dates). Significant influences are marked with three asterisks, according to the significance code. Due to very low significance value of 10⁻¹⁶ the time of sampling contributes significantly on the yield as well as the individual plant itself, expressing AB on significantly different levels from plant to plant.

The F-value, in both cases very small, 2.2e-16: is the test statistic used to decide whether the sample means are within sampling variability of each other. It can be used to test the hypothesis H₀. Which is equivalent as asking whether the model has statistically significant predictive capability. The F-value is the ratio of the Model Mean Square to the Error Mean Square (Mean Square Error of 3.76). Under the correctly assumed null hypothesis that the model has no predictive capability the F-value would be very large and the null hypothesis is rejected if the F ratio is larger than 0.05.

The output of the HSD post hoc test is a table showing groups of significance, means with the same letter are not significantly different from each other. Thus leading to the conclusion that the last two trials conducted at the 19.10.2016 and 28.10.2016 are significantly differing from the first trial checked on the 10.10.2016. As the first trial was undertaken three weeks after transplanting to soil the yield showed up to be lower than the yield after a certain maturation period. The yields for trial two and three showed significant similarities thus leading to the conclusion that after about a month on soil the expression of antibody reaches a certain level. It might change after this time, but due to restrictions in time there were no further investigations undertaken to determine the yield after two months, when plants are in flower, which might be interesting as well.

It is not possible to apply a general rule for the determination of the minimum timescale from soil to screen, but in this specific case the antibody yield varied significantly within the first month on soil leading to the conclusion that plants should not be checked within the first month after transplanting but rather at a certain and well defined developmental stage, e.g. intermediate bud stage where the concentrations are elevated to obtain comparable results.

To test the H₀₂ another HSD post hoc test was performed showing that plants do significantly vary in terms of yield from each other.

Finally it can be stated, that the effects described above do significantly influence the yield and are worth to be investigated further i.e. as a step to generate starting material for further crossings. It is also possible to achieve much better antibody yields as shown e.g. by (Paul et al., 2014) were $15.2 \frac{mg}{g}$ leaf fresh mass in transgenic tobacco and $25 \frac{mg}{g}$ leaf fresh mass after transient expression have been achieved.

4.6 CLONING OF THE ANTIBODY-CBM EXPRESSION VECTOR

The PCR-based cloning approach offered the possibility to operate in a sequence lacking restriction sites. For this purpose specific dual-primers were designed to accomplish the correct annealing for the first and second stage binding.

While the two flanking primers (forward 1 and reverse 4) were designed by a standard procedure, it was slightly more challenging to design primer 3 and 6, which amplified originally from one plasmid and had also a chimeric tail, usually eight base pairs as described in the literature (Sambrook & Russel, 2001) for the alignment of the full construct.

Primer five and three contained the artificial linker (GTCTCTTTCTCCTGGAAAG) between HC and CBM but without the stop codon. Primers were designed to have similar melting temperatures and could therefore be used in the same thermocycler program.

4.7 BINDING CAPACITY AND SPECIFICITY OF THE CBM

The binding capacity of the CBM was analyzed in several approaches which consistently showed a clear upshift of about 397 bp compared to the positive control is indicating a successful attachment of the CBM to the HC.

. The intention of the CBM was to attach the AB to cellulose which would be a cost efficient method to purify it as well as a convenient way to fix it to a cellulose matrix for application. The overall goal in terms of cost efficiency would be the attachment of the AB to the plant cellulose enabling the whole plant material to be used as a bio filter for environmental sanitation programs.

First of all a regular purification procedure as described above combined with a western-blot to find all residues of the antibody in the different steps of the downstream process. As the cellulose of the cell wall might be difficult to access for the CBM or not sufficiently present the addition of cellulose was an alternative approach. This approach showed no significant results, in terms of antibody retention within the pellet. And led to the conclusion, that the cellulose of the primary and secondary cell wall is not the limiting factor for the binding of the CBM.

Other experiments tried to elute the antibody from the matrix by the application of cosmotropic agents such as a 1 M Ammonium sulfate solution. The goal of this approach

was to increase the hydrophobic effects by increasing the amount of intra-protein-specific order and precipitate the proteins from the bulk solution. After observing the apparently enhanced binding capacity, compared to the regular MC10E7 AB, to G-protein crosslinked sepharose beads the whole procedure was repeated evaluating the affinity of the CBM to pure sepharose beads. As we have observed a slightly higher affinity of the antibody-CBM-conjugate to the G-protein beads than the primary IgG. One assumption was the potential interaction of the CBM with the unbranched polymer of agarobiose units.

4.7.1 ANALYSIS OF THE CBM PROPERTIES

In the first biological repetition we tried to reveal any effects of the expression system (*Nicotiana tabacum* and *Nicotiana benthamiana*) on the purification procedure. *N. tabacum* seems to express a bit stronger than *N. benthamiana* but on the other hand, has more degradation products. Therefore a successful binding of the antibody to the pellet cannot be stated. To verify the result of the first trial the *N. benthamiana* and *N. tabacum* expression system was compared once again. The sample tissue was combined, homogenized and used as starting material for each extraction method. The regular extraction procedure for *N. benthamiana* yielded a protein with the molecular mass of 174 kD indicating a successful fusion product of HC and CBM. As well as some degradation product of about 55 kDa and 40 kDa. The amount of degradation product is lower in the pellet derived from the first centrifugation step of the crude lysate, which indicates, that mainly the fully assembled antibody seems to stick to the pellet [2]. After washing the pellet a second time the amount of antibody in the supernatant was lowered significantly and showed virtually no LC, which could be explained by the limit of detection for a western blot and the low molecular weight.

The three different elution procedures were checked: first of all the elution with purified water [4] which removed some antibody from the pellet but in the same amount also some AB degradation products, which are more effectively eluted from the pellet via the Glycine treatment. If evaluated in a semi-quantitative way the elution with water and glycine at pH 3 showed similar results. In contrast, the treatment with Tris removed the plant-derived antibody more effectively from the pellet, which might indicate that the CBM binding capacity is reduced under alkali conditions. This was observed with other members of the CBM family too (Linder et al., 1999). Although the pellet was washed two times with PBS buffer, prior to the three elution methods, high amounts were obtained, probably reaching 25% of the antibody produced in total. This brings up the question if this is due to the properties of the CBM or occurring also in the standard extraction procedure.

Here the first supernatant shows significant levels of antibody as well as the degradation products at 55 kDa and 40 kDa. The first pellet of NT showed lower antibody concentrations than in the NB trial, which might indicate that the extra-cellular matrix of *N. tabacum* is less favorable for the CBM binding. Here we need to account the different amounts loaded on the gel, the liquid phase applied was 100 µL and the pellet was 50 mg which makes a direct comparison difficult. The degradation product is mostly found in the second supernatant [3]. For the same three elution methods applied (water, Tris and Glycine) the relative success didn't differ significantly. The water and Tris elution showed quite similar results where the elution with glycine [6] removed lower molecular weight components of about 18 kDa and 20 kDa which do probably not represent the LC which runs in the positive control [7] lightly lower at about 15 kDa.

The next approach tried to identify the plant derived antibody residuals in the individual steps of the regular extraction procedure from *N. benthamiana*. The supernatant of the first and second wash showed familiar patterns as before, with a significantly lower level of degradation product in the second supernatant.

For the first pellet a loading mistake must be assumed as the plant derived antibody is virtually not present in the first pellet but in the second one. It seems that after two washing steps the plant derived antibody is removed to a high degree and the third supernatant is not showing significant amount of plant derived antibody. As experienced from the first trial the Tris extraction method seemed to work quite well, this time the sample was brought to pH 8 with hydrochloric acid to check if the successful elution was just due to the pH shift. But the elution was not significantly better than the beads elution with glycine at pH 3 whereas the elution from protein-A beads with glycine pH 3 failed and left plenty of plant derived antibody on the beads. The eluted beads were washed and applied directly to the SDS-PAGE sample preparation. Concluding, it can be said, that the protein-A beads bind the plant derived antibody very efficiently but it cannot be eluted efficiently with glycine at pH 3.

The intended goal of the third biological repetition was to produce sufficient amounts of antibody to conduct all trials necessary to find out more about the properties and specific behaviors in combination with Cellulose. To fix the plant derived antibody to the pellet and have as little amounts in the supernatant as possible.

Another intention was to determine the long term stability of the antibody bound to the protein-A beads for three days at 5 °C followed by a regular elution procedure with glycine at pH 3. The eluted antibody showed clear coagulations and precipitated as milky white mass at the tube bottom. The binding to G-protein binding should therefore be kept at manufacturers recommendations and not exceed 12 h for IgG antibodies. The precipitate and the upper phase were sampled via a syringe needle and applied individually to the western blot. According to expectations the clear upper phase did not contain significant amounts of antibody, so it was no surprise the band was absent. But for the lower phase with all the precipitated antibody there should be a strong bands visible at 77 kDa and 25 kDa which were not present. Such Possible explanation as the high degradation of the antibody was taken into consideration, but couldn't hold true as the blot was performed under denaturing conditions and the paratopes should be sufficiently exposed for the secondary antibody to successfully form an antibody sandwich if there would be any primary AB present.

The flow through (*Fig. 41*), from the washing steps of the protein-A beads, contains a fraction which is visible as a clear band, slightly lighter than the regular LC. This band might be an indicator for a degraded LC and the antibody was already partially disassembled or never fully assembled. The boiled beads on the other hand show a clear pattern for the fully assembled antibody as well as some degradation products at a slightly lower molecular weight. Neither for HC nor for LC double bands or smear-signals occur, instead the signals are clearly visible against the degradation-product-free background. This might indicate that the long-term avidity of the fully assembled HC and LC bind more efficiently to the protein A beads than degradation products, which are easily washed off.

It can be concluded, that the attachment of the CBM to the C-terminal end of the AB provided completely new properties in terms of avidity to different substrates, which are still not fully understood. There seem to be a negligible differences in both expression systems, although

the retained AB in the pellet was overall slightly higher in the NB expression system. The standard extraction procedure with protein A and Glycine at pH 3 failed and left plenty of plant derived antibody on the bead which might lead to the conclusion, that the protein-A beads bind the plant derived antibody-CBM-conjugate with a high avidity. Also different elution methods, starting with the retention of AB within the pellet by high ammonium sulfate concentrations followed by an elution with distilled water as described by (Sugimoto et al., 2012) were not successful. This can also be explained by the big number of homologues of these CBDs and CBMs in the CBM2 superfamily.

4.7.2 ELISA - CBD BINDING CAPACITY

For a quantitative evaluation of the CBM binding affinity the most applicable method, protein-A extraction as well as two new methods were tested. All three procedures started with the homogenized and resuspended primary pellet obtained by a regular PBS extraction.

The primary pellet, derived from the first centrifugation step, displayed in all three measurements a similar value of about $9.8 \frac{ng}{mL}$ of AB and indicates a consistent measurement, as all three samples were taken from the same crude pellet and were not further treated. After that 0.2 g of crude pellet in a 1:1 ratio with PBS pH 7.4. After the incubation with protein-A beads the antibody was eluted with Glycine at pH 3 and both fractions analyzed. First fraction was the remaining beads after elution which showed definitely an elevated concentration compared to the crude pellet, indicating that the protein-A beads were able to bind antibody left in the protein-A solution but the elution was not completely successful. But when observing the eluted fraction, an elevated concentration was measured there indicating that not all antibody remained in the pellet but more than half of it was eluted properly, which is compared to former recovery factors tenfold less. When accounting the spherical bead volume and the reduction of the void fraction the recovery function indicates about 25% losses, which is significantly above the usual 5% losses (Melnik et al., 2016, in preparation) with the regular MC10E7.

The same procedure performed with sepharose led to an equivalent concentration for the first two samples, of about $10 \frac{ng}{mL}$ for the crude pellet and about $5 \frac{ng}{mL}$ for the PBS solution as expected. But the results of the elution pattern clearly reject the hypothesis of an elevated affinity of the CBM-antibody-conjugate with cross linked sepharose beads. Because the concentration of the incubation solution ($\sim 5 \frac{ng}{mL}$) was significantly higher than the antibody after elution ($\sim 2.5 \frac{ng}{mL}$). This leading to the conclusion that it might have been just the incubation solution replaced by glycine and eluted off the sepharose beads.

The second hypothesis (H0₂) tested was the defined degradation of cellulose via cellulase to recover the AB attached to defined polysaccharide fragments. The first two samples confirmed the measured concentration of the primary pellet and the cellulase solution ranging from $\sim 5 \frac{ng}{mL}$ to $\sim 10 \frac{ng}{mL}$. After inhibiting the cellulase the solution was cleared by a centrifugation step as described above and incubated with 150 μ L protein-A beads to determine the concentration of antibody in the supernatant after the degradation with cellulase.

When comparing the crude pellet, derived from the first centrifugation step, with the same pellet treated with cellulase, the antibody concentration was clearly reduced from the crude pellet to the cellulase treated pellet, which might be explained by the cellulase treatment or the higher AB affinity of the protein-A beads. But when comparing the results of the elution from the beads $13 \frac{ng}{mL}$ with the obtained concentration by pure protein-A application ranging also at $12.5 \frac{ng}{mL}$ the effect cannot be explained by the cellulase activity. Which must have led to an enhanced availability of AB for the protein-A extraction and a higher recovery than just $13 \frac{ng}{mL}$.

But as this is not the case it can be stated, that the degradation of the pellet with cellulase has therefore not significantly enhanced the recovery of AB from the pellet and cannot provide the specific conditions needed for an efficient extraction of the CBM-antibody conjugate. The sepharose beads also did not attach significant levels of antibody, compared to the incubation solution leading to the conclusion that there is no elevated affinity to sepharose provided by the CBM.

4.8 SUBCELLULAR LOCALIZATION

The confocal images of Clone D (12.10.2016) obtained by transferring the M4-27-2 were clearly indicating the presence of antibodies within the endomembrane system. In contrast, the signal from the successfully secreted antibody was only hardly visible in the apoplastic space, contrary to the endomembrane system where a colocalization with ER-tracker red showed clusters of inclusion bodies. This might be an indication, that the ER machinery is approaching its processing limits due to an excess of heavy chain protein. Similar observations were also made with GFP leading to a ER overload (Kintaka et al., 2016). On the other hand is the particular expression level of 12 mg/kg far below the yield of Kintaka and might also be due to incorrect assembled HC polypeptides.

The unassembled HC may be retained within the ER, but as the total yields indicate, that there is probably no abundance of HC overloading the ER. They contain the recombinant protein, or ordinary cell constituents in a normal or degenerating condition and appear either single size or, more often, in various proportions (Martelli, 1977).

Samples taken from Clone D at a later stage of plant development (28.10.2016) were prepared and observed in the same way and additionally stained with 2 μL of ER-tracker. A partial colocalization was observed which indicates that one part of the antibody is located within the endomembrane system, and still on the way to secretion. The antibody was finally detected as successfully secreted and might have shown an affinity to the secondary cell wall, probably due to the porous structure. It might be also interesting for future projects to avoid a DS-Red accumulation within the ER and instead target the DS-Red protein to certain plastids. This might release stress from the ER-apparatus, which is working at full blast due to the amount to artificial protein expressed. Finally it can be said, that the MC10E7 was successfully detected in the apoplastic space. A partial colocalization was observed by the use of the ER-tracker red which indicates that a part of the antibody is still located within the endomembrane system, and on the way to secretion.

4.9 INTROGRESSION AND GENE FLOW

Finally the potential environmental concerns about this technology should be addressed, as the possibility of a genetically modified crop to transfer foreign genes by pollen flow to related plant species has been mentioned as an environmental concern. And is controversially discussed (NIJS et al., 2004). One side goal of this work is to address concerns from the public side and provide some information to improve the frequently emotional discussions to an objective level. The intention, when including the easily traceable DsRed marker into the transient plants, was to contribute to more transparent GMO policy. And to provide a backtrack option in case of doubts and uncertainty of origin.

Most molecular approaches targeting the control of gene flow among crops and wild relatives have primarily focused on maternal inheritance, male sterility, as well as seed sterility. But also several other strategies may be useful in restricting gene flow, including apomixis (asexual seed formation), cleistogamy (self-fertilization in bud stage), genome incompatibility, chemical induction of transgenes. No strategy has still been proven broadly applicable to all crop species and maybe a combination of approaches may be considered for engineering the next generation of crops. One alternative approach to avoid introgression of genetic information into wild relatives is the expression of foreign proteins in chloroplasts of higher plants. Cells of higher plants carry substantial amounts of mitochondrial DNA 250 000 bp up to 2 million bp which is about tenfold the amount of mammalian mitochondrial DNA (Knippers, 1997). Some foreign genes have been already integrated into the non-chromosomal chloroplast genome of *Nicotiana tabacum*, giving up to 10 000 copies per cell and resulting in the accumulation of recombinant proteins up to 47 % of the total soluble protein. Chloroplast transformation uses two flanking sequences that insert foreign DNA into the spacer region between the functional genes of the chloroplast genome and thus targeting the foreign genes to a precise location and eliminates the 'position effect' upon expression that is frequently observed in transgenic plants with genes inserted into the nuclear genome, which might be also possible for the AB sequence. Gene silencing has up to now not been observed with chloroplast transformation, although it is a common phenomenon with chromosomal transformation. Therefore chloroplast genetic engineering is minimizing several environmental concerns (Daniell, 2002).

Finally it can be said, that the crop to wild gene flow is a common phenomenon for out-breeders and depends strongly on the relatedness of the involved plant taxa. Therefore the environmental safety of this taxa in an agroecosystem should be thoroughly addressed. Some factors should be taken into consideration like: flowering asynchrony and limited sexual compatibility, abundance as well as environmental conditions to evaluate the chances of the transfer of the gene encoding for MC10E7 to wild relatives is possible, and as tobacco is considered to be an out breeder to about 25% its possible. But as soon as the gene might be transferred it confers no evolutionary advantage over other competitors when observed outside the anthropogenic agroecosystem. Instead leads sometimes to a metabolic burden with negative selection pressure. In general, plants used for the recombinant production of mammalian proteins are not intended for cultivation in the open field, but rather for contained growth environments such as greenhouses.

4.10 OUTLOOK AND FURTHER PERSPECTIVES

Contamination of surface waters and natural pools is still an unaddressed problem when the application of chlorine, to inhibit the growth of the microbial flora, is not an option. One solution may be development of on-site analysis with lateral flow immunoassays (dipstick assay) utilizing a plant derived antibody to significantly reduce the costs per dipstick. Or the biotechnological environmental clean-up by water purification adsorbents as it might be further explored in other work. This option would require huge amounts of antibody at a very low price, and one option for achieving this in the future would be an optimized, inexpensive and scalable plant expression system.

The production of stably transformed *N. tabacum* lines has therefore laid the basis for further yield optimization. The highest yield was achieved by the single construct infiltration, although several other plants from the tandem delivery system also performed well and could be used as parents for further crossing projects. The crossing of lines preselected for highest yield might be one of the ways to enhance the overall gene copy number and might lead to a higher expression and a higher yield. Specific bottlenecks, such as the HC overproduction, as described above in section 4.4 might be tackled by a crossing strategy with the best LC expressing plant to avoid free HC accumulation in the ER lumen.

According to the information gained from the CBM-MC10E7 conjugate experiments it can be stated, that -although the AB itself retains its outstanding affinity and specificity- the CBM causes new properties to the MC10E7 which are still not fully understood. On one hand the CBM was confirmed to be attached successfully to the antibody via numerous western blots. The specificity and selectivity of the CBM-antibody conjugate was not clarified completely as too low concentrations of antibody were recovered from the batches. This might be a goal for future investigations focusing on the properties in a quantitative ELISA to check if the CBM really offers a higher affinity to microcrystalline cellulose compared to the standard MC10E7. There was a clear tendency throughout all experiments, that the CBM-antibody conjugate had a higher affinity to the G-protein beads and was only poorly eluted. However, empty sepharose beads did not show similar attributes and had no elevated affinity to the CBM-antibody conjugate. Further investigations according the binding properties of the CBM might lead to a better understanding and could be performed in a quantitative ELISA combined with a microcrystalline cellulose coating carried out in high binding microtiter plates (MTP's). Another question arising during the work with several successfully transformed *A. tumefaciens* strains was the significant difference in transfection potential. Some strains performed clearly better in terms of transient expression than others. Also the production of polysaccharides during up-scale led to certain difficulties. Due to limited time resources it was not possible to address these questions within this thesis. The production of specific adsorbents for the on-site sanitation was not attempted in this work, but CBM-antibody binding to micro cellulose-based filter matrices was explored and should be further addressed in future projects.

Finally it can be concluded that the use of stable *N. tabacum* lines expressing the full-size recombinant antibody MC10E7 is suitable for the intended use, which is the production of user-friendly test strips to trace microcystin in water and this provides a basis for future research projects.

5 APPENDIX A

This Appendix brings together the used abbreviations as well as measurement units and explanations are given to support the understanding and facilitate the search for synonym.

Ab	Antibody
HC	Heavy Chain
LC	Light Chain
CBM (CBD)	CBM(domain)
DsRed	Red fluorescent protein from Discosoma
bp	Base pairs
<i>g</i>	Gravitational force
CV	Column volume, packed beads
PD's	Protein drugs
bw	Body weight
BSA	Bovine serum albumin
PB	Phosphate buffer
PFA	Paraformaldehyde
SAP	shrimp alkaline phosphatase
CHO	Chinese hamster ovary
SAR	Scaffold attachment region
GMP	Good manufacturing practice
BT	<i>Bacillus thuringiensis</i>
Pa	Pascal
FP	Fluorescent protein
SNP	Single nucleotide polymorphism
NEB	New England Biolabs
TS	Thermo Scientific
PCR	Polymerase chain reaction
Taq	<i>Thermus aquaticus</i>
kDa	Kilo-daltons
LB	Laemmli Buffer
NB	<i>Nicotiana benthamiana</i>
NT	<i>Nicotiana tabacum</i>
rpm	Revolutions per minute
MTP	Micro titer plates
MC-LR	Microcystin-leucine-arginine
SGS	suppressors of gene silencing
TBSV	Tomato bushy stunt virus
GFP	Green fluorescent protein
GOI	Gene of interest

6 APPENDIX B

In this Appendix, specific sequences used in the text above are summed up to facilitate a constant reading flow. Some common sequences for vectors and plasmids are excluded to maintain a manageable extract.

Primer	sequence	Tm	Use
HHC-882_F	CAACTGGTACGTGGATGG	60.6°	CPEC assembly
TRA-HHC1629_R	GAGTCGCAAATATTTCTAGGG	59.7°C	CPEC assembly
CBM2-HHC_F	CCTGGAAAGGGTCCTACACCTACGCCAAC	63.7°C 76.4	CPEC assembly
CBM2-TRA_R	CTCTAGATCATCATCCAACAGTGCAAGGAGC	63.3°C 74.0°C	CPEC assembly
DR-CBM2_F	GCGGCCGCTGGTCCTACACCTACGCCAAC	63.7°C 83.3°C	CPEC assembly
DR-CBM2_R	GCGGCCGCTCCAACAGTGCAAGGAGCAC	66.9 84.7°C	CPEC assembly
HHC_CBM2_R	GTAGGACCCTTTCCAGGAGAAAGAGAC	56.1°C 68.9°C	CPEC assembly
TRA-CBM2_F	CTGTTGGATGATGATCTAGAGATATCAC	55.6°C 64.1°C	CPEC assembly
HHC41_F	CCGGTGGTTCACTACGTCTC	60,11	Screening HC
HHC429_R	TCCAAGAGCAGCAGTTCCAC	60,25	Screening HC
HLC40_F	ACCATTGGACAACCAGCCTC	60,25	Screening LC
HLC593_R	GCGTAAACCTTGTGCTTCTCG	60,14	Screening LC

7 APPENDIX C

Additional sequences excluded from the text to provide a better readability.

Humanized heavy (gamma) chain HHC2 (pC27-2) peptide sequence

GAGGTTATGGTCGTTGAATCTGGGGGGGGTTTGTAGTGAAGCCCGGTGGTTCACCTACGTCTC
TCGTGCGCAGCAAGCGGCTTCACGTTCTCCAGGTATGCTATGAGTTGGTTTAGGCAGACT
CCAGAACGGAGACTGGAATGGGTAGCGACTATTAACAGTGTTGGATCATATTCTTACTAC
CCTGACAGTGTTAAAGGACGCTTTACAATATCCAGAGATAATGTCCGAAATACCCTTTTT
TTGCAAATGAGCTCTCTTAGATCTGAGGATACTGCTATCTATTACTGTACCAAGGGCGCT
GACTATGCCATGGATTATTGGGGACAAGGAACATCTGTAACAGTGTCATCAGCGTCGACT
AAGGGGCCCTCTGTGTTTCCACTTGCTCCATCTTCTAAGTCTACTTCAGGTGGAAGTCTGCT
GCTCTTGGATGCCTTGTGAAGGATTACTTCCAGAGCCAGTTACTGTTTCATGGAAGTCT
GGTGCTCTTACTTGTGGTGTTCACACTTTCCAGCTGTGCTTCAGTCATCTGGACTTTAC
TCACTTTCTTCTAGTGCTGCTGCCATCTTCTTCTCTTGGAACTCAGACTTACATCTGC
AACGTGAACCACAAGCCATCTAACACAAAAGTGGATAAGAAGGTGGAGCCAAAGTCTTGC
GATAAGACTCATACTTGTCCACCATGTCCAGCTCCAGAACTTCTTGGAGGACCTTCTGTG
TTCCTTTTCCACCAAAGCCAAAGGATACTCTTATGATTTCTAGGACTCCAGAGGTTACA
TGC GTTGTGGTTGATGTGTCTCACGAAGATCCAGAGGTGAAGTTCAACTGGTACGTGGAT
GGTGTGAGAGTTCACAACGCTAAGACTAAGCCAAGGGAAGAGCAGTACAACCTTACTTAC
AGGGTGGTGTCTGTGCTTACTGTTCTTCCAGGATTGGCTTAACGGAAAAGAGTACAAG
TGCAAGGTATCAAAACAAGGCTCTTCCAGCTCCAATTGAAAAGACTATTTCTAAGGCTAAG
GGACAACCTAGAGAGCCACAGGTTTACACTCTTCCACCATCTAGGGATGAGCTTACTAAG
AACCAGGTGTCACTTACTTGTGTTGGTGAAGGGATTCTACCCATCTGATATTGCTGTTGAG
TGGGAGTCTAATGGACAACCAGAGAACAACCTACAAGACTACTCCACCAGTGCTTGATTCT
GATGGATCTTTCTTCTTACTCTAAGCTTACTGTGGATAAGTCTAGGTGGCAGCAGGGA
AATGTTTTCTTGTCTGTGATGCATGAGGCTCTTCAATCACTACACTCAGAAAGTCT
TTGTCTCTTCTCCTGGAAAG

Humanized heavy (gamma) chain HHC2 (pC27-2) amino acid sequence

MVVESGGGLVKPGGSLRLSCAASGFTFSRYAMSWFRQTPERRLEWVATINSVGSYSYPPDSVKGRFTISRDNVR
NTLFLQMSSLRSEDTAIYYCTKGADYAMDYWGQGTSTVTVSSASTKGPSVFPLAPSSKSTSGGTAALGCLVKDYF
PEPVTVSWNSGALTSGVHTFPAVLQSSGLYSLSSVTVTPSSSLGTQTYICNVNHKPSNTKVDKKVEPKSCDKHTH
CPPCPAPELLGGPSVFLFPPKPKDTLMISRTPEVTCVVDVSHEDPEVKFNWYVDGVEVHNAKTKPREEQYNST
YRVVSVLTVHLQDWLNGKEYCKVSNKALPAPIEKTISKAKGQPREPQVYTLPPSRDELTKNQVSLTCLVKGFYPS
DIAVEWESNGQPENNYKTTTPVLDSDGSFFLYSKLTVDKSRWQQGNVFSCSVMHEALHNHYTQKSLSLSPGK

Humanized light (kappa) chain HHC2 (pC27-2) peptide sequence

GATGTTGTGATGACCCAGACTCCTCTCACTTTGTGCGTTACCATTTGGACAACCAGCCTCCATATCTTGCAAGT
CAAGTCAGAGCCTCTTAGAGGGTGATGAAAAGACATATTTGAATTGGTTGTTACAGAGGCCAGGCCAGTCTC
CAAAGCGCCTAATCTATCTGGTGTCTAAACTTGACTCTGGAGTCCCTGACAGGTTCACTGGCAGTGGATCAG
GGACAGATTTCACTGAAAATCAGCAGAGTGAGGCTGAGGATTTGGGAGTTTATTATTGCTGGCAAGGTA
CACATTTTCTCAGACGTTCCGGTGGAGGTACCAACCTGGAATCATACGTACGGTGGCTGCTCCATCTGTGT
TTATTTTCCCACCATCTGATGAGCAACTTAAGTCTGGAAGTCTTCTGTTGTGTGCCTTCTTAACAACCTTCTAC
CCAAGGGAAGCTAAGGTTCAAGTGGAAAAGTGGATAACGCTCTTCAGTCTGGAAACTCTCAAGAGTCTGTGACT
GAGCAGGATTCTAAGGATTCACTTACTCTTTCTTCTACTCTTACTCTTTCTAAGGCTGATTACGAGAAGCA
CAAGGTTTACGCTTGCGAAGTTACTCATCAGGGACTTTCTTCTCCAGTACTAAGTCTTTCAACAGGGGAGAG
TGCTGA

Humanized light (kappa) chain HHC2 (pC27-2) amino acid sequence:

MTQTPLTSLVTIGQPASISCKSSQSLLEGDGKTYLNLWLLQRPQQSPKRLIYLVSKLDSGVPDRFTGSGSGTDFTLK
ISRVEAEDLGVIYCWQGFHFPQTFGGNTLEIIRTVAAAPSVFIFPPSDEQLKSGTASVVCLLNNFYPREAKVQWKV
DNALQSGNSQESVTEQDSKSTYLSSTLTLSKADYEKHKVYACEVTHQGLSSPVTKSFNRGEC

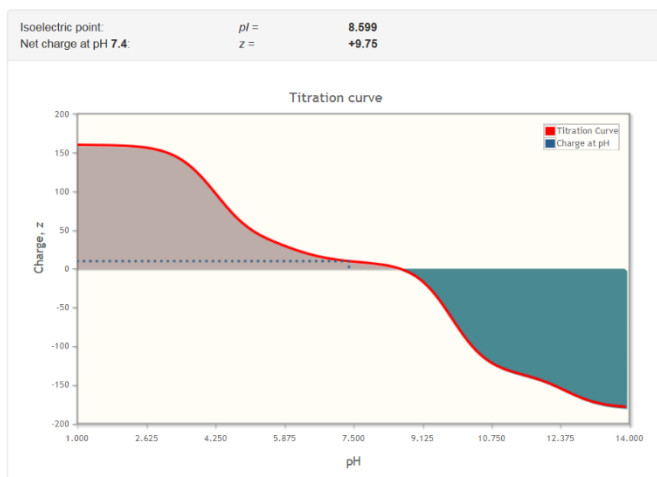
Theoretical calculated data:

Amino acid composition for the fully assembled MC10E7 antibody

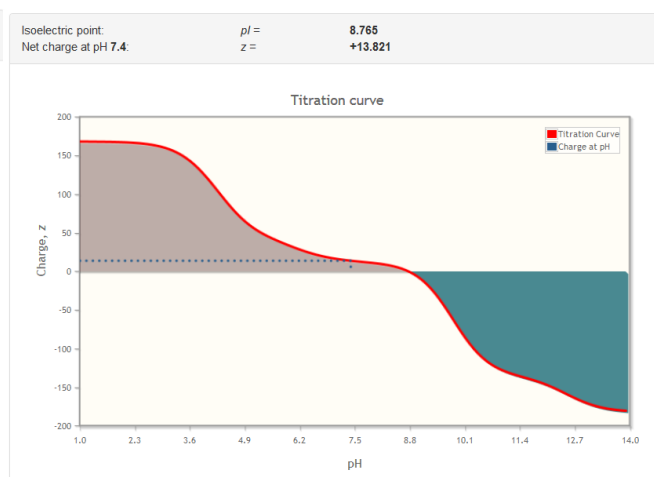
Name	3-Letter	1-Letter	Class:	Number:	Count, %
Alanine	Ala	A	Hydrophobic	58	4.39 %
Arginine	Arg	R	Basic	44	3.33 %
Asparagine	Asn	N	Hydrophilic	50	3.78 %
Aspartic Acid	Asp	D	Acidic	56	4.24 %
Cysteine	Cys	C	Hydrophilic	32	2.42 %
Glutamic Acid	Glu	E	Acidic	64	4.84 %
Glutamine	Gln	Q	Hydrophilic	54	4.08 %
Glycine	Gly	G	Hydrophilic	92	6.96 %
Histidine	His	H	Basic	24	1.82 %
Isoleucine	Ile	I	Hydrophobic	30	2.27 %
Leucine	Leu	L	Hydrophobic	108	8.17 %
Lysine	Lys	K	Basic	88	6.66 %
Methionine	Met	M	Hydrophobic	14	1.06 %
Phenylalanine	Phe	F	Hydrophobic	46	3.48 %
Proline	Pro	P	Hydrophobic	90	6.81 %
Pyrrolysine	Pyl	O	Basic	0	0 %
Selenocysteine	Sec	U	Acidic	0	0 %
Serine	Ser	S	Hydrophilic	168	12.71 %
Threonine	Thr	T	Hydrophilic	108	8.17 %
Tryptophan	Trp	W	Hydrophobic	22	1.66 %
Tyrosine	Tyr	Y	Hydrophobic	56	4.24 %
Valine	Val	V	Hydrophobic	118	8.93 %

Total: 1322 100 %

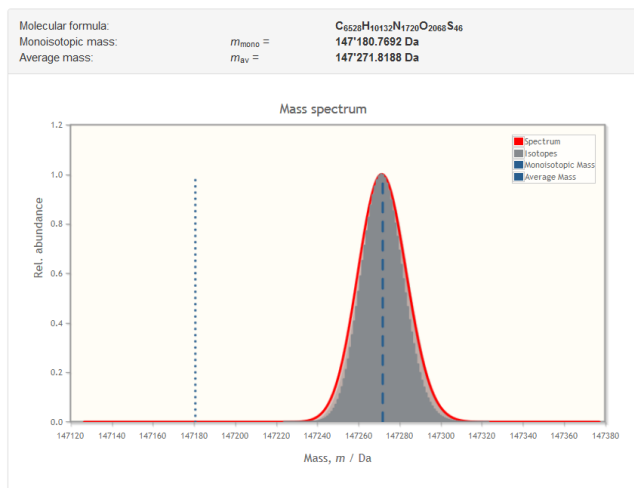
Isoelectric point: $2 \cdot \text{HC} + 2 \cdot \text{LC}$



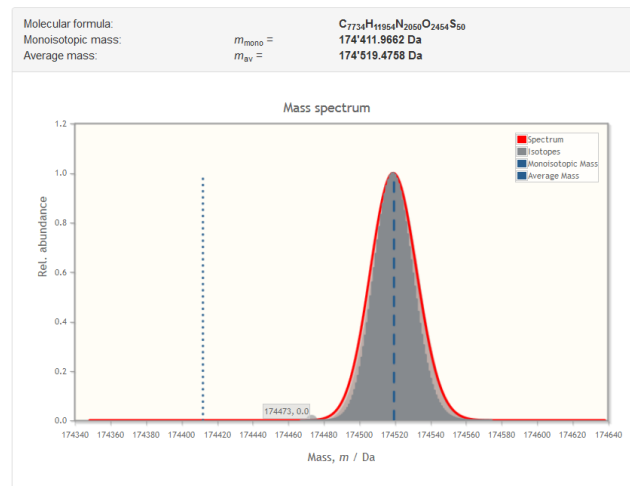
Isoelectric point: $2 \cdot (\text{HC} + \text{CBM}) + 2 \cdot \text{LC}$



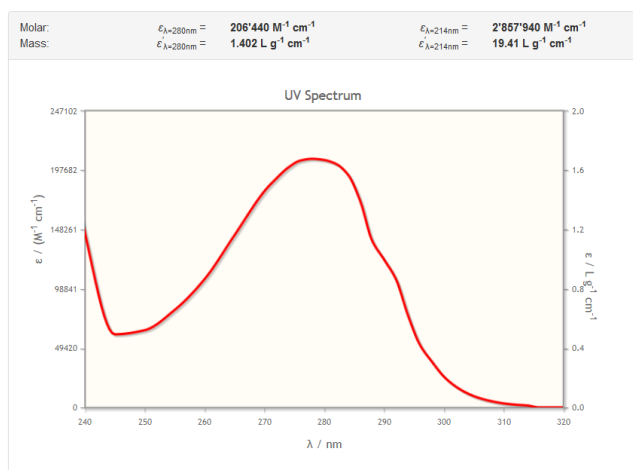
molar mass: MC10E7



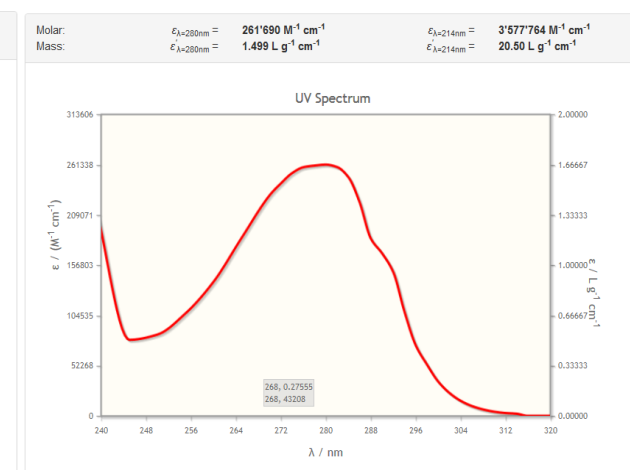
molar mass: MC10E7 + CBM



UV absorption coefficient: MC10E7



UV absorption coefficient: MC10E7 + CBM



8 LIST OF FIGURES

Fig. 1: Structure of Microcystin-LR (Dawson, 1998).	4
Fig. 2: Schematic drawing of an IgG antibody Thermo Fischer, 2016.	5
Fig. 3: N-glycosylation pattern for secreted glycoproteins, typical for plant derived glycosylation pattern are the beta(1,2)-xylose and alpha(1,3)-fucose residues.	6
Fig. 4: N-glycosylation pattern, high mannose type without secretion (e.g. retained in the ER)	6
Fig. 5: exo-beta-1,4-glucanase derived from <i>Cellulomonas fimi</i> , showing the sulfide double bonds and the N terminal end, pointing inwards where the linker is attached	9
Fig. 6: T4 Ligase catalyzed ATP dependent phosphodiester bond formation (Hardin, 2001).	11
Fig. 7: Graphical illustration of the PCR-based cloning for the CBM attachment to the HC, shown in three different excise reactions and one final assembly reaction.	14
Fig. 8: Equipment for the vacuum infiltration procedure.	34
Fig. 9: A successful infiltration of the leaf is easily observable, as fully infiltrated leafs do show a transparent appearance (left) compared to non infiltrated leafs (right)	35
Fig. 10: Manual syringe infiltration into the abaxial side of <i>N. tabacum</i> L. cv. Petit Havana SR1 leafs.	35
Fig. 11: Removing of the not transformed midvein before homogenization.	35
Fig. 12: Homogenization of leaf material with mortar and pestle under constant cooling with liquid nitrogen.	36
Fig. 13: developmental stages of plant regeneration, captured at one week, 5 weeks and 11 weeks	39
Fig. 14: Chronological observation of a single embryonal callus to plant stage. Starting at A: 1 week B: 3 weeks C: 5 weeks D: 7 weeks, E: 9 weeks transfer to rooting media, F: 11 weeks, transplantation to magenta boxes.	39
Fig. 15: Initial plasmids:	40
Fig. 16: pJet1.2 shuttle vector with lethal restriction site Eco47IR	41
Fig. 17: PCR-based screening for integration of the HLC2 into the pJET1.2 vector.	42
Fig. 18: Integrated LC in forward orientation at the pJet, pM2.	42
Fig. 19: gel purified product pM2 for further processing	42
Fig. 20: Colony cracking screen for the <i>E. coli</i> transformation.	43
Fig. 21: PCR screening with pJet_F and Ds_Red_R primers for the correct insertion	44
Fig. 22: gel purified product pM3 for further processing	44
Fig. 23: Pre-screen for the <i>E. coli</i> transformation of LC and DsRed into the HC expression vector.	44
Fig. 24: PCR screening for the correct insertion of LC and DsRed into the expression vector, successful integration in colony 9 and 27.	45
Fig. 25: restriction digest with Eco RI and Eco RV show the expected pattern for an insertion.	45
Fig. 26: (Robinson et al., 2015) showing a schematic explanation of the distinct degradation or incomplete assembly of IgG	46
Fig. 27: Transient expression of antibody in <i>N. benthamiana</i> using the final <i>A. tumefaciens</i> clone pM4-27-2. Distinct degradation bands occurred at about 40 kDa	46
Fig. 28: Transient expression of the single construct in NT, observed after local DsRed expression	46
Fig. 29: Transient expression of the single construct in NB, observed via the local DsRed expression	47
Fig. 30: PCR pre- screening (HHC-882_F and TRA-HHC1629_R) of colonies after the quick ligation procedure.	47
Fig. 31: PCR based screening for the correct insertion of the assembled expression vector	48
Fig. 32: Colony cracking screen after <i>A. tumefaciens</i> transformation.	48
Fig. 33: The samples from <i>Nicotiana tabacum</i> (1-2 supernatant, 5-6 pellet, 9-10 pH shifted pellet and 13-14 eluate) followed by the <i>Nicotiana benthamiana</i> samples (3-4 supernatant, 7-8 pellet, 11-12 pH shifted pellet and 15-16 eluate)	50
Fig. 34: Second biological repetition NT, comparison of different elution methods from the pellet-immobilized antibody. Wildtype NT served as negative control and purified AB as positive control	50
Fig. 35: Second biological repetition NB, comparison of different elution methods.	51
Fig. 36: Comparison of different extraction stages, and elution procedures at pH3 and 8.	52
Fig. 37: The regular extraction procedure (prot A) of NT sampled at every step.	53

Fig. 38: Experiment [A]: to analyze the fixation on the AB to the pellet, acquiring 1M ammonium sulfate and cellulose mixed to the crude lysate, trying to retain most of the AB in the pellet.....	54
Fig. 39: Experiment [B]: Showing the extraction with A-protein. to identify the possible losses.	55
Fig. 40: Experiment [C]: repetition of experiment A, Cellulose fixation and elution with water.	56
Fig. 41: Experiment [D]: regular extraction with protein A and glycine pH3: The differences of the white layer and the rest of the pellet is examined together with the pellet of the last biological repetition and the long-term stability experiment.....	57
Fig. 42 Flowchart of the three compared extraction procedures	57
Fig. 43 ELISA analysis for the protein-A extraction.....	58
Fig. 44: ELISA analysis for the sepharose beads extraction procedure sampled at the four main stages.....	58
Fig. 45: ELISA analysis of the cellulase treatment of the first pellet.....	58
Fig. 46: First screening to optimize the blotting conditions, successful detection of the LC in plant 3 and 5.....	59
Fig. 47: Full screen for LC detection.....	59
Fig. 48: For the HC detection the procedure was repeated enriched and concentrated via a binding and several washing steps with protein A.	60
Fig. 49: Targeted pollination of HC plant 15 with pollen from LC plant 6.	60
Fig. 50: Schematic drawing of the crossed HC and LC containing plants.	60
Fig. 51: Overview of the regenerative stages of NT from leaf-disc to rooting media.	61
Fig. 52: Selection based on the expression of DsRed for the detection of successfully transformed clones, the shoot arising from the lower part of the callus was detected as negative due to the absence of DsRed. Both plants were irradiated but only the anterior shoot was emitting red light indicating the presence of DsRed and therefore likely the presence of the antibody transgene.	62
Fig. 53: Clone B and C showed homogenous distribution all over the surface, but especially strong in the flower buds and the tips of the youngest leaves. Both plants showed a weak growth and slightly untypical leaves.	62
Fig. 54: Clone D showed an inverted phenotype to Clone A with no DS-Red in the younger leafs and strong expression in the first three lower leaves.....	62
Fig. 55: Clone A showed enriched fields of DS-red in the younger leaves but exclusively adjacent to the veins. While the first four leaves and their internodes showed no signal at all the younger leaves especially their veins were shining bright.	62
Fig. 56: Yield distribution for the total harvests.	64
Fig. 57: Distribution of the antibody yield for the prescreen procedure.....	64
Fig. 58: Illustration of significance levels for the individual trials.	66
Fig. 59: Illustration of significance levels for the highest producing plants..	67
Fig. 60: regular infiltration pattern.	68
Fig. 61: massive yellow chlorosis.....	68
Fig. 62: Regular sized spots.	68
Fig. 63: sclerotic spots.	68
Fig. 64: Crude lysate for the individual patterns.	68
Fig. 65: Antibody prduction, comparison of expression.	68
Fig. 66: Fluorescent microscopy image for the subcellular localization of the AB in clone D. The spots of successfully secreted AB is marked with red arrows	69
Fig. 67: [A] Localization of the AB in the apoplastic space, indicating a successful secretion. [B] Subcellular localisation of the AB still on the way to secretion, dark circular areas are excluded chloroplasts	69
Fig. 68: The following pictures show the (1) an emission of the antibody, (2) emission ER-tracker and (4) a confocal image. A partial colocalization was observed as bright structure in the middle (red arrow) which is a result of the overlay of the magenta and green wave spectra, leading to a white signal, which indicates that a fraction of the antibody is still within the endomembrane system.....	70
Fig. 69: [A] Detection of the Antibody within the endomembrane system. The colocalization of the AB (red arrows) signal and ER tracker results in white area that indicate that part of the antibody is retained within the ER forming RB-like structures.....	70

9 LIST OF TABLES

Table 1: Comparison of production systems for recombinant human pharmaceutical proteins, (Ma et al., 2015).	3
Table 2: Restriction digestion	10
Table 3: Quick ligation reaction	12
Table 4: Colony touch down mix	13
Table 5: General temperature profile for thermocycler	13
Table 6: Excise reaction one	14
Table 7: Master-mix, excitation reaction	15
Table 8: Excise reaction two	15
Table 9: Thermocycler program for reaction 1 and 2	16
Table 10: Excise reaction three	16
Table 11. final assembly reaction	17
Table 12: Low melting point agarose mix for 1% separation.	17
Table 13: Extraction buffer for CTAB genomic DNA precipitation.	21
Table 14: The cracking buffer (Sambrook & Russel, 2001).	21
Table 15: Resolving gel 12%, Concentration for 50 mL	23
Table 16: Stacking gel 4%, Concentration for 50 mL	23
Table 17: Polymerization initiators for stacking and resolution gel	23
Table 18: Transfer buffer	24
Table 19: Tris-Buffered Saline (TBS; 10×, pH 7.5) COLD SPRING HARBOUR (2014)	24
Table 20: Blocking buffer	24
Table 21: Developing solution BCIP/NBT	25
Table 22: Dicarboxylate Coatingbuffer, pH9.6	25
Table 23: DEA-buffer	26
Table 24: Fixation solution for sample embedding	26
Table 25: Dehydration steps	27
Table 26: Infiltration steps	27
Table 27: Dehydration and rehydration steps	28
Table 28: Differences in the isoelectric point calculated by ProMoSt, ExPASy and Native	29
Table 29: Concentrations of antibiotics used for selection	30
Table 30: Composition LB-medium	30
Table 31: Composition LB-Agar	31
Table 32: Composition SOC-medium	31
Table 33: Composition YEB-medium	31
Table 34: Composition YEB-Agar	32
Table 35: Composition induction medium	32
Table 36: Composition infiltration medium	32
Table 37: Composition MS-Vitamin stocks	32
Table 38: Composition Murashige & Skoog shooting medium	33
Table 39: Composition murashige & skoog rooting medium	33
Table 40: Composition AB-salts	33
Table 41: Extraction buffer	36
Table 42: PMSF stocks 1000x	36
Table 43: Comparison of yield for the five and seven day expression system.	63
Table 44: Total harvest of Antibody.	64
Table 45: Analysis of Variance Table, response: yield	65
Table 46: Posthoc test for comparison of individual AB yields per plant.	66
Table 47: Posthoc test for comparison of individual AB yields per plant.	67

1. REFERENCES

1. AGARWAL et al. (1989) 'Scaffold Attachment Region-Mediated Enhancement of Retroviral Vector Expression in Primary T Cells', *JOURNAL OF VIROLOGY*, pp. 3720–3728.
2. AN et al. (1985) 'High Efficiency Transformation of Cultured Tobacco Cells', *Plant physiology*, vol. 79, no. 2, pp. 568–570.
3. Baird et al. (2000) 'Biochemistry, Mutagenesis, and Oligomerization of DsRed, a Red Fluorescent Protein from Coral', *Proceedings of the National Academy of Sciences of the United States of America*, Vol. 97, No. 22, pp. 11984–11989.
4. Barbi, T., Drake, P. M. W., Drever, M., van Dolleweerd, C. J., Porter, A. R. and Ma, J. K.-C. (2011) 'Generation of transgenic plants expressing plasma membrane-bound antibodies to the environmental pollutant microcystin-LR', *Transgenic research*, vol. 20, no. 3, pp. 701–707.
5. Barta, A., Sommergruber, K., Thompson, D., Hartmuth, K., Matzke, M. A. and Matzke, A. J. (1986) 'The expression of a nopaline synthase - human growth hormone chimaeric gene in transformed tobacco and sunflower callus tissue', *Plant molecular biology*, vol. 6, no. 5, pp. 347–357.
6. Baulcombe, D. (2004) 'RNA silencing in plants', *Nature*, vol. 431, no. 7006, pp. 356–363.
7. Bechtold et al. (1998) *In Planta Agrobacterium Mediated Transformation of Adult Arabidopsis thaliana plants by Vacuum Infiltration*, Totowa N.J., Humana Press.
8. Bialczyk, J., Kochanowski, A., Czaja-Prokop, U. and Chrapusta, E. (2014) 'Removal of microcystin-LR from water by polymers based on N -vinylformamide structure', *Water Science & Technology: Water Supply*, vol. 14, no. 2, p. 230.
9. BOSELEY (2015) *Ebola crisis: - the Guardian briefing* [Online]. Available at <https://www.theguardian.com/world/2014/sep/25/-sp-ebola-crisis-briefing> (Accessed 14 February 2017).
10. Carthew, R. W. and Sontheimer, E. J. (2009) 'Origins and Mechanisms of miRNAs and siRNAs', *Cell*, vol. 136, no. 4, pp. 642–655.
11. Chen, Q., Lai, H., Hurtado, J., Stahnke, J., Leuzinger, K. and Dent, M. (2013) 'Agroinfiltration as an Effective and Scalable Strategy of Gene Delivery for Production of Pharmaceutical Proteins', *Advanced techniques in biology & medicine*, vol. 1, no. 1.
12. Chorus, I. and Bartram, J. (1999) *Toxic cyanobacteria in water: A guide to their public health consequences, monitoring, and management*, London, New York, E & FN Spon.

13. Christou, P. and Klee, H., eds. (2004) *Handbook of plant biotechnology* [Online], Chichester, Wiley. Available at <http://www.loc.gov/catdir/description/wiley041/2003027341.html>.
14. Cline, J. (1996) 'PCR fidelity of pfu DNA polymerase and other thermostable DNA polymerases', *Nucleic Acids Research*, vol. 24, no. 18, pp. 3546–3551.
15. COCO-MARTIN, JAN W. OBERINK, FREEK BRUNINK, TINY A. M. VAN DER VELDEN-DE GROOT and and E. COEN BEUVERY (1992) 'Instability of a Hybridoma Cell Line in a Homogeneous Continuous Perfusion Culture System', pp. 653–666.
16. Daniell, H. (2002) 'Molecular strategies for gene containment in transgenic crops', *Nature biotechnology*, vol. 20, no. 6, pp. 581–586.
17. Dawson, R. (1998) 'the toxicology of microcystins', *Toxicon*, vol. 36, no. 7, pp. 953–962.
18. Ecker, D. M., Jones, S. D. and Levine, H. L. (2015) 'The therapeutic monoclonal antibody market', *mAbs*, vol. 7, no. 1, pp. 9–14.
19. Eisenbrand (2007) 'Microcystins in algae products used as food supplements: DFG - Senate Commission on Food Safety', no. 1, pp. 1–5.
20. El Semary (2010) 'Modern Methods for Detection and Elimination of Microcystins Toxins Produced by Cyanobacteria', *Journal of Applied Sciences*, pp. 1662–1666.
21. Encorbio (2016) *Ammonium Sulfate Calculator: Ammonium Sulfate Precipitation is a simple and effective means of fractionating proteins* [Online], ©EnCor Biotechnology Inc. Available at <http://www.encorbio.com/protocols/AM-SO4.htm> (Accessed 14 December 2016).
22. Feher et al. (2003) 'Transition of somatic plant cells to an embryogenic state: Review of Plant Biotechnology and Applied Genetics', *Plant Cell, Tissue and Organ Culture* 74: 201–228,
23. Fischer et al. (2014) 'Molecular Farming in Plants: The Long Road to the Market', in Howard, J. A. and Hood, E. E. (eds) *Commercial Plant-Produced Recombinant Protein Products*, Berlin, Heidelberg, Springer Berlin Heidelberg, pp. 27–41.
24. Fujiki, H. and Suganuma, M. (2011) 'Tumor Promoters - Microcystin-LR, Nodularin and TNF- α ; and Human Cancer Development', *Anti-Cancer Agents in Medicinal Chemistry*, vol. 11, no. 1, pp. 4–18.
25. Garabagi, F., Gilbert, E., Loos, A., McLean, M. D. and Hall, J. C. (2012) 'Utility of the P19 suppressor of gene-silencing protein for production of therapeutic antibodies in Nicotiana expression hosts', *Plant biotechnology journal*, vol. 10, no. 9, pp. 1118–1128.
26. Giritch, A., Marillonnet, S., Engler, C., van Eldik, G., Botterman, J., Klimyuk, V. and Gleba, Y. (2006) 'Rapid high-yield expression of full-size IgG antibodies in plants coinfecting with

- noncompeting viral vectors', *Proceedings of the National Academy of Sciences of the United States of America*, vol. 103, no. 40, pp. 14701–14706.
27. Gurbuz, F., Uzunmehmetoglu, O. Y., Diler, O., Metcalf, J. S. and Codd, G. A. (2016) 'Occurrence of microcystins in water, bloom, sediment and fish from a public water supply', *The Science of the total environment*, vol. 562, pp. 860–868.
 28. Gutierrez, S. P., Saberianfar, R., Kohalmi, S. E. and Menassa, R. (2013) 'Protein body formation in stable transgenic tobacco expressing elastin-like polypeptide and hydrophobin fusion proteins', *BMC biotechnology*, vol. 13, p. 40.
 29. Hardin, C. C. (2001) *Cloning, gene expression, and protein purification: Experimental procedures and process rationale* [Online], New York, Oxford Univ. Press. Available at <http://www.loc.gov/catdir/enhancements/fy0610/00045312-d.html>.
 30. Harris, B. (1999) 'Exploiting antibody-based technologies to manage environmental pollution', *Trends in Biotechnology*, vol. 17, no. 7, pp. 290–296.
 31. Hart, H., Craine, L. E. and Hart, D. J. (2002) *Organische Chemie*, 2nd edn, Weinheim, Wiley-VCH.
 32. Hensel, G., Floss, D. M., Arcalis, E., Sack, M., Melnik, S., Altmann, F., Rutten, T., Kumlehn, J., Stoger, E. and Conrad, U. (2015) 'Transgenic Production of an Anti HIV Antibody in the Barley Endosperm', *PloS one*, vol. 10, no. 10, pp. e0140476.
 33. Hiatt, A. and Pauly, M. (2006) 'Monoclonal antibodies from plants: a new speed record', *Proceedings of the National Academy of Sciences of the United States of America*, vol. 103, no. 40, pp. 14645–14646.
 34. Hofbauer, A., Peters, J., Arcalis, E., Rademacher, T., Lampel, J., Eudes, F., Vitale, A. and Stoger, E. (2014) 'The Induction of Recombinant Protein Bodies in Different Subcellular Compartments Reveals a Cryptic Plastid-Targeting Signal in the 27-kDa γ -Zein Sequence', *Frontiers in bioengineering and biotechnology*, vol. 2, p. 67.
 35. Ibelings, B. W., Fastner, J., Bormans, M. and Visser, P. M. (2016) 'Erratum to: Cyanobacterial blooms. Ecology, prevention, mitigation and control: Editorial to a CYANOCOST Special Issue', *Aquatic Ecology*, vol. 50, no. 4, p. 735.
 36. Ibrahim, W. M., Salim, E. H., Azab, Y. A. and Ismail, A.-H. M. (2016) 'Monitoring and removal of cyanobacterial toxins from drinking water by algal-activated carbon', *Toxicology and industrial health*, vol. 32, no. 10, pp. 1752–1762.
 37. Kelly, K. (2009) *Early civilizations: Prehistoric times to 500 C.E* [Online], New York NY, Facts on File. Available at <http://site.ebrary.com/lib/alltitles/docDetail.action?docID=10340565>.

38. Kintaka, R., Makanae, K. and Moriya, H. (2016) 'Cellular growth defects triggered by an overload of protein localization processes', *Scientific reports*, vol. 6, p. 31774.
39. Knippers, R. (1997) *Molekulare Genetik: 76 Tabellen*, 7th edn, Stuttgart, Thieme.
40. Köhler, W., Schachtel, G. and Voleske, P. (2012) *Biostatistik: Eine Einführung für Biologen und Agrarwissenschaftler*, 5th edn, Berlin, Springer-Spektrum.
41. Komarova, T. V., Baschieri, S., Donini, M., Marusic, C., Benvenuto, E. and Dorokhov, Y. L. (2010) 'Transient expression systems for plant-derived biopharmaceuticals', *Expert review of vaccines*, vol. 9, no. 8, pp. 859–876.
42. Lakatos, L., Szittyá, G., Silhavy, D. and Burgyan, J. (2004) 'Molecular mechanism of RNA silencing suppression mediated by p19 protein of tombusviruses', *The EMBO journal*, vol. 23, no. 4, pp. 876–884.
43. Le Noir, M., Lepeuple, A.-S., Guieysse, B. and Mattiasson, B. (2007) 'Selective removal of 17beta-estradiol at trace concentration using a molecularly imprinted polymer', *Water research*, vol. 41, no. 12, pp. 2825–2831.
44. Li, X., Zhao, Q., Zhou, W., Xu, L. and Wang, Y. (2015) 'Effects of chronic exposure to microcystin-LR on hepatocyte mitochondrial DNA replication in mice', *Environmental science & technology*, vol. 49, no. 7, pp. 4665–4672.
45. Linder, M., Nevanen, T. and Teeri, T. T. (1999) 'Design of a pH-dependent cellulose-binding domain', *FEBS Letters*, vol. 447, no. 1, pp. 13–16.
46. Ma, J. K.-C., Drossard, J., Lewis, D., Altmann, F., Boyle, J., Christou, P., Cole, T., Dale, P., van Dolleweerd, C. J., Isitt, V., Katinger, D., Lobedan, M., Mertens, H., Paul, M. J., Rademacher, T., Sack, M., Hundleby, P. A. C., Stiegler, G., Stoger, E., Twyman, R. M., Vcelar, B. and Fischer, R. (2015) 'Regulatory approval and a first-in-human phase I clinical trial of a monoclonal antibody produced in transgenic tobacco plants', *Plant biotechnology journal*, vol. 13, no. 8, pp. 1106–1120.
47. Marillonnet et al. (2004) 'In planta engineering of viral RNA replicons: Efficient assembly by recombination of DNA modules delivered by *Agrobacterium*', *PNAS*, no. 18, vol. 101, pp. 6852–6857.
48. Mason et al. (1996) 'Expression of Norwalk virus capsid protein in transgenic tobacco and potato and its oral immunogenicity in mice', *May Immunology*, Vol. 93, pp. 5335–5340.
49. Meucci, V. and Arukwe, A. (2005) 'Detection of vitellogenin and zona radiata protein expressions in surface mucus of immature juvenile Atlantic salmon (*Salmo salar*) exposed to waterborne nonylphenol', *Aquatic toxicology (Amsterdam, Netherlands)*, no. 1, pp. 1–10.

50. Moe, S. J., Haande, S. and Couture, R.-M. (2016) 'Climate change, cyanobacteria blooms and ecological status of lakes: A Bayesian network approach', *Ecological Modelling*, vol. 337, pp. 330–347.
51. Morscheid (2006) 'Toxinbildende Cyanobakterien (Blaualgen) in bayrischen Gewässern: Massenentwicklung, Gefährdungspotential, wasserwirtschaftlicher Bezug', no. 125.
52. Mülhardt, C. (2013) *Der Experimentator Molekularbiologie/Genomics* [Online], 7th edn, Berlin, Heidelberg, Springer Berlin Heidelberg. Available at <http://dx.doi.org/10.1007/978-3-642-34636-1>.
53. NATURE (1989) *production of antibodies in transgenic plants* [Online]. Available at https://upload.wikimedia.org/wikipedia/commons/thumb/a/a0/Variety_of_glycans.svg/440px-Variety_of_glycans.svg.png (Accessed 18 January 2016).
54. NIJS, H., Bartsch, D. and Sweet, J. (2004) *Introgression from genetically modified plants into wild relatives* [Online], Wallingford, CABI Publishing. Available at <http://www.cabi.org/CABeBooks/default.aspx?site=107&page=45&LoadModule=PDFHier&BookID=215>.
55. O'NEILL, e. (1986) 'Overproduction from a Cellulase Gene with a High Guanosine-Plus-Cytosine Content in Escherichia coli', *American Society for Mikrobiology*, vol. 1986, Vol. 42 Nr. 4, pp. 737–743.
56. Orzaez, D., Granell, A. and Blazquez, M. A. (2009) 'Manufacturing antibodies in the plant cell', *Biotechnology journal*, vol. 4, no. 12, pp. 1712–1724.
57. Park, J.-W., Faure-Rabasse, S., Robinson, M. A., Desvoyes, B. and Scholthof, H. B. (2004) 'The multifunctional plant viral suppressor of gene silencing P19 interacts with itself and an RNA binding host protein', *Virology*, vol. 323, no. 1, pp. 49–58.
58. Paul, M., Reljic, R., Klein, K., Drake, P. M. W., van Dolleweerd, C., Pabst, M., Windwarder, M., Arcalis, E., Stoger, E., Altmann, F., Cosgrove, C., Bartolf, A., Baden, S. and Ma, J. K.-C. (2014) 'Characterization of a plant-produced recombinant human secretory IgA with broad neutralizing activity against HIV', *mAbs*, vol. 6, no. 6, pp. 1585–1597.
59. Pawar Sandip (2017) *Agrobacterium Tumefaciens: Answers and Explanations* [Online]. Available at <https://upscgk.com/Online-gk/10414/agrobacterium-tumefaciens-is> (Accessed 18 April 2017).
60. Peters & Stoger (2011) 'Transgenic crops for the production of recombinant vaccines and anti-microbial antibodies', *Human Vaccines*, vol. 7, no. 3, pp. 367–374.
61. Petrovska, B. B. (2012) 'Historical review of medicinal plants' usage', *Pharmacognosy reviews*, vol. 6, no. 11, pp. 1–5.
62. Plattner, H. and Hentschel, J. (2006) *Zellbiologie: 20 Tabellen*, 3rd edn, Stuttgart, Thieme.

63. Pogue, G. P., Vojdani, F., Palmer, K. E., Hiatt, E., Hume, S., Phelps, J., Long, L., Bohorova, N., Kim, D., Pauly, M., Velasco, J., Whaley, K., Zeitlin, L., Garger, S. J., White, E., Bai, Y., Haydon, H. and Bratcher, B. (2010) 'Production of pharmaceutical-grade recombinant aprotinin and a monoclonal antibody product using plant-based transient expression systems', *Plant biotechnology journal*, vol. 8, no. 5, pp. 638–654.
64. Poste, A. E., Hecky, R. E. and Guildford, S. J. (2011) 'Evaluating microcystin exposure risk through fish consumption', *Environmental science & technology*, vol. 45, no. 13, pp. 5806–5811.
65. Reinert, J. and Yeoman, M. M. (1982) *Plant Cell and Tissue Culture: A Laboratory Manual*, Berlin, Heidelberg, Springer Berlin Heidelberg.
66. Robinson, M.-P., Ke, N., Lobstein, J., Peterson, C., Szkodny, A., Mansell, T. J., Tuckey, C., Riggs, P. D., Colussi, P. A., Noren, C. J., Taron, C. H., Delisa, M. P. and Berkmen, M. (2015) 'Efficient expression of full-length antibodies in the cytoplasm of engineered bacteria', *Nature communications*, vol. 6, p. 8072.
67. Sack, M., Hofbauer, A., Fischer, R. and Stoger, E. (2015a) 'The increasing value of plant-made proteins', *Current opinion in biotechnology*, vol. 32, pp. 163–170.
68. Sack, M., Hofbauer, A., Fischer, R. and Stoger, E. (2015b) 'The increasing value of plant-made proteins', *Current opinion in biotechnology*, vol. 32, pp. 163–170.
69. Sack, M., Rademacher, T., Spiegel, H., Boes, A., Hellwig, S., Drossard, J., Stoger, E. and Fischer, R. (2015) 'From gene to harvest: insights into upstream process development for the GMP production of a monoclonal antibody in transgenic tobacco plants', *Plant biotechnology journal*, vol. 13, no. 8, pp. 1094–1105.
70. Safarnejad, M. R., Jouzani, G. S., Tabatabaei, M., Twyman, R. M. and Schillberg, S. (2011) 'Antibody-mediated resistance against plant pathogens', *Biotechnology advances*, vol. 29, no. 6, pp. 961–971.
71. Sainsbury, F. and Lomonossoff, G. P. (2008) 'Extremely high-level and rapid transient protein production in plants without the use of viral replication', *Plant physiology*, vol. 148, no. 3, pp. 1212–1218.
72. Sainsbury, F., Thuenemann, E. C. and Lomonossoff, G. P. (2009) 'pEAQ: versatile expression vectors for easy and quick transient expression of heterologous proteins in plants', *Plant biotechnology journal*, vol. 7, no. 7, pp. 682–693.
73. Sambrook & Russel (2001) 'Molecular Cloning: A Laboratory Manual', Volume 1.
74. Saxena, P., Hsieh, Y.-C., Alvarado, V. Y., Sainsbury, F., Saunders, K., Lomonossoff, G. P. and Scholthof, H. B. (2011) 'Improved foreign gene expression in plants using a virus-encoded

- suppressor of RNA silencing modified to be developmentally harmless', *Plant biotechnology journal*, vol. 9, no. 6, pp. 703–712.
75. Schahs, M., Strasser, R., Stadlmann, J., Kunert, R., Rademacher, T. and Steinkellner, H. (2007) 'Production of a monoclonal antibody in plants with a humanized N-glycosylation pattern', *Plant biotechnology journal*, vol. 5, no. 5, pp. 657–663.
 76. Shaner, N. C., Steinbach, P. A. and Tsien, R. Y. (2005) 'A guide to choosing fluorescent proteins', *Nature methods*, vol. 2, no. 12, pp. 905–909.
 77. Sharp, P. A., Sugden, B. and Sambrook, J. (1973) 'Detection of two restriction endonuclease activities in *Haemophilus parainfluenzae* using analytical agarose-ethidium bromide electrophoresis', *Biochemistry*, vol. 12, no. 16, pp. 3055–3063.
 78. Shoseyov, O., Shani, Z. and Levy, I. (2006) 'Carbohydrate binding modules: biochemical properties and novel applications', *Microbiology and molecular biology reviews : MMBR*, vol. 70, no. 2, pp. 283–295.
 79. Siddiqui, S. A., Sarmiento, C., Truve, E., Lehto, H. and Lehto, K. (2008) 'Phenotypes and functional effects caused by various viral RNA silencing suppressors in transgenic *Nicotiana benthamiana* and *N. tabacum*', *Molecular plant-microbe interactions : MPMI*, vol. 21, no. 2, pp. 178–187.
 80. Silhavy, D., Molnar, A., Lucioli, A., Szittya, G., Hornyik, C., Tavazza, M. and Burgyan, J. (2002) 'A viral protein suppresses RNA silencing and binds silencing-generated, 21- to 25-nucleotide double-stranded RNAs', *The EMBO journal*, vol. 21, no. 12, pp. 3070–3080.
 81. Stöger, E. (2013) 'Editorial: from plant biotechnology to bio-based products', *Biotechnology journal*, vol. 8, no. 10, pp. 1122–1123.
 82. Sugimoto, N., Igarashi, K. and Samejima, M. (2012) 'Cellulose affinity purification of fusion proteins tagged with fungal family 1 cellulose-binding domain', *Protein expression and purification*, vol. 82, no. 2, pp. 290–296.
 83. Tiberg et al. (1995) 'Allergy to green algae (*Chlorella*) among children', *Journal of Allergy and Clinical Immunology*, vol. 96, no. 2, pp. 257–259.
 84. Tippkötter, N., Stuckmann, H., Kroll, S., Winkelmann, G., Noack, U., Scheper, T. and Ulber, R. (2009) 'A semi-quantitative dipstick assay for microcystin', *Analytical and bioanalytical chemistry*, vol. 394, no. 3, pp. 863–869.
 85. Tosens, T., Niinemets, U., Vislap, V., Eichelmann, H. and Castro Diez, P. (2012) 'Developmental changes in mesophyll diffusion conductance and photosynthetic capacity under different light and water availabilities in *Populus tremula*: how structure constrains function', *Plant, cell & environment*, vol. 35, no. 5, pp. 839–856.

86. Tremblay, R., Wang, D., Jevnikar, A. M. and Ma, S. (2010) 'Tobacco, a highly efficient green bioreactor for production of therapeutic proteins', *Biotechnology advances*, vol. 28, no. 2, pp. 214–221.
87. Voinnet et al. (2015) 'Suppression of gene silencing: A general strategy used by diverse DNA and RNA viruses of plants', *Proceedings of the National Academy of Sciences of the United States of America*, vol. 112, no. 34, E4812.
88. Weiner et al. (2009) 'Monoclonal antibodies for cancer immunotherapy', *Lancet*, pp. 1033–1040.
89. Weisshaar et al. (1991) 'Light-inducible and constitutively expressed DNA-binding proteins recognizing a plant promoter element with functional relevance in light responsiveness', *The EMBO journal*, vol.10 no.7, pp. 1777–1786.
90. Xu, P., Zhang, X.-X., Miao, C., Fu, Z., Li, Z., Zhang, G., Zheng, M., Liu, Y., Yang, L. and Wang, T. (2013) 'Promotion of melanoma cell invasion and tumor metastasis by microcystin-LR via phosphatidylinositol 3-kinase/AKT pathway', *Environmental science & technology*, vol. 47, no. 15, pp. 8801–8808.
91. Zeck, A., Eikenberg, A., Weller, M. G. and Niessner, R. (2001) 'Highly sensitive immunoassay based on a monoclonal antibody specific for [4-arginine]microcystins', *Analytica Chimica Acta*, vol. 441, no. 1, pp. 1–13.
92. Zeitlin, L., Pettitt, J., Scully, C., Bohorova, N., Kim, D., Pauly, M., Hiatt, A., Ngo, L., Steinkellner, H., Whaley, K. J. and Olinger, G. G. (2011) 'Enhanced potency of a fucose-free monoclonal antibody being developed as an Ebola virus immunoprotectant', *Proceedings of the National Academy of Sciences of the United States of America*, vol. 108, no. 51, pp. 20690–20694.
93. Zhang, S. and Cahalan, M. D. (2007) 'Purifying Plasmid DNA from Bacterial Colonies Using the Qiagen Miniprep Kit', no. 6, e247.
94. Zheng, N., Xia, R., Yang, C., Yin, B., Li, Y., Duan, C., Liang, L., Guo, H. and Xie, Q. (2009) 'Boosted expression of the SARS-CoV nucleocapsid protein in tobacco and its immunogenicity in mice', *Vaccine*, vol. 27, no. 36, pp. 5001–5007.
95. Zuo et al. (2000) 'Chemical-inducible systems for regulated expression of plant genes', *Current opinion in biotechnology*, no. 11, pp. 146–151.
96. Ma, J.K., Drossard, J., Lewis, D., Altmann, F., Boyle, J., Christou, P., Cole, T., Dale, P., van Dolleweerd, C.J., Isitt, V., Katinger, D., Lobedan, M., Mertens, H., Paul, M.J., Rademacher, T., Sack, M., Hundleyby, P.A., Stiegler, G., Stoger, E., Twyman, R.M., Vcelar, B. and Fischer, R. (2015) Regulatory approval and a first-in-human phase I clinical trial of a monoclonal antibody produced in transgenic tobacco plants. *Plant Biotechnol J* 13, 1106-1120.

This ANOVA estimates the influences on the yield according to the parameters of the individual plant and the trial (in total three trials at three dates). Significant influences are marked with three asterisks, according to the significance code. The F value is 77.05, and p-value is very low too. In other words, the variation of plant yield means among different plants is much larger than the variation of AB yield within each trial. Hence it can be concluded that for the confidence interval (p-value is less than 0.05) the alternative hypothesis H1 can be accepted and stated, that there is a significant relationship between the time of sampling as well as a significant difference between the individual plants.

The single factorial ANOVA only states, that within a group of means there is a significant difference. The post-hoc-test (Fig. 58-59) offers a comparison in pairs and provides information which means significantly differ from each other.

Posthoc test for comparison of trials
Study: model.trial ~ "trial"

HSD Test for yield
Mean Square Error: 3.763431

	yield	std	r	Min	Max
trial 1	3.88125	1.845795	16	2.2	8.6
trial 2	9.20000	2.002998	16	7.3	14.5
trial 3	8.92500	1.967570	16	7.1	13.9

alpha: 0.05 ; Df Error: 45
Critical Value of Studentized Range: 3.427507
Honestly Significant Difference: 1.662304

Trial means labeled with the same letter are not significantly different from each other.

Table 46: Posthoc test for comparison of individual AB yields per plant.

	Trial	Means $\frac{mg}{kg}$	Groups
1	Trial 2	9.2	a
2	Trial 3	8.925	a
3	Trial 1	3.881	b

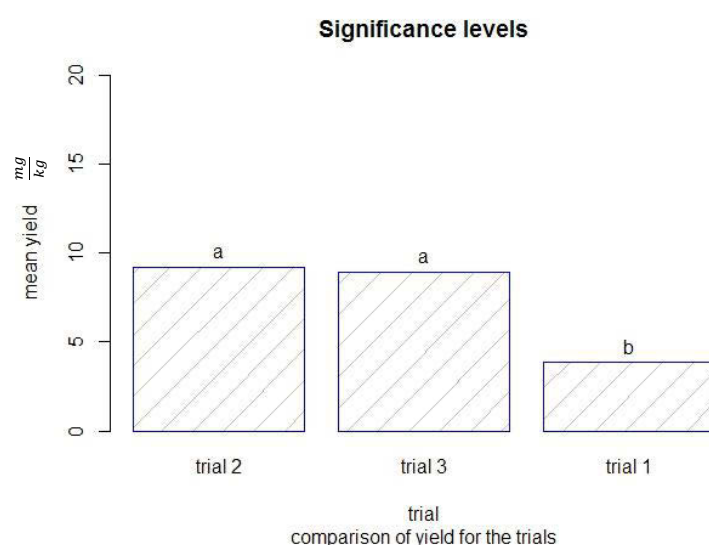


Fig. 58: Illustration of significance levels for the individual trials.

Posthoc test for comparison of yields

Study: model2 ~ "plant"

HSD Test for yield

Mean Square Error: 7.452542

	yield	std	r	Min	Max
11	7.283333	3.257248	6	3.0	10.0
15	6.433333	2.601282	6	2.9	8.6
16	6.650000	2.893268	6	2.2	9.1
17	6.550000	2.413918	6	3.4	8.4
5	6.116667	2.706597	6	2.2	8.4
6	6.233333	2.631856	6	2.8	9.0
7	7.416667	2.325869	6	4.0	9.1
D	12.000000	2.895514	6	8.0	14.5

alpha: 0.05 ; Df Error: 40

Critical Value of Studentized Range: 4.520535

Honestly Significant Difference: 5.038096

Means with the same letter are not significantly different.

Table 47: Posthoc test for comparison of individual AB yields per plant.

	plant	Means $\frac{mg}{kg}$	Groups
1	D	12	a
2	7	7.41	ab
3	11	7.28	ab
4	16	6.65	b
5	17	6.55	b
6	15	6.43	b
7	6	6.23	b
8	5	6.11	b

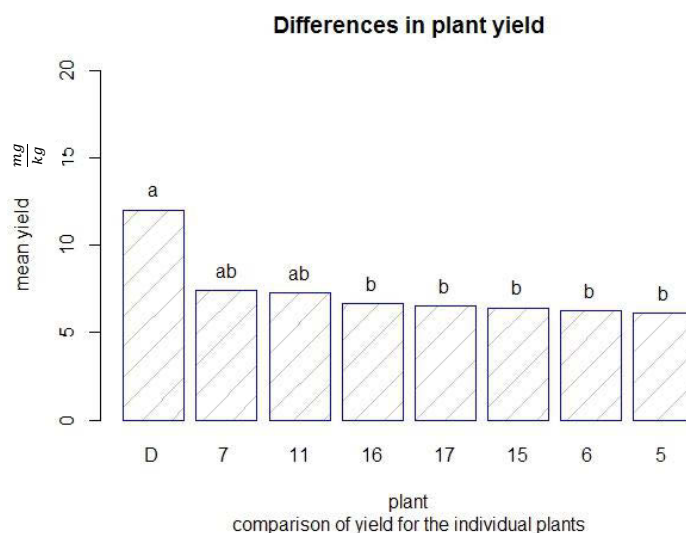


Fig. 59: Illustration of significance levels for the highest producing plants..

Another side experiment in terms of plant derived antibody expression was the investigation of postinfiltration leaf chlorosis (Fig. 60-63) and partial necrosis due to environmental or infiltration stress. This approach was not intended to evaluate the effects on a semi-quantitative or even statistical basis but just to get an impression of the visible symptoms and the potential effects on the plant derived antibody yield. Four different leaf samples were collected. First of all *NB* leaf infiltrated by vacuum infiltration (7dpi), then a highly chlorotic *NT* leaf of an intentionally for this experiment overwatered plant (7dpi), followed by a conventional infiltration pattern of *NT* (7 dpi) and a highly necrotic tissue of *NT* (7 dpi) probably induced by an insufficient removal of medium and thus elevated sucrose concentrations.

3.4.4 SUBCELLULAR LOCALIZATION

3.4.4.1 ANTIBODY FLUORESCENT-MICROSCOPY

For the fluorescence microscopy the best producer, clone D was selected. The kappa chain was successfully detected via an immunostaining assay, as explained in chapter 2.1.22 to 2.1.24 and was visible in the apoplastic space shown by the red arrows. Although the signal obtained is rather low, consistent with the WB results, it can be observed as faint deposits in the apoplastic space (Fig. 66).

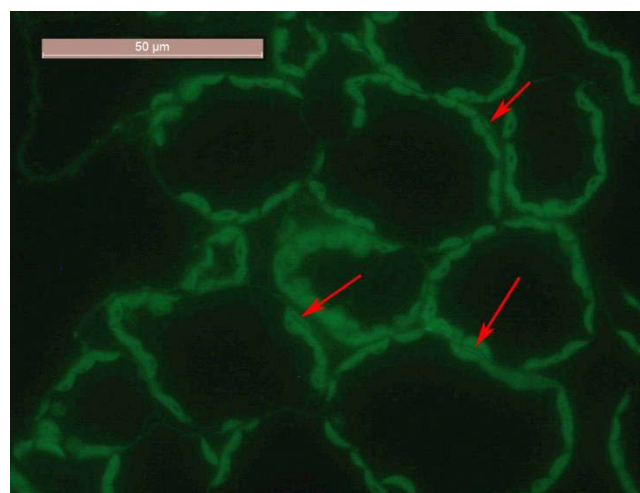


Fig. 66: Fluorescent microscopy image for the subcellular localization of the AB in clone D. The spots of successfully secreted AB is marked with red arrows

3.4.4.2 CONFOCAL MICROSCOPY

Given the low expression level of the protein, a different localization approach was tried in order to improve the signal to noise ratio.

Images were captured using the Leica SP5 CLSM with filter settings for autofluorescence, secondary antibody (excitation 488 nm, emission 500–530 nm), ER-Tracker (excitation 488 nm, emission 500–531 nm). Images were processed using Leica confocal software, ImageJ and Adobe Photoshop CS5.

The confocal images of Clone D derived from the single construct cloning project were prepared as described in Chapter 2.1.25 and localized with a mouse anti human antibody. The images indicated a strong accumulation of AB either in the cytoplasm or ER area. The AB was only hardly visible in the apoplastic region. In contrast to the Cytoplasm / ER where real clusters of antibodies were located.

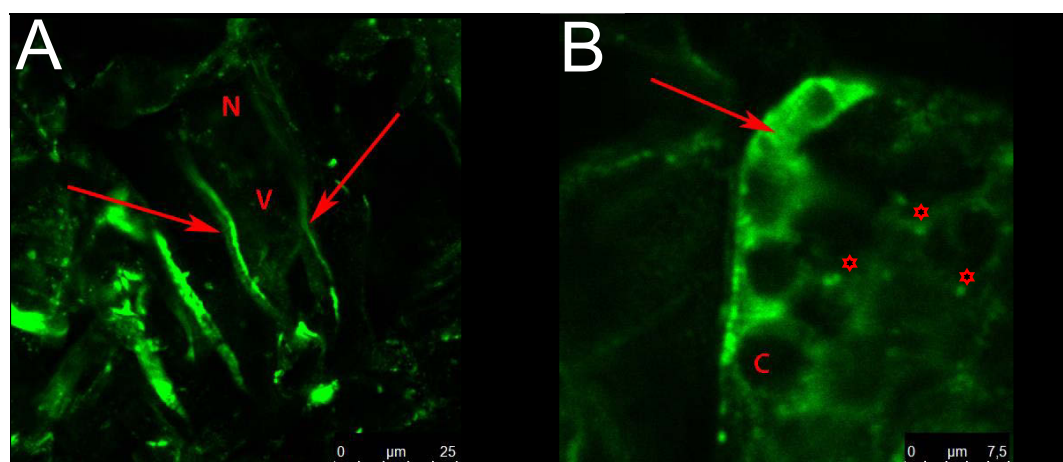


Fig. 67: [A] Localization of the AB in the apoplastic space, indicating a successful secretion. [B] Subcellular localisation of the AB still on the way to secretion, dark circular areas are excluded chloroplasts

Significant signals (Fig. 67 A) derived from the apoplastic space (arrows), could be an indication for successful secretion of the AB. Russel body like inclusion bodies (next to the asterisk).

The arrows indicate an antibody which is already on the way to secretion. See also the signal in between the chloroplasts (c) corresponding to the HC (γ -chain) in the endomembrane system.

Second observation:

In the second observation, an ER marker was used (Fig. 68) to better determine the nature of the punctuate structure where the antibody seems to accumulate to confirm the ER origin of the RB like structures (Clone D). The ER Tracker has a high affinity for the potassium channels, very abundant in the ER and therefore it stains preferably this organelle.

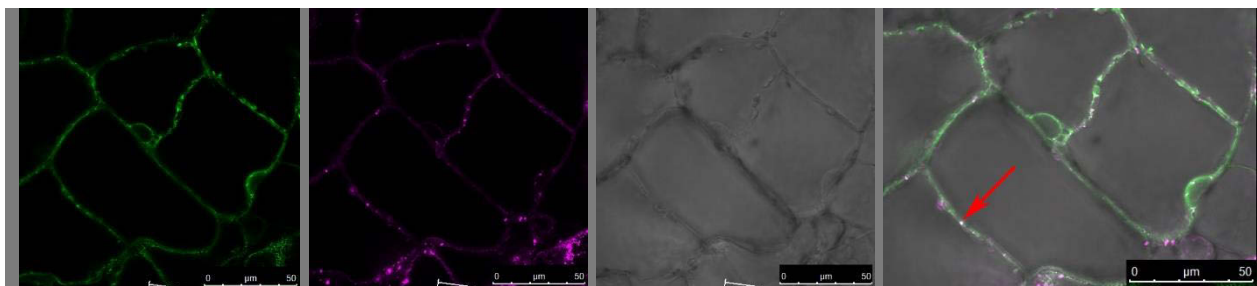


Fig. 68: The following pictures show the (1) an emission of the antibody, (2) emission ER-tracker and (4) a confocal image. A partial colocalization was observed as bright structure in the middle (red arrow) which is a result of the overlay of the magenta and green wave spectra, leading to a white signal, which indicates that a fraction of the antibody is still within the endomembrane system.

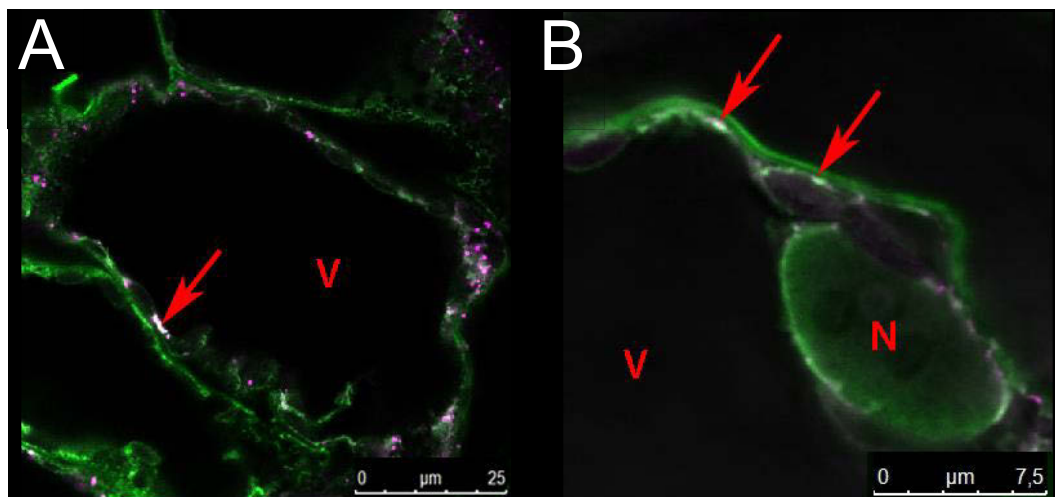


Fig. 69: [A] Detection of the Antibody within the endomembrane system. The colocalization of the AB (red arrows) signal and ER tracker results in white area that indicate that part of the antibody is retained within the ER forming RB-like structures.

In image (Fig.69 [B]) the nucleus is shown in detail surrounded by chloroplasts. In both sub compartments of the cell no antibody was detected, whereas in the region of the plasma membrane, in the upper part of the picture. For the above mentioned reasons, the antibody can therefore be confirmed as successfully secreted into the apoplastic space (Fig.68 A). Although the ER-tracker-red, seems to reveal the presence of diluted structures of accumulated HC as shown in Fig. 69.